AN ABSTRACT OF THE THESIS OF

Robert E. Peterson for the degree of Doctor of Philosophy in Oceanography presented on May 3, 1977.

Title: A Study of Suspended Particulate Matter: Arctic Ocean and Northern Oregon Continental Shelf.

Abstract approved: Redacted for privacy
LaVerne D. Kulm

Total suspended mass (TSM) was determined by gravimetric methods for 53 water samples collected 60 miles north of Ellesmere Island in the Arctic Ocean. The four water masses of the Arctic Ocean, if present at this location, could not be defined by either TSM or light scattering characteristics. TSM was nearly constant at all depths, varying from 6 to 9 μgm/ℓ. The limited range in TSM and scattering precluded calibration of the optical instrument for mass prediction purposes. Oxidizable organic matter varied between 44 and 62% and showed the highest value in waters thought to have a Bering Sea origin. An organic matter/particulate carbon ratio of 1.6 is suggested when these results are compared with an earlier particulate organic carbon study performed in a more central part of the Canada Basin. A size distribution for inorganic suspended particles was calculated assuming Stokes settling, an average inorganic suspended mass concentration, and a flux to the seafloor estimated from accumulation rates observed in sediment cores.

TSM, light transmission, and other suspended particulate parameters were measured for 107 samples from the northern Oregon

continental shelf during April, 1975. Average particulate characteristics were determined for the mixed layer, pycnocline, clearest layers, mid-depth turbid layers, and bottom nepheloid layers. X-ray diffraction revealed a common mineralogy of quartz, feldspars, chlorite, and illite for all samples. Ratios of carbon/nitrogen, organic matter/carbon, and TSM/volume concentration (apparent particle density) were calculated. The nephelometer was calibrated to allow prediction of TSM for an observed range of beam attenuation (c) from 0.4 to 2.0 m^{-1}. This corresponds to a range in TSM of 100 to 2000 $\mu gm/\ell$. Regression analysis gave the following equations for TSM prediction:

"c" in mixed layer and pycnocline

$$TSM = (c - 0.45)/0.00079 \qquad r = 0.99$$

"c" below seasonal pycnocline

$$TSM = (c - 0.42)/0.00064 \qquad r = 0.97$$

The particle-free intercept is very close to the experimentally determined value of c for pure water (0.33 to 0.43 m^{-1}) cited in the literature. TSM prediction can be made with uncertainties of less than $\pm$ 70 $\mu gm/\ell$ for most values of c.

Nephelometer profiles from two across-shelf transects and two 36 hour anchor stations were converted to TSM profiles. Integrated profiles suggest values of about 2.7 to 7.8 mg TSM in a column of water above 1 cm^2 of seafloor, with the higher values found at offshore stations. Temporal variations in mass per seafloor area at the anchor stations are nearly as large as spatial variations observed during the transects. Predicted TSM was contoured in 100 $\mu gm/\ell$

increments as a function of time at the anchor stations and as a function of distance offshore for the transect stations. Distributions of mass clearly reflect the dynamics of coastal upwelling. A deep, onshore flow of relatively cold, clear water can be identified in one time series. A shallow flow of relatively warm, turbid water moves offshore and descends along an inclined isopycnal. Steep gradients in TSM near the surface apparently fluctuate with internal waves propagating along the seasonal pycnocline.

A Study of Suspended Particulate Matter: Arctic Ocean and Northern Oregon Continental Shelf

by

Robert E. Peterson

A THESIS

Submitted to

Oregon State University

in partial fulfillment of
the requirements for the
degree of

Doctor of Philosophy

Completed May 3, 1977

Commencement June 1978

APPROVED:

Redacted for privacy

Professor of Oceanography

Redacted for privacy

Dean of School of Oceanography

Redacted for privacy

Dean of Graduate School

Date thesis is presented: May 3, 1977

Typed by Janice L. Peterson for Robert E. Peterson.

ACKNOWLEDGEMENTS

I would like to express my gratitude to G. Ross Heath for his acceptance of me as a graduate student and for his providing me with the opportunity to pursue the study of suspended particles in the ocean. His counseling and encouragement on several occasions prevented me from going the way of those who start but never finish.

Numerous people tutored me in an informal way during discussions of various topics, especially (in alphabetic order) R. Bartz, T. Chriss, M. Clauson, I. N. McCave, H. Pak, and J.R.V. Zaneveld. The criticisms of the thesis committee members -- G.R. Heath, L.D. Kulm, J.R.V. Zaneveld, H. Pak, E.J. Dasch, and J. Corliss -- were quite helpful in producing the final text. L.D. Kulm kindly offered to serve as the committee chairman in the absence of G.R. Heath. To all these people, and any I should have mentioned but have forgotten to, I offer a sincere thank you.

Finishing this degree became a team effort -- the partner being Jan Peterson. She was most helpful with computer programming, final typing, and emotional support. The project would probably not have been completed without her.

I would also like to acknowledge the encouragement and interest shown by my parents during all phases of my formal education. I am very grateful for the many opportunities that they have provided for me.

TABLE OF CONTENTS

LIST OF FIGURES

LIST OF FIGURES, continued

LIST OF TABLES

LIST OF PLATES

A STUDY OF SUSPENDED PARTICULATE MATTER: ARCTIC OCEAN AND NORTHERN OREGON CONTINENTAL SHELF

CHAPTER I. INTRODUCTION

This research began as an investigation into the nature of suspended particulate matter in the open ocean environment. The area has long been neglected by sedimentologists when compared to the advances made in the study of marine sediments. The reasons for this neglect are primarily technical, since the extremely low mass concentration of suspended material in the open ocean has made it difficult to collect samples of a sufficient size for typical sedimentological analyses. Therefore, this project has included the construction of equipment to collect samples and the refinement of several methods to study them.

The early goals were to collect large enough samples of suspended material (perhaps tens of milligrams) to determine mineralogy by X-ray diffraction. A prototype in situ filtering system was available at O.S.U., but it was lost at sea during the early stages of the project. This resulted in rescheduling the program to allow for equipment construction. The experience is described in Appendix IV and may be helpful to those who attempt similar projects in the future. In addition, documentation for the use of Nuclepore filters in the study of suspended material has been obtained and is presented in Appendix IV in detail.

Samples were collected for study from four rather widely dispersed geographical areas. This was the result of chance opportunities

to go to sea and not necessarily by experimental design! The first set was obtained in November, 1973, from Ice Island T-3 in the Arctic Ocean. Water samples were collected using large volume sampling bottles instead of the *in situ* filtering equipment. The data set is the third reported observation of suspended particulate matter in the Arctic Ocean and the first from the region north of Ellesmere Island.

The *in situ* filtering system was used twice at sea: once during a cruise to the Blanco Fracture Zone in the northeast Pacific Ocean in July, 1974, and again during a transit of the R/V Yaquina from Hawaii to Oregon in December, 1974. The data collected during these latter two cruises was limited and has not been analyzed other than to determine the total suspended mass of particles. The results are tabulated in Tables IX and X of Appendix IV.

Finally in April, 1975, a substantial amount of data pertaining to suspended particulate matter was collected during a cruise on the Oregon continental shelf. The field work was a combined effort of three disciplines: phytoplankton ecology, optical oceanography, and geological oceanography. During this cruise, particulate matter was collected using small volume water samplers. The cruise occurred during upwelling conditions on the Oregon coast and revealed new information on the relation between suspended particles and upwelling dynamics.

Throughout the following text the abbreviation "TSM" (for total suspended matter) will be used to refer to the material retained on a 0.4 μm pore size filter. The values are dry weight concentrations expressed in micrograms per liter.

CHAPTER II. SUSPENDED PARTICULATE MATTER IN THE ARCTIC OCEAN

Introduction

Goals and Previous Work

During November, 1973, members of the Optical and Physical Oceanography groups at O.S.U. participated in a joint research project on Arctic Ice Island T-3, then located about 60 nautical miles north of Ellesmere Island. The effort included *in situ* measurements of light scattering and temperature, and the collection of water samples for gravimetric analysis and Coulter Counter size analysis of the suspended particulate matter. Unfortunately, the latter equipment failed to function properly during the project. The author's participation included the study of the suspended particulate matter, with an immediate goal of learning whether or not the various water masses of the Canada Basin could be distinguished on the basis of their suspended particles.

Figure 1 is an index map to the part of the Arctic Ocean involved in the following discussion, and the locations of previous investigations of suspended matter and optical properties are noted as well. The first reported results of mass concentration measurements of suspended matter in the Canada Basin can be found in Jacobs and Ewing (1969). They used a 200 ℓ water sampler and centrifugation techniques to make their determinations. Kinney et al. (1971) made mass concentration measurements by filtration methods and performed analyses for particulate carbon and nitrogen. Nephelometer records were obtained from T-3 by a Lamont-Doherty group between 1965 and 1969

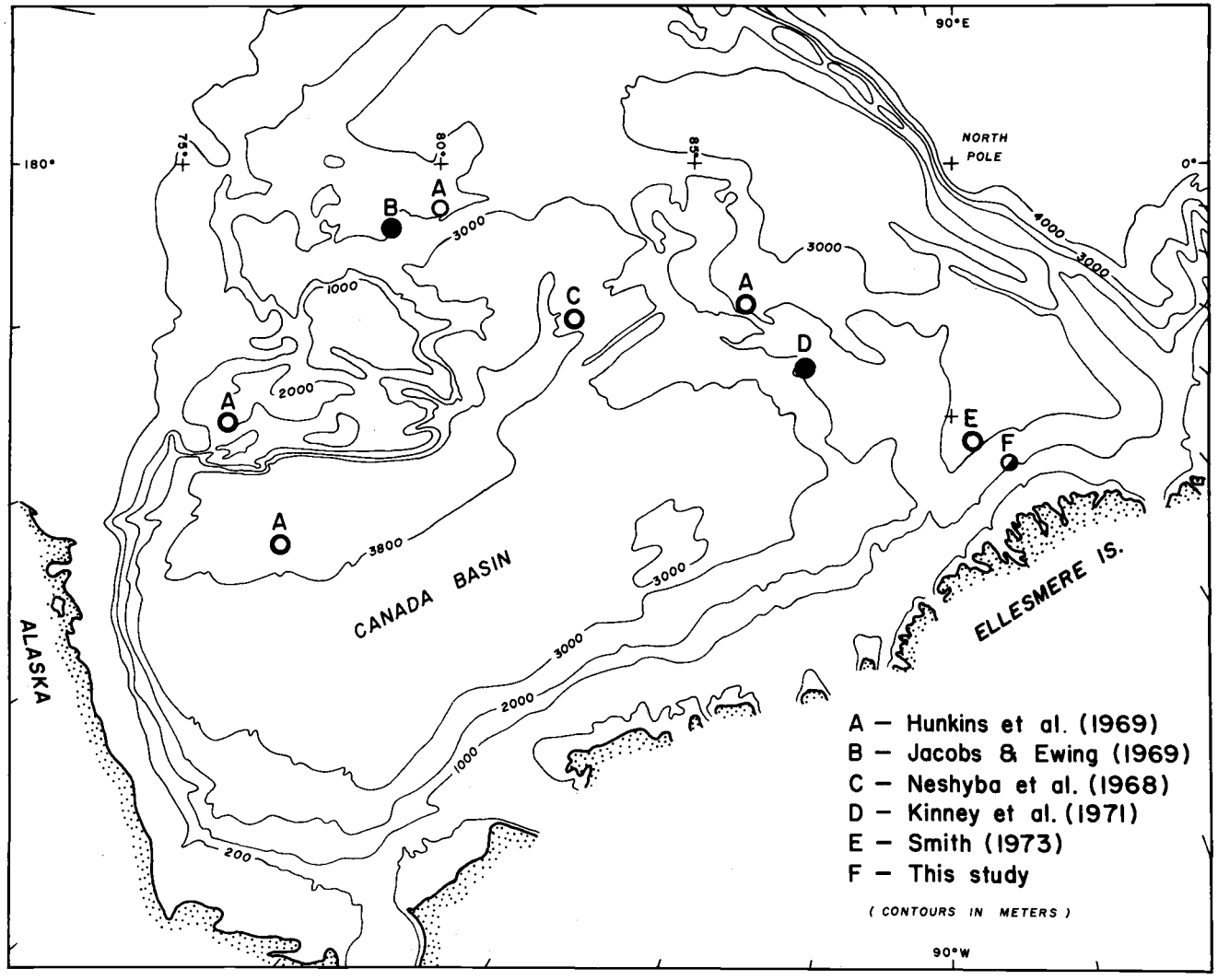

Figure 1. Index map to the Canada Basin, Arctic Ocean. Open symbols indicate locations of previous optical measurements and closed symbols indicate locations of previous collections of suspended particulate matter.

and are reported in Hunkins et al. (1969). Isolated observations of light scattering were made by Neshyba et al. (1968) and beam attenuance was determined for the upper 120 m of the water column by Smith (1973).

Oceanographic Setting

A complete summary of the existing knowledge of physical oceanography in the Arctic Ocean may be found in Coachman and Aagaard (1974). The present report is principally concerned with the currents and water masses of the Canada Basin, whose oceanography has been studied almost exclusively from drifting ice stations.

The surface circulation in the Canada Basin is generally clockwise at a rate of 1 to 2 nautical miles per day as determined by monitoring the drift of ice stations (Coachman, 1969). The surface circulation extends to 200 to 300 m and may include water masses of several geographic origins. The waters of intermediate depths, down to about 900 m, cross the Canada Basin in a southeasterly direction at a rate of about 1 nautical mile per day (Coachman and Barnes, 1963). The deep circulation of this basin is poorly known, but is presumed to be generally counterclockwise and is apparently more vigorous on the ridges and slopes than in the central abyssal plain (Hunkins et al., 1969).

The waters of the Canada Basin are stratified into a two-layer system -- the layers being defined by a sharp pycnocline which occurs between 50 and 200 m and prevents extensive vertical mixing (Coachman and Aagaard, 1974). Physical oceanographers generally refer to three

main water masses: Arctic Surface (0 to 200 m), Atlantic (200 to 900 m), and Arctic Deep (below 900 m). A fourth water mass is usually identifiable immediately below the mixed layer, between 50 and 200 m, and is principally of Pacific origin (Kinney et al., 1970). Figure 2 summarizes the basic properties of these four water masses. During our field work, we did not have the equipment necessary to establish the presence or absence of these various water masses, so Kinney's results were used as a guide to the depths chosen for water sampling.

The region around T-3 is completely covered with pack ice year round. The drift track of the island during our two week stay was irregular and covered an area of several square kilometers. Ice island motion could not be ascertained from any inclination of the hydrowire during the period of water sample collection.

Equipment and Methods

Water samples were collected with a 30 ℓ Niskin bottle and a 40 ℓ PVC sampler built by the Oceanography Department of the University of Washington. Both samplers operated by means of an internal rubber which pulls together two end-caps. Internal rubbers have been suspected as a potential source of particulate contamination (unpublished Coulter Counter results of the Optical Oceanography group at O.S.U., 1974) and rubber parts in general as a source of trace element contamination -- particularly Zn, Cr, Cp, Cs, Sb, and Sc (Bertine and LaFleur, 1972). Further evidence for particulate contamination will be discussed presently.

Seawater was vacuum-filtered directly from the sampler through

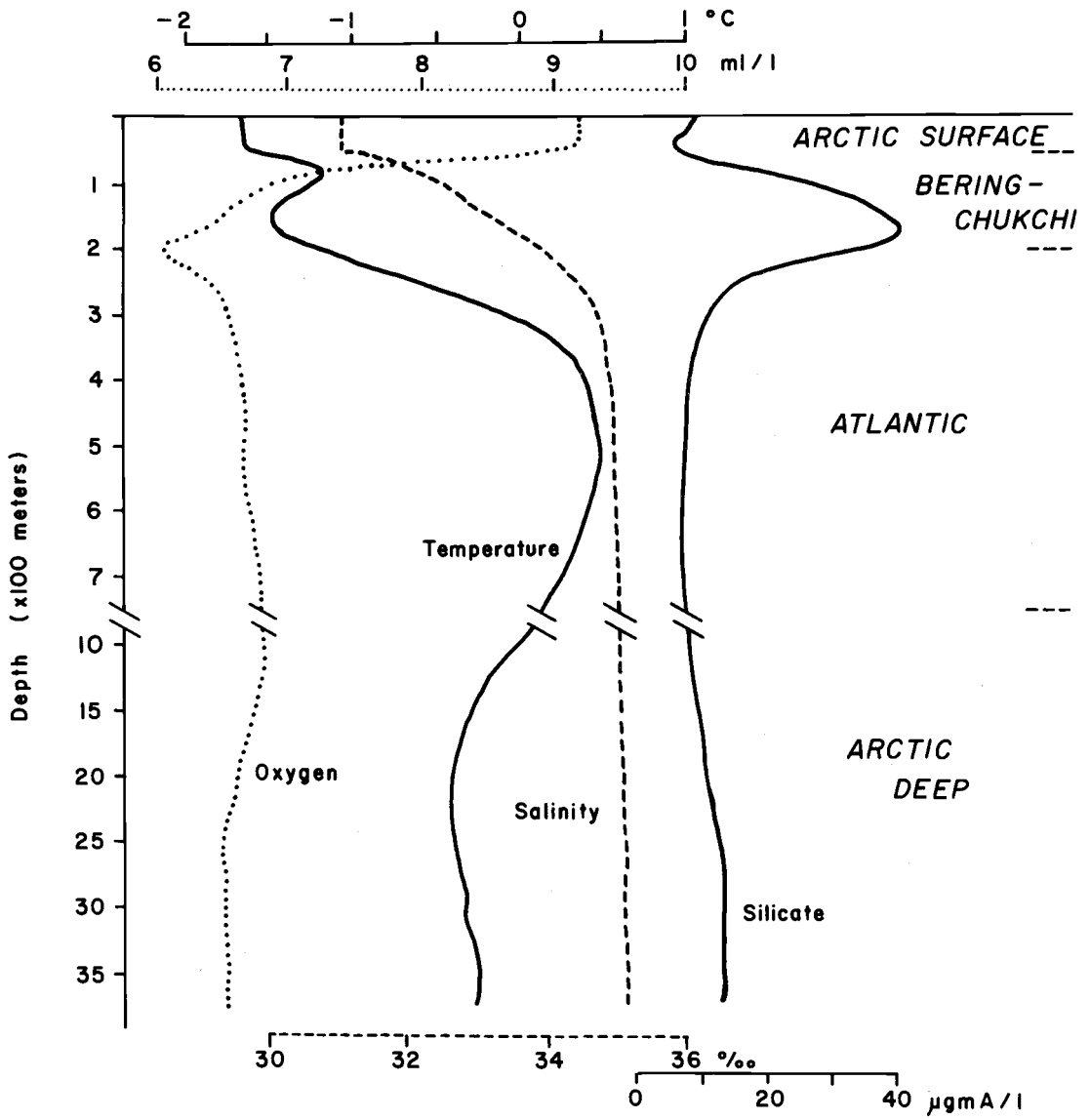

Figure 2. Characteristics of the four water masses present in the Canada Basin (modified from Kinney et al., 1971).

a 47 mm diameter Nuclepore filter with 0.4 μm pore size. The volume of water filtered was measured to an estimated precision of ± 0.03 ℓ . Weighing of the filters was accomplished according to the techniques described in Appendix IV and resulted in a precision of ± 38 μgm for the weight of particles recovered. Two filters from each water mass were treated with hydrogen peroxide to determine the organic matter content by weight loss. Sections of filters were mounted in Hyrax for optical microscopy and affixed to aluminum pedestals and gold-coated for scanning electron microscopy.

Results

Gravimetric analyses

Station data and measured results for the entire sample set are tabulated in Appendix I. Figure 3 is a plot of all the total suspended mass (TSM) concentration values obtained as a function of the time at which the water samples were collected. The overall range of values observed is 3 to 31 μgm/ℓ , although the majority of values occur in the range 5 to 12 μgm/ℓ . The points connected by dashed lines represent filters through which more than one water sample was filtered and in nearly all cases give lower TSM values than single volume samples for the same water mass. The underlined symbols indicate filters that were selected for organic matter digestion.

Two aspects of this plot suggest erroneous values for some of the data points: the curvilinear nature of the Arctic Deep water samples taken with the Niskin sampler (solid circles) and the differences in Arctic Deep and Atlantic values obtained by the Niskin and the

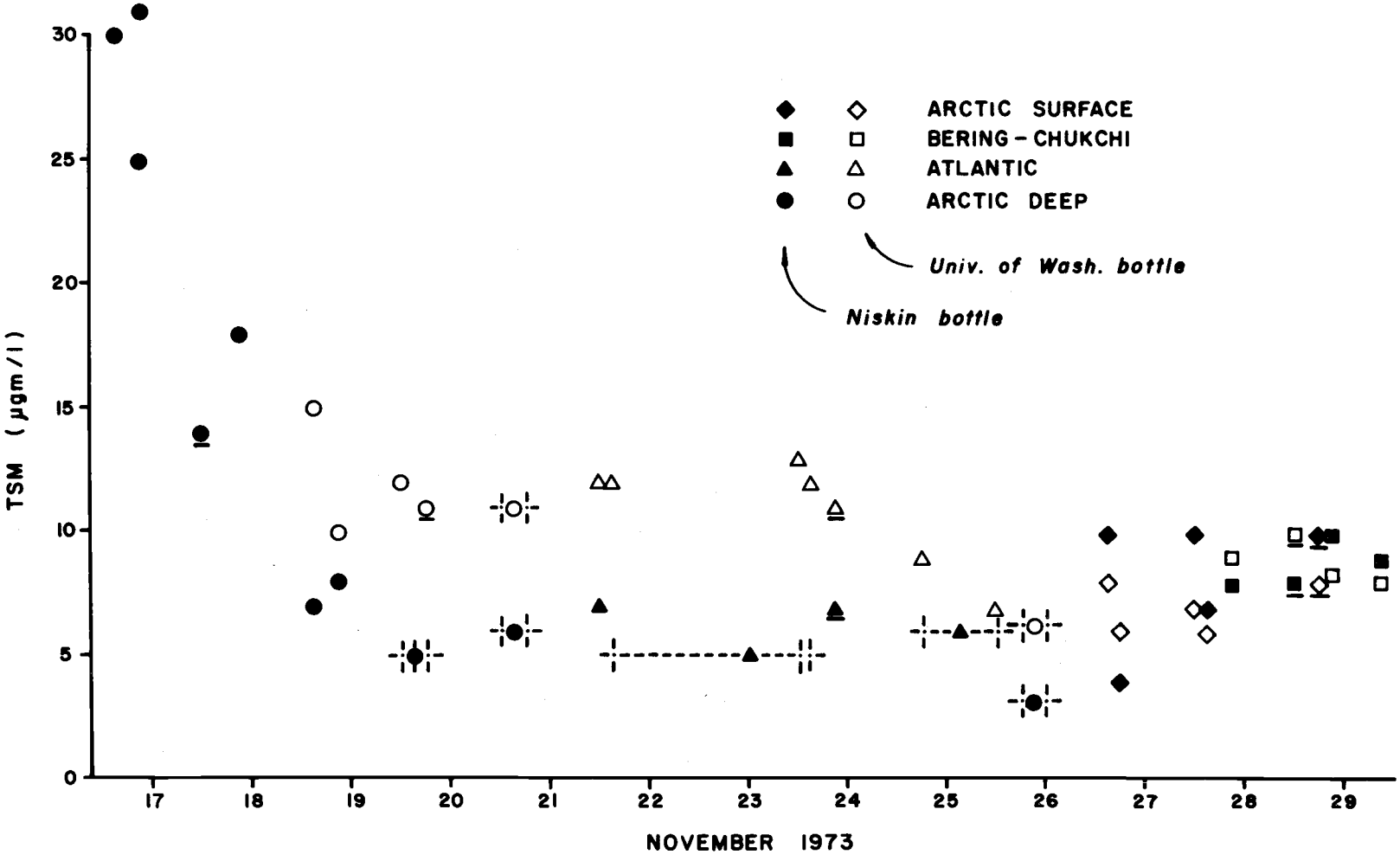

Figure 3. TSM as a function of the time of sample collection. Dashed lines indicate filters through which more than one water sampler volume was processed. Underlined symbols indicate filtered particulates which were treated to determine organic matter. TSM precision is about ± 1.5 µgm/ℓ .

University of Washington sampler. The first trend is judged not to be due to a natural variation in the suspended load, as might be observed during the passage of a mass of more turbid water, since the nephelometer records did not show any concurrent variations. It is suggested that the relatively high TSM values are caused by the addition of contaminants during sampling, possibly by particles from the hydrowire and/or particles shaken loose from inside the Niskin as it was tripped. This effect would become less pronounced with increased use as the less firmly attached particles on the wire or the Niskin were removed. The second aspect -- differences in values for samples collected with different bottles -- suggests even more that particulate contamination from the sampler itself was present, since values obtained from the Niskin are consistently lower for Arctic Deep and Atlantic water masses. The data for 25 to 29 November appear to be less influenced by possible contamination. Variability for a particular water mass is decreased and there do not seem to be consistent differences between samplers.

As a result of the above observations, a number of data points have been deleted from the estimates of mass concentration for Arctic Deep and Atlantic water masses. Figure 4 is an edited version of the data set, showing which values were included. The calculated results are shown in Table I.

A semi-quantitative estimate of the proportion of oxidizable organic matter in each of the water masses is also presented in Table I. The values were obtained by dividing the average weight loss due to hydrogen peroxide digestion by the average mass

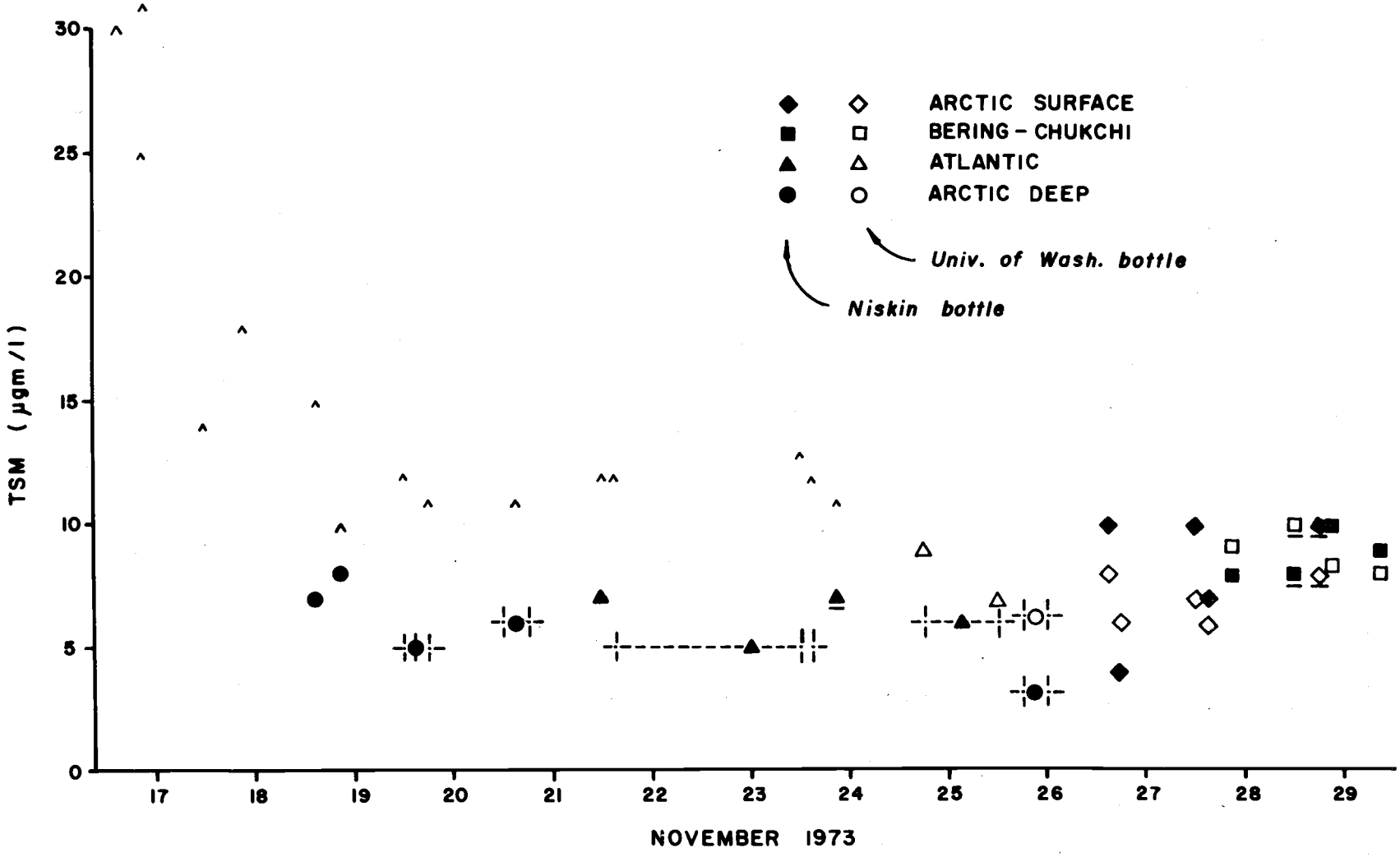

Figure 4. TSM as a function of the time of sample collection, with samples suspected to be contaminated removed (tick marks represent deleted data points). These are the data points used to calculate the average TSM values for each of the water masses.

TABLE I. GRAVIMETRIC RESULTS

Water mass	Number of samples	TSM (µgm/ℓ)	Organic matter (µgm/ℓ)	Inorganic matter (µgm/ℓ)	Percent organic
Arctic surface (50 m)	10	7.6 (4 - 10)	3.7 (3.6 - 3.8)	3.9	49
Bering-Chukchi (150 m)	8	8.9 (8 - 10)	5.5 (4.9 - 6.1)	3.4	62
Atlantic (600 m)	6	6.8 (5 - 9)	3.0 (1.4 - 4.7)	3.8	44
Arctic Deep (1220 m)	6	5.8 (3 - 8)	3.0 (2.5 - 3.5)	2.8	51
(Mean values		7.28	3.80	3.48)	

Note: The organic concentrations are averages of two samples. Numbers in parentheses are maximum and minimum values encountered.

concentration of the water mass. The weighing error is large compared to the leaching weight loss, so the results must be described as semi-quantitative.

Microscopy

Microscope analysis of filters from each of the water masses gives several impressions. The majority of particles in the surface water masses are biogenic -- usually diatoms. In the deeper waters, particles tend to be smaller, and consist of more lithogenous material and skeletal fragments as opposed to whole organisms. Numerically, particles on the order of 2 μm seem to predominate.

In addition to diatoms and lithogenous fragments, numerous seven-spined silicoflagellates were encountered in the surface waters. Clear aggregates containing small black dots were found in an Arctic Deep sample and were very similar in appearance to rubber scraped from a Niskin internal rubber. In several slides, reddish, isotropic mineral fragments were observed that are thought to be rust and occasional opaque, metallic grains similar to fly-ash were also noted (comparisons were made with reference photos in McCrone, 1974, volume II). These observations tend to corroborate the addition of contaminants to the natural particle population.

Although aggregates were present on most filters, they did not predominate. The impression given during scanning electron microscopy was that single particles are more common than large aggregates. Few particles smaller than 0.4 μm were observed, which suggests that Nuclepore filters do indeed function well as size-separating screens,

unless of course no smaller than 0.4 μm particles were present in suspension -- an unlikely possibility. The scanning electron micrographs also revealed the destructive effects filtering has on some particles. The implication of these effects for studies estimating size distributions by microscope techniques on filtered samples is obvious (c.f. Feely, 1976). Plates 1 - 4 are selected micrographs of the filters.

PLATES 1-4. Scanning electron micrographs of Arctic Ocean filters. Pores in filters are 0.4 μm diameter. Sampling depths were as follows: Arctic surface water (50m), Bering-Chukchi water (150m), Atlantic water (600m), and Arctic Deep water (1220m).

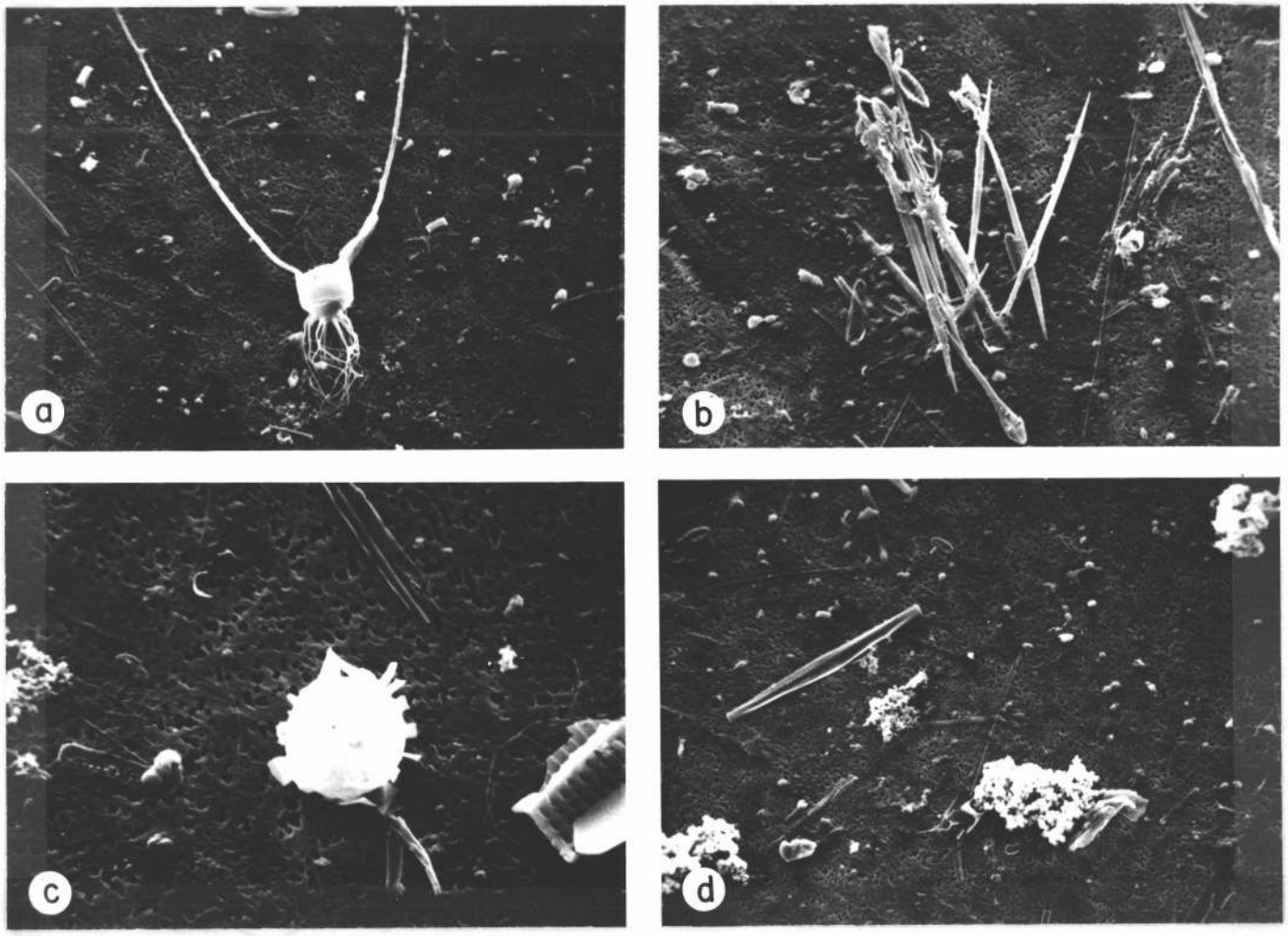

Plate I. (a) Arctic surface water; diatom. (b) Arctic surface water; spines, frequently observed. (c) Arctic surface water; sphere with delicate plate-like extrusions. Note delicate threads on filter surface. (d) Arctic surface water; diatoms.

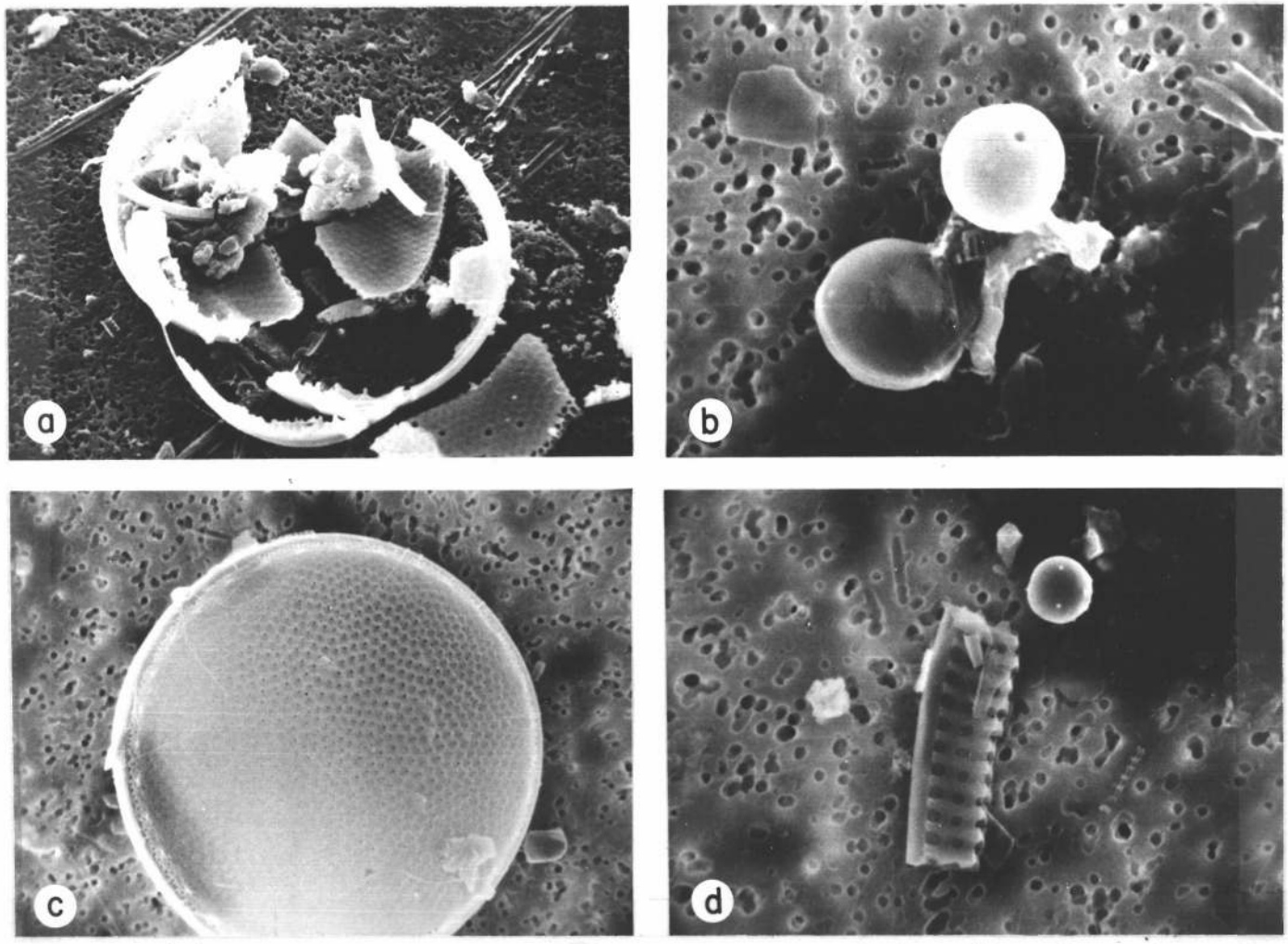

Plate II. (a) Arctic surface water; diatom, fragmented during filtration. Note clay mineral aggregate inside diatom. (b) Bering-Chukchi water; diatom, sphere with hole. (c) Bering-Chukchi water; diatom with clay minerals attached. (d) Bering-Chukchi water; fragments.

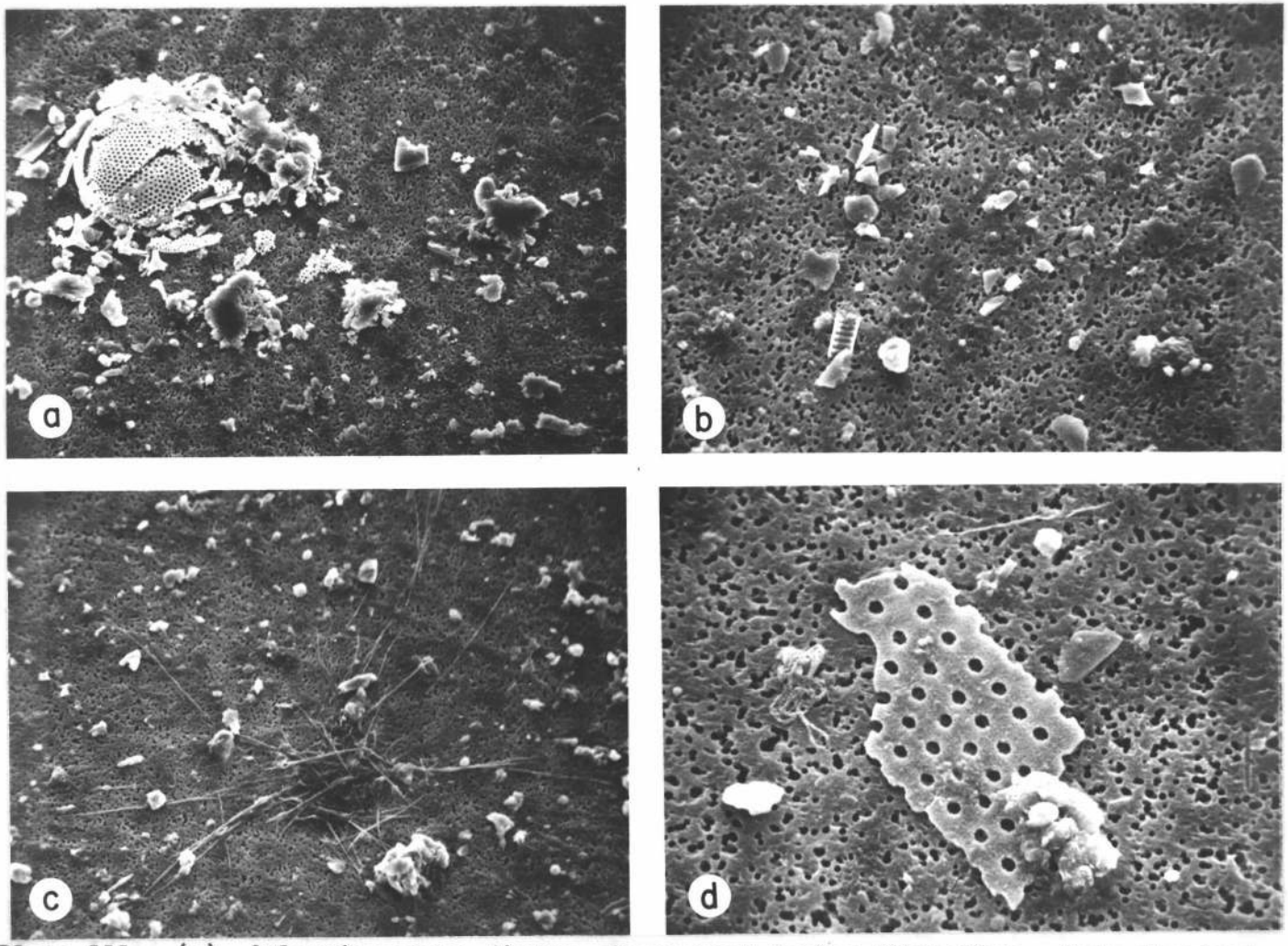

Plate III. (a) Atlantic water; diatom, fragmented during filtration. Note abundant mineral grains. (b) Atlantic water; mineral grains. (c) Arctic deep water; spines from organism collapsed by filtration. (d) Arctic deep water; mineral grains and biogenous fragments.

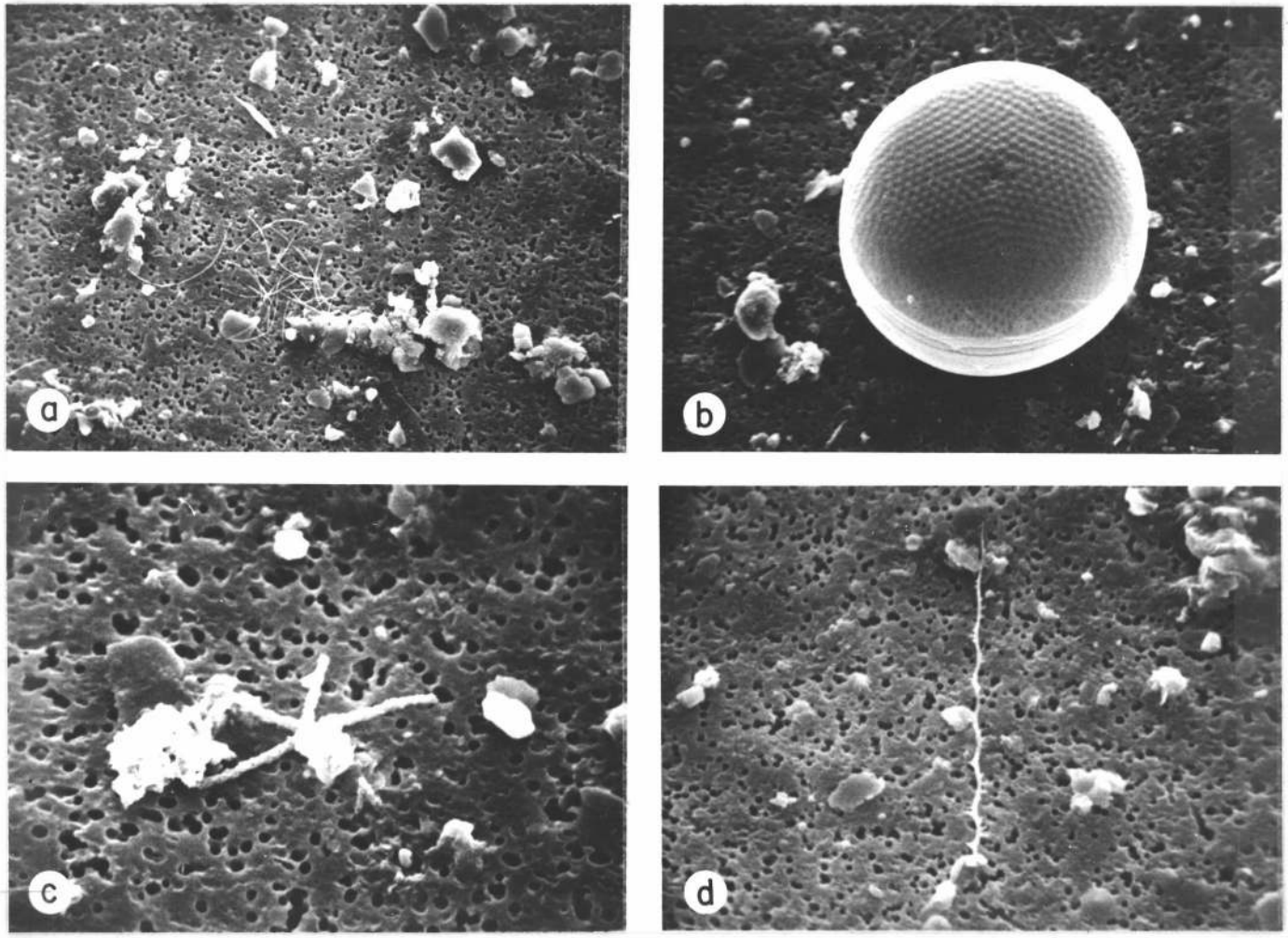

Plate IV. (a) Arctic deep water; mineral grains and very fine threads. (b) Arctic deep water; diatom, note central pore. (c) Arctic deep water; unknown. (d) Arctic deep water; unknown.

Discussion

Mass Concentration and Light Scattering

The estimates of TSM concentration for each of the four water masses sampled show some correlation with the *in situ* light scattering records (Table II). The scattering intensities in this table were determined from seven profiles by averaging the value recorded at each of the four depths chosen for filtration (J.R.V. Zaneveld, personal communication). The discrepancy between the 1200 m depth at which light scattering intensity was measured and the 1220 m depth at which filtration was accomplished is not significant.

The light scattering profiles show very little structure compared to other ocean areas. Typically, the upper hundred meters or so contain the greatest intensity and variability in scattering, which agrees with the earlier data reported by Neshyba et al. (1968). It would be difficult, however, to assess the natural importance of this increased scattering, since water immediately below the hydrohole in the ice may give erroneous scattering values due to light penetration from the hydrohut and to particulate matter derived from hydrohole activity.

During three of the nephelometer casts, the nephelometer was allowed to settle onto the seafloor, yet no indication of even a thin bottom nepheloid layer was observed. Based on more widespread nephelometry in the Canada Basin reported in Hunkins et al. (1969), this could indicate the absence of sedimentologically important bottom currents in this region.

TABLE II. COMPARISON OF LIGHT SCATTERING AND TSM

Depth (m)	Cast Number 1	2	4	5	6	7	8	Range
50	1.86	2.06	2.12	1.90	1.96	1.96	2.09	0.26
150	1.83	2.07	1.87	1.93	1.85	1.88	2.05	0.24
600	1.75	1.94	1.87	1.78	1.82	1.86	1.92	0.20
1200	1.78	1.96	1.92	1.74	1.74	1.84	1.87	0.22
Range	0.11	0.13	0.25	0.19	0.22	0.12	0.22	

a. Relative scattering intensities from SCOUT nephelometer profiles measured at depths comparable to those sampled for suspended particulate matter.

Depth (m)	Average Scattering Intensity	Average TSM (μgm/ℓ)
50	1.99	7.6
150	1.93	8.9
600	1.85	6.8
1200	1.84	5.8

b. Comparison of average scattering intensity and average TSM at four depths sampled.

In several of the nephelometer records, occasional spikes of increased scattering were observed. The best explanation for such a signal is blocking of the instrument's light path by a relatively large diameter particle, perhaps on the order of a millimeter or larger (H. Pak, personal communication). Particles of this size do exist in the water column, as is demonstrated by the photomicrographs of sections of filters, but they are rare, and the probability of one settling through the light path seems very small. Pak suggests that zooplankton may have been attracted by the light and swam through the beam. Amphipods were observed in the water in the hydrohole, and other zooplankton are known to exist at all depths in this region of the Arctic Ocean (Hopkins, 1969).

Comparison with Previous Gravimetric Results

The gravimetric data obtained by Jacobs and Ewing (1969) and by Kinney et al. (1971) are presented in Table III for comparison with the data reported here. The results of this study differ from the two previous studies in two ways: 1. The mass concentration of suspended matter north of Ellesmere Island is nearly constant throughout the water column, whereas in areas more centrally located in the Canada Basin, there is a significantly higher TSM in surface layers, and 2. Mass concentrations north of Ellesmere are in general lower than at the other localities (refer to Figure 1 for locations of previous studies).

A partial explanation for both trends may be the age of the water masses at various locations. The circulation of all water masses

TABLE III. SUMMARY OF TSM MEASUREMENTS IN THE CANADA BASIN

Water Mass	Sample Depth (m)	Jacobs & Ewing (1969) (μgm/ℓ)	Kinney et al. (1971) (μgm/ℓ)	This Study (μgm/ℓ)
Arctic Surface (0 - 50 m)	5		31	
	12	32		
	20		32	
	50		55	8
Bering-Chukchi (50 - 200 m)	75	19	30	
	100		22	
	140		18	
	150			9
	155	18		
	200		10	
Atlantic (200 - 900 m)	500	49	15	
	600			7
	750		10	
Arctic Deep (below 900 m)	1000	6		
	1100		9	
	1220			6
	2000	9		
	2210	8		
	2260	9		
	2302	10		

in the Canada Basin, except the Arctic Deep water whose motion is largely unknown, progresses from the Jacobs and Ewing locality to the author's locality. If the removal rate of suspended particles exceeds the supply to the suspension, the oldest waters should have the lowest concentration. Age estimates for Atlantic and Pacific waters in the Arctic Ocean suggest that the waters north of Ellesmere may be older than in most other parts of the Ocean, perhaps having a residence time of roughly 10 years (see summary of residence times in Coachman and Aagaard, 1974). This is sufficient time for lithogenous particles of about 5 μm diameter to settle through 3800 meters of water, the depth for a large portion of the Canada Basin. Unfortunately, there is no direct way to support this simple model, since the supply rates of particles to suspension by ice-rafting, eolian sources, and primary production, as well as the rates of other removal processes such as accelerated settling by fecal pellet production, are unknown.

An alternative, but unsettling explanation for the differences between the Kinney data and that of this study is contamination during Kinney's water sample collection, just as it was suspected in the results presented here. If the first ten 30 ℓ Niskin samples taken by the author (including those identified as contaminated in a previous paragraph) are compared with the samples of Kinney, assuming his sequence of sampling to be surface-to-deep, a good correlation exists (Figure 5). It is possible that all the variability exhibited in his data is due to the same sort of contamination suspected in many of the author's samples, since Kinney also used Niskin bottles for his work. This is pure speculation, however, since the actual sequence in

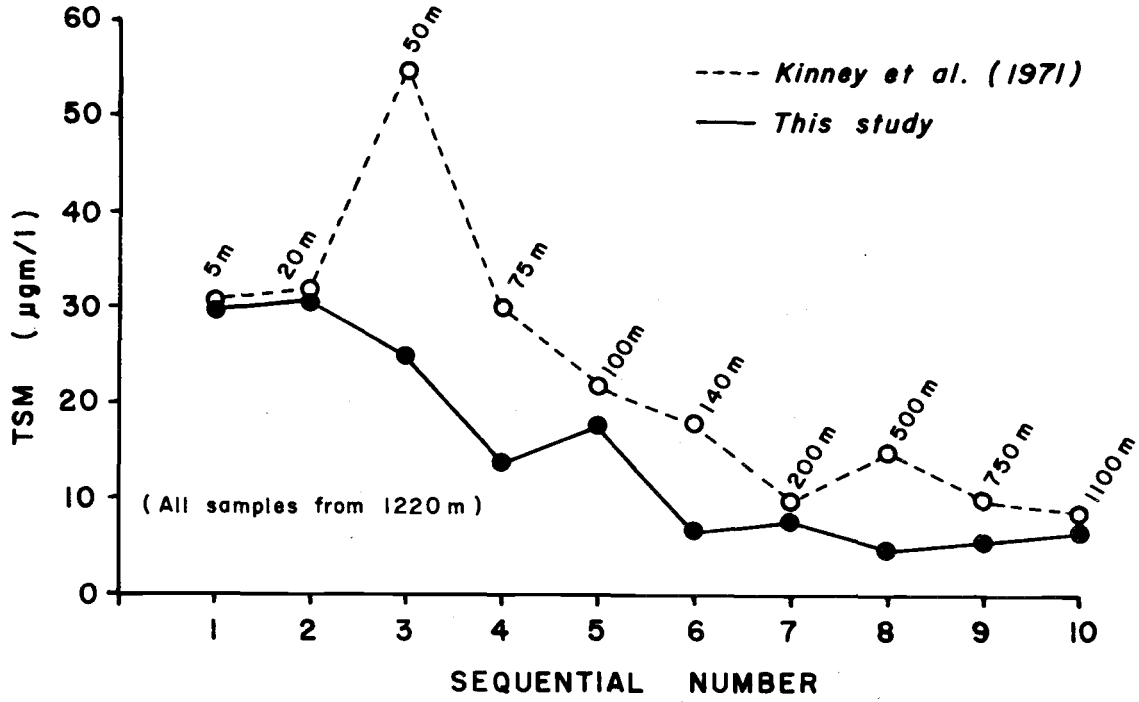

Figure 5. Comparison of TSM from two studies, using the sequence in which samples were collected as the basis for the comparison. Kinney's sequence of sampling is assumed. If the assumption is correct, note the high degree of correlation, regardless of depth from which the sample was taken.

which his samples were collected could not be determined.

Organic Matter in Suspended Particulates

The relatively large proportion of organic matter found in six of the samples (Table I) is probably due to a very low terrigenous and/or eolian contribution -- low primary productivity notwithstanding. This conclusion was also made by Kinney et al. (1971) following their analysis of particulate and dissolved carbon in the Canada Basin. Their TSM and POC values were averaged for each water mass, and the POC was converted to organic matter by multiplying by two. This result was divided by TSM to give percent organic matter which could then be compared to the results listed in Table I. Both studies indicate that a major portion of the TSM is organic and that Bering-Chukchi water contains the greatest proportion. It is interesting also that the percentages presented here are similar to the 50% organic matter reported for a dust sample by Darby et al. (1974) north of Barrow, Alaska, at 75N-150W.

The factor used to convert particulate carbon to organic matter is not precise and the value two was selected as an estimate. For suspended particulate matter from the Oregon continental shelf, values in the range of 1 to 2 are generally found, although considerable variability exists (see Figure 12, Chapter III). Carroll (1970) used 1.72 in her study of Arctic seafloor sediment, which is a value frequently encountered in soils analysis (Jackson, 1958). Gordon (1970) used a value of 1.8 in his studies of suspended particulates in the North Atlantic.

Making the assumption that the organic matter percentages

obtained by peroxide leaching are reasonable for the Canada Basin, the conversion factor was calculated using Kinney's TSM and POC values according to the following expression:

$$\text{ORGMAT: ORG CAR} = \frac{(\%\ \text{ORG MAT})\ (\text{TSM})}{(\text{POC})}$$

The results (Table IV) suggest a value of about 1.6 for the organic matter/particulate carbon ratio. The differences between water masses are judged to be insignificant due to the errors associated with the TSM, POC, and % organic matter values. The value 1.6 for this ratio seems reasonable for the biogenous material one might expect to find in Arctic waters. Since primary productivity is very low compared to other ocean areas, the proportion of biogenic material that is relatively refractory (compared to living organisms) should be increased, causing a decrease in the ratio by virtue of the methods used to determine it. That is, the more refractory material will still be measured by the combustion techniques used to determine POC but will tend to be missed by peroxide leaching methods.

Relation Between Suspended Particles and Seafloor Sediment

An attempt has been made to relate the mass of suspended inorganic material to the mass of sediment accumulating on the seafloor of the Canada Basin. If these two parameters are known, it is possible to estimate a size distribution for the suspended material, allowing reasonable assumptions. The decision to compare suspended inorganic material to the rate of accumulation of seafloor sediment

TABLE IV. PARTICULATE ORGANIC CARBON DATA OF KINNEY et al. (1971) COMPARED TO RESULTS OF THIS STUDY

Water Mass	Average TSM (µgm/ℓ)	Average POC (µgm/ℓ)	Organic Matter (%)
Arctic Surface	37.0	9.8	53
Bering-Chukchi	16.7	7.3	87
Atlantic	12.5	3.8	61
Arctic Deep	9.0	2.7	60

a. Kinney's data converted to percent organic matter assuming an organic matter to carbon ratio of two. TSM precision is ± 4 µgm/ℓ and POC is ± 2 µgm/ℓ .

Water Mass	% Organic Matter (this study)		Organic matter: Carbon
Arctic Surface	49		1.86
Bering-Chukchi	62		1.43
Atlantic	44		1.45
Arctic Deep	51		1.70
		(Average	1.61)

b. Organic matter to carbon ratio assuming oxidizable organic matter results of this study and TSM and POC values from Kinney.

was prompted by the 1% or less organic matter in the sediments (Carroll, 1970; Green, 1960). The low percentage is presumed due to lack of preservation of pelagic organic matter, whether by non-deposition or post deposition destruction, rather than to dilution by inorganic components.

The boundaries of the Canada Basin have been set as the area enclosed by the 3000 m contour (refer to Figure 1). The volume of the basin is represented by the sum of the volumes above the 3000 m contour and between the 3800 and 3000 m contours. The other parameters necessary for the calculations are listed in Table V. Sediment bulk density was estimated from wet bulk densities of similar sediments measured in the southern Bering Sea (Hamilton, 1976; Lee, 1973) and in the Greenland-Norwegian Sea (Keller, 1971). The wet bulk density values were converted to dry values assuming a moisture content of 40 to 60% (dry weight basis) for Canada Basin sediment (Clark, 1969; also Keller, 1971, for Greenland-Norwegian Sea sediment). A grain density had to be included in the calculations involving Stokes settling and was taken to be 2.55 gm/cm^3, which is an average of 2.4 for a Bering Sea diatom ooze and 2.7 for North Pacific pelagic clay (Hamilton, 1974).

The seafloor accumulation rate was calculated by multiplying the average pelagic sedimentation rate reported in the literature by the estimated dry bulk density for the sediments, and resulted in a value of 1.35×10^{-4} $gm/(cm^2)(yr)$. Next, the time interval in the sediment was determined for which the seafloor mass of material was equal to the total inorganic suspended mass in the Canada Basin.

TABLE V. PARAMETERS USED IN SIZE DISTRIBUTION MODEL

Parameter	Value
Area within 3000 m contour	9.184×10^{15} cm^2
Area within 3800 m contour	1.696×10^{15} cm^2
Volume above 3000 m contour	2.755×10^{21} cm^3
Volume between 3000 and 3800 meters	0.136×10^{21} cm^3
Total volume of Canada Basin	2.891×10^{21} cm^3
Concentration of suspended inorganic material	3.48 µgm/ℓ (2.8 - 3.9)
Pelagic sedimentation rate[1]	0.15 cm/1000 yrs (0.1 - 0.2)
Sediment moisture content[2]	40 - 60% (dry weight basis)
Sediment grain density[3]	2.55 gm/cm^3 (2.4 - 2.7)
Sediment dry bulk density[4]	0.90 gm/cm^3 (0.8 - 1.0)
Stokes constants (K)	5.52×10^3 $(cm\ sec)^{-1}$ (4.98 - 6.07)
R:M (see text for explanation)	1.23×10^{-3} cm/sec (0.65 - 2.27)

Sources:
1. Hunkins and Kutschale (1967); Ku and Broecker (1967); Clark (1969)
2. Clark (1969); Keller (1971)
3. Hamilton (1974)
4. Hamilton (1976); Lee (1973)

This was calculated according to the following expression:

$$\text{Time interval} = \frac{\left(\begin{array}{c}\text{suspended mass}\\ \text{concentration}\end{array}\right)\left(\begin{array}{c}\text{volume of}\\ \text{basin}\end{array}\right)}{\left(\begin{array}{c}\text{area of}\\ \text{basin}\end{array}\right)\left(\begin{array}{c}\text{accumulation}\\ \text{rate}\end{array}\right)}$$

It has been assumed that the inorganic mass concentration has an average value for the whole basin. The resulting interval is 8 years, with the value in the range of 4 to 15 years when the uncertainties of the parameters are considered. This is of the same order as the age of Atlantic and Pacific water masses in this part of the Arctic Ocean (Coachman and Aagaard, 1974, Figures 11 and 19). Though it is difficult to define a precise meaning for this time interval, it suggests a sort of average residence time for inorganic particles in the basin. If all particulate input and circulation were to stop, nearly all the inorganic mass in suspension should have accumulated at the seafloor in about 8 years.

If the flux of particles from suspension to the seafloor can be estimated by the accumulation rate of pelagic sediment at the seafloor, it is possible to calculate a size distribution for the suspended particles. It is assumed that the accumulation rate at the present is the same as that revealed by analysis of the sedimentation rate in cores from the Canada Basin and that Stokes settling is the main process responsible for the flux. The next assumption made is that the size distribution is a hyperbolic function of the form:

$$\begin{array}{c}\text{Number of particles of}\\ \text{diameter D per cm}^3\end{array} = ND^{-C}$$

where D is expressed in micrometers, the coefficient N in particles per cubic centimeter, and the slope C is a dimensionless number. This function has been suggested by Bader (1970) as being typical for natural collections of many types of small particles, including marine suspensions and aerosols. (Frequently, the hyperbolic size distribution is given in the cumulative form, where the function is the number of particles larger than diameter D; in the following equstions, the differential of that form is used).

The mass concentration of suspended inorganic particles can be expressed as follows:

$$\underset{(M)}{\text{mass concentration}} = \int_{D_l}^{D_u} \left(\frac{\rho \pi D^3}{6}\right) N D^{-C} \, dD \qquad (1)$$

where D_u and D_l refer to upper and lower size limits for particle diameter and ρ is particle density. The first term describes the mass of each particle and the second the number of particles, both as a function of diameter. Upon integration, this equation becomes:

$$M = \left(\frac{\rho \pi N}{6(4-C)}\right)\left(D_u^{4-c} - D_l^{4-c}\right) \qquad (2)$$

The rate of removal from suspension can be expressed as a function of the mass of particles in suspension and the rate at which they are settling to the seafloor by Stokesian settling:

$$\text{flux from suspension}_{(R)} = \int_{D_l}^{D_u} \left(\frac{\rho\pi D^3}{6}\right)(ND^{-C})\,(KD^2)\,dD \qquad (3)$$

Again, the first and second terms reflect particle mass and number as a function of diameter respectively. The third term is Stokes settling velocity, where the constant K includes gravity (g), relative density $(\rho-\rho_w)$, and fluid viscosity (μ) terms such that:

$$K = \left(\frac{1}{18}\right)\left(\frac{1}{\mu}\right)(\rho-\rho_w)\,g$$

After integrating, equation (3) becomes:

$$R = \left(\frac{\rho\pi NK}{6\,(6-C)}\right)\left(D_u^{\,6-c} - D_l^{\,6-c}\right) \qquad (4)$$

We now have two equations in two unknowns (N and C of the size distribution) which can be solved simultaneously by taking the ratio R:M, with the following result:

$$\frac{R}{M} = K\left(\frac{4-C}{6-C}\right)\left(\frac{D_u^{\,6-c} - D_l^{\,6-c}}{D_u^{\,4-c} - D_l^{\,4-c}}\right) \qquad (5)$$

The flux from suspension (R) is estimated by the seafloor accumulation rate calculated earlier. The mass concentration of suspended inorganic material (M) is estimated from the filtration results listed in Table I. The ratio is 1.23×10^{-3} cm/sec. Note that the ratio R:M is in velocity units. This may be thought of as an average

settling velocity and would correspond to opal particles (ρ =2.0) with diameters of about 6 μm, or clay particles (ρ =2.7) with diameters of about 4 μm.

At this point, equation (5) is solved by iteration for values of C which will produce the desired ratio R:M. The dimensionality of equation (5) is confusing, since the empirical function for the number size distribution contains mixed units, i.e. N is expressed in "number of particles per cubic centimeter" and D in micrometers. To maintain dimensional consistency in equation (5), those terms normally expressed in centimeters must now be converted to micrometers. After C has been calculated and we wish to solve for N in either equation (2) or (4), we must also use micrometers in place of centimeters for the parameters of those equations.

Numerous solutions for equation (5) were calculated to learn the effects of various upper and lower limits for particle diameter. The slope of the size distribution is far more sensitive to changes in the lower limit than in the upper, as is evident in Figure 6. The variability of C introduced by the uncertainties in the values of the other parameters used in equations (2) and (4) was also determined and is shown by the error bars extending from the dotted line for the R:M value in Figure 6. In choosing the appropriate size limits for this analysis, we are constrained by the fact that the suspended mass concentration includes all inorganic material larger than about 0.5 μm in diameter. Microscopic inspection of filters revealed no particles with a dimension larger than about 225 μm, and we should probably expect to find particles of this size in a 30 ℓ sample only rarely

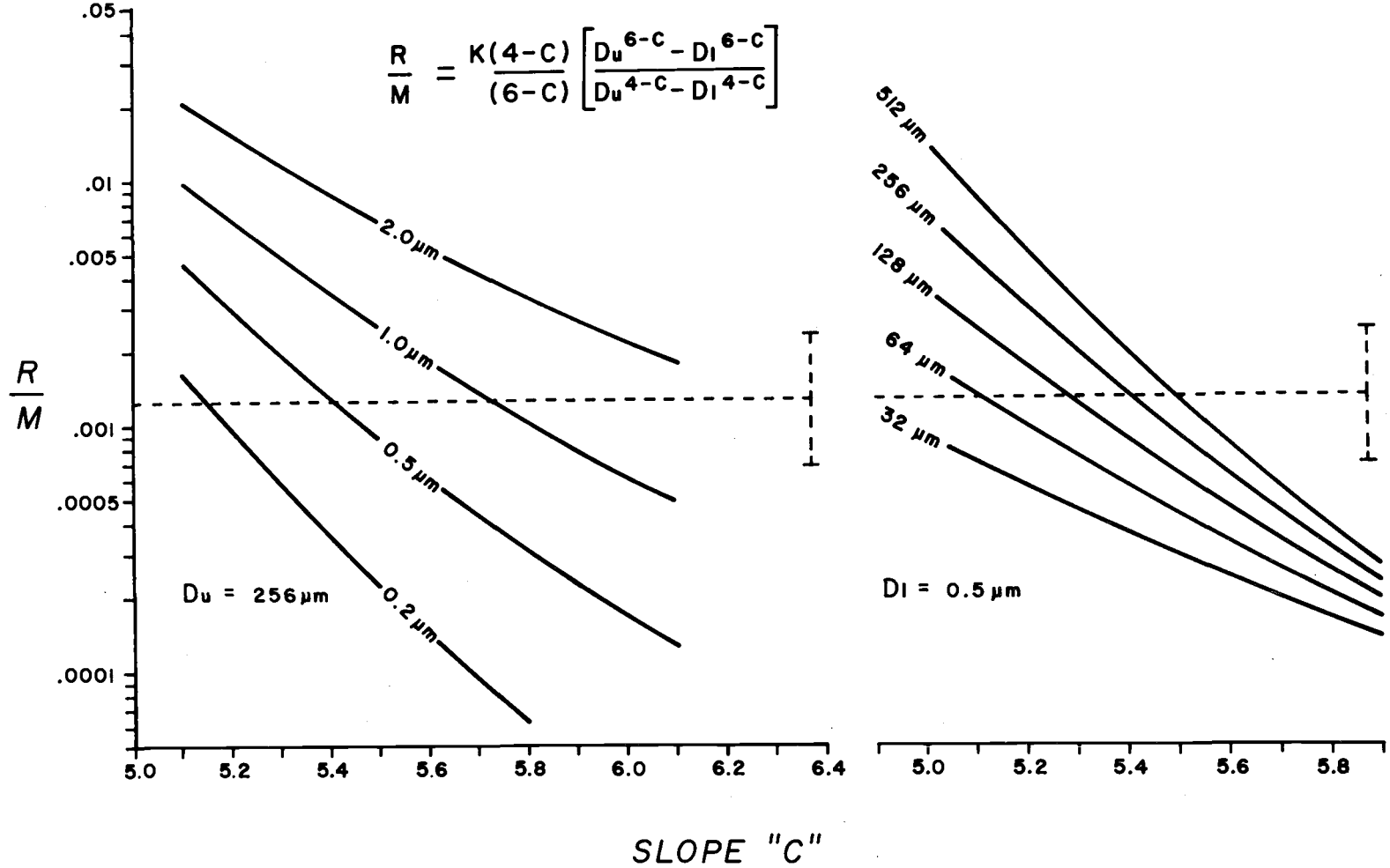

Figure 6. Variability in size distribution slope which results from choosing various upper and lower diameters to delineate the distribution. Dashed line represents estimated value and uncertainty range for R/M. See text for further explanation.

(McCave, 1975). Hence, the size range 0.5 to 256 μm was chosen for the diameter limits. From the curve in Figure 6 for this size range, slope C can be read as 5.42 with an uncertainty of ± 0.16 due to the uncertainty of the R:M ratio. (Note: an additional uncertainty of ± 0.03 would be added by recognizing also the natural variability in the parameters used to calculate K, the Stokes constants).

Once C has been decided upon, N can be solved for in either equation (2) or (4) and is found to be 1383 particles per cubic centimeter. Uncertainties in the various parameters become compounded at this stage and lead to a large range in values for N. As an example using equation (4), the maximum and minimum values for mass concentration, particle density, and slope C will produce values for N ranging from 1043 to 1640 particles per cubic centimeter. We now have a complete description of the size distribution:

$$\text{Number of particles of diameter D per cm}^3 = 1383\ D^{-5.42}$$

More commonly, this description is presented as a cumulative size distribution, where:

$$\text{Number of particles larger than diameter D per cm}^3 = \int_{D_l}^{D_u} ND^{-c}\ dD$$

$$= N \left[\frac{D_l^{-c+1}}{-c+1} \right]_{D_l}^{D_u}$$

$$= 312.9\ D^{-4.42}$$

These values for the concentration constant and slope (313 particles per cm^3 and 4.4 respectively) compare favorably with Coulter Counter values for deep ocean water found in the literature. McCave's (1975) summary of such values suggests a range of 2000 to 10,000 for the constant and a slope of 2.4 to 3.6 for water samples containing the entire particle population. If the organic fraction was removed, the effect would be to reduce the number concentration of particles and probably to steepen the slope of the distribution (increase the value), indicating a predominance of finer particles. Thus, the values obtained for the shape of the size distribution in this study seem reasonable.

Figure 7 is a plot of the number of particles larger than a certain diameter one may expect to find in a 30 ℓ sample of Canada Basin water. Recall that this plot includes the inorganic particles only. It can be seen that the hyperbolic distribution becomes unrealistic when the diameter becomes very small.

For an extrapolation such as the one just described to be confirmed, an independent observation is required. The most appropriate method in this case would be to analyze Canada Basin water samples with a Coulter Counter. Oxidizable organic matter would have to be removed prior to counting, and techniques for doing this have been attempted by Kranck (1975) and are in the experimental stage at O.S.U. using ozone digestion.

From the size distribution generated by these calculations, it

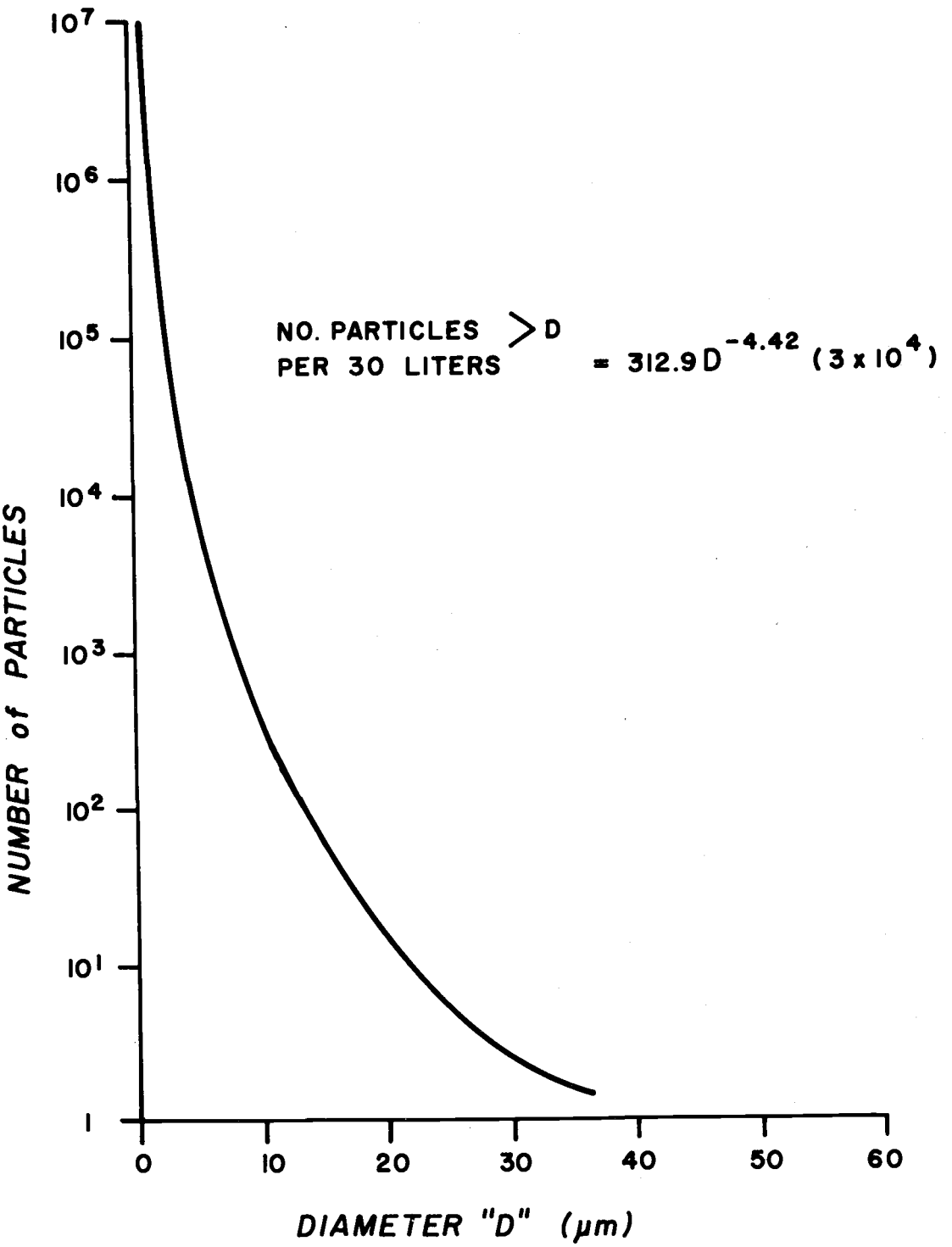

Figure 7. Number of particles to be expected in a 30 ℓ sample of Canada Basin water as a function of particle diameter. The size distribution has been derived from a mathematical model.

would be possible to estimate the mass flux to the seafloor by size class, as McCave has done in his theoretical treatment of the subject (1975). Another intriguing possibility for using these equations involves the assumption that the slope of the inorganic fraction is constant and about 4.4 for the Canada Basin. If this is the case, we could estimate the mass concentration of suspended inorganic particles going back in time by using the sediment accumulation rate determined with depth in a core in equation (5). The lack of sufficient resolution of the variability in sedimentation rate determinations precludes this exercise at the present.

A Final Note on the Model

One basic assumption of this size distribution model -- that the flux from suspension is governed primarily by Stokes settling of individual particles -- should be carefully scrutinized, since in many parts of the world ocean this is not the case. The proximity of very small particles to their source, such as diatoms in deep water sediments directly under zones of high productivity and the abundance of clay-sized mineral fragments in fecal pellets, argues that individual particle deposition may not be the only important process involved, but that some process of accelerated sinking (relative to Stokes settling) is also occurring (c.f. McCave, 1975, for an extensive bibliography of these arguments).

However, there is some justification for suggesting that accelerated sinking is not dominant in the Canada Basin. First, primary productivity is extremely low and most zooplankton activity

is limited to one or two months each year, the remainder of the time apparently being spent in some dormant stage (Hopkins, 1969). Hopkins has estimated the average zooplankton biomass for a region slightly to the northeast of this study and he found values of 0.62 μgm/ℓ , 0.14 μgm/ℓ , and 0.04 μgm/ℓ for Arctic surface, Atlantic, and Arctic deep waters respectively. Thus, the dry weight of zooplankton in the surface layers represents 10% or less of the total material in suspension. Assuming active fecal pellet production for only one or two months per year, it seems unlikely that zooplankton might process a significant portion of the suspended material into rapidly sinking fecal pellets.

The other evidence suggesting simple settling as a dominant process is the lack of identifiable fecal pellets or numerous large agglomerates during optical and scanning microscopy. The majority of particles observed are discreet grains of either diatoms or mineral fragments. It could still be argued, however, that the particles collected in a 30 ℓ sample of water bear little quantitative relation to the accumulation of sediment at the seafloor, and that the latter process is controlled by rapidly sinking and relatively large particles that are missed by sampling only 30 ℓ of water, a hypothesis proposed by McCave (1975) and supported by the size distribution model. Until a better understanding of deep ocean sedimentation processes is obtained, this size distribution model should be viewed as simply an academic exercise.

CHAPTER III. SUSPENDED PARTICULATE MATTER IN CONTINENTAL SHELF WATERS OFF OREGON

Introduction

The data presented in the following sections were collected during a cruise of R/V Yaquina in April of 1975 (Y7504C). The efforts were jointly sponsored by the Optical and Phytoplankton groups of O.S.U. Oceanography. The primary goal of the project was the characterization, in as many ways as possible, of suspended particulate matter at a typical continental shelf station along the northern Oregon coast. The sampling scheme included both temporal and spatial observations over a limited geographical area. Figure 8 is an index map to the sampling locations.

Measurements of in situ light attenuation, temperature, and conductivity were obtained. Water samples were analyzed for Coulter Counter size distributions and light scattering, and filtered for gravimetric analyses and determinations of particulate carbon and nitrogen. In addition, observations of wind and sea conditions were made and a "profiling" current meter was used to discern current motion with depth at several stations. Two across-shelf transects of stations were completed ranging in depth from 37 to 163 m, and two 36 hour anchor stations were occupied at 120 and 70 m for time-series measurements.

The aspects of the data that will be discussed in this study are the gravimetric analyses of filtered particulate matter, the relation between suspended particulates and light attenuation, and some features of the composition of the filtered particulates.

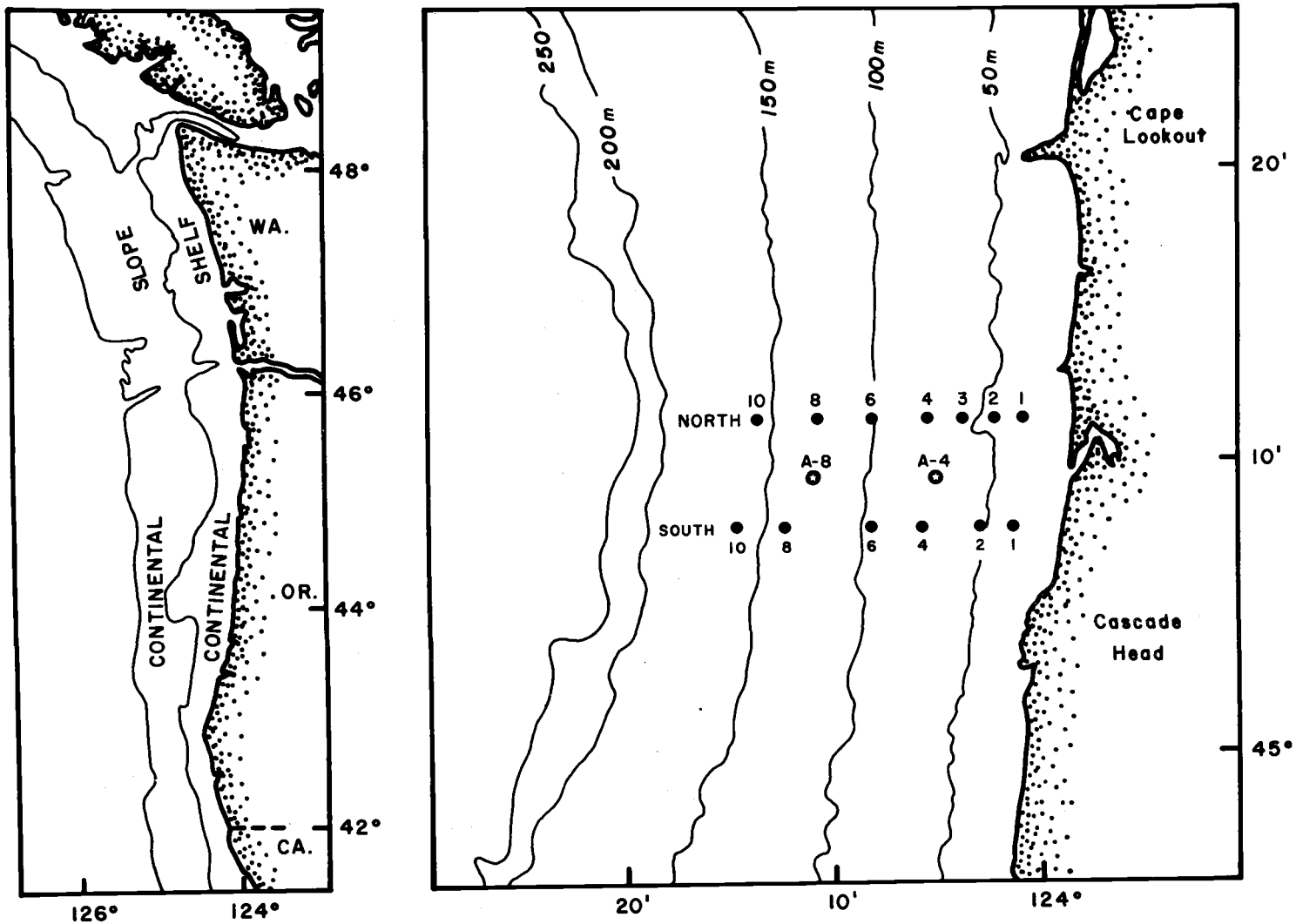

Figure 8. Index map to the northern Oregon continental shelf. Sampling locations for cruise Y7504C are indicated.

Previous work in any of the above areas is scarce for the Oregon continental shelf. Although numerous measurements of optical properties have been made by investigators at O.S.U., few relate to suspended particulate matter directly (c.f. Pak, 1969). Harlett (1972) obtained measurements of light transmission and near-bottom current velocities which were used to speculate on the transport of fine-grained material over the continental shelf (Harlett and Kulm, 1973; Komar et al., 1974).

Methods

Water Samples

Water samples were collected in 5 ℓ Niskin bottles. The Niskins were mounted in a rosette attached to the nephelometer package, which also included a CTD and pinger. They were tripped by command from the ship at various depths chosen for sampling. Three bottles per cast were available for filtration and the features chosen to sample were the seasonal pycnocline, the clearest water observed, and the bottom nepheloid layer. Occasionally, a turbid layer was observed at mid-depths, and attempts were made to sample this layer.

The shipboard display of data was the basis for deciding at which depths the Niskin bottles should be tripped. The resolution provided by this display was not as good as the simultaneously stored digital record. Hence, subsequent analysis of the digital records revealed that the "core" of a mid-depth turbid layer was never sampled, although several Niskins did sample the "flanks" of these features. In addition, it was discovered that several samples intended to come from the pycnocline actually came from the mixed layer.

The water was drained from the Niskins into plastic carboys and filtered immediately through 0.4 μm Nuclepore filters, using a vacuum apparatus. Sea salts were removed by a triple rinse with distilled water and the filters were stored in plastic PetriSlides. Subsequent treatment of the filters included removal of organic matter by hydrogen peroxide leaching and resuspension of the inorganic fraction for X-ray diffraction. These procedures are described in detail in Appendix IV.

Measurement of Beam Attenuation

The optical measurements were obtained with a beam transmissometer designed and built by Mr. Bob Bartz of the Optical group. The instrument projects and receives red light (wavelength 660 nm) over a folded one meter path, and provides a deck readout and digital record. Attenuation of this wavelength light is not significantly influenced by the presence of dissolved organic substances (yellow matter), and therefore is primarily the result of scattering by suspended particulates and attenuation by pure water (Jerlov, 1968). The parameter actually measured by the instrument is the ratio of the intensity of light received to the intensity of the light projected. The natural logarithm of this ratio is the beam attenuation coefficient.

X-Ray Diffraction

Planchets for X-ray diffraction were made by combining several resuspensions of the inorganic fractions into a single suspension and filtering it through a pressed silver planchet. The scheme used

to select filters for combining into a single X-ray sample was based on the original shipboard classification of the samples by water column feature. As already mentioned, subsequent analysis of the digital records revealed that this was not always the most correct classification. Unfortunately, the few samples correctly associated with the mid-depth turbid layer did not provide enough material for X-ray diffraction.

The planchets were run in untreated and ethylene glycol solvated condition. Solvation was accomplished at 60^{0} C for one hour in a saturated atmosphere. Instrument conditions were as follows: CuK radiation and a step scan of $.02^{0}$/step with a time constant of 4 sec.

Table VI provides pertinent information concerning the X-ray samples. An attempt was made to have the same amount of material on each X-ray mount, but differing recovery efficiencies for surface and deep samples during the resuspension process thwarted this attempt.

Other data

Particulate carbon and nitrogen values were provided by Mr. Dave Menzies of the Phytoplankton group and were obtained using a Carlo Ebba CHN analyzer. Volume concentration and size distribution values were provided by Mr. Jim Kitchen of the Optical group and were obtained using a Coulter Counter.

Results

Hydrographic Features

The data recorded for a typical station by the nephelometer

TABLE VI. DESCRIPTION OF X-RAY DIFFRACTION SAMPLES

Water column feature	X-ray ident.	Station	Filter	Mass recovered (mg)	Average recovery (%)	Planchet conc. (mg/cm^2)
Surface Group	4301	S1	24M	9.42	88	3.14
		N1	27M			
		A4-2	97P			
		A4-6	110P			
		A4-8	117P			
		A4-10	123P			
	4302	S6	14P	9.69	89	3.23
		S4	18P			
		N2	30P			
		A8-7	68P			
		A8-9	74P			
Clearest Layers	4303	S4	17C	10.45	100	3.48
		S2	20C			
		S1	22C			
		N2	29C			
		N4	35C			
		A4-2	96C			
		A4-4	103C			
Nepheloid Group	4304	A8-13	86C	11.63	99	3.88
		A4-6	109N			
		A4-8	116N			
		A4-10	122N			
	4305	A4-2	95C	11.81	99	3.94
		A4-4	102N			
		A4-8	114N			
		A4-10	121N			
	4306	A8-3	53N	14.67	95	4.89
		A8-5	59N			
		A8-9	72N			
		A8-11	78N			

Note: Letters after filter numbers indicate feature which was sampled: mixed layer (M), pycnocline (P), clearest layer (C), and nepheloid layer (N).

package are shown in Figure 9. This particular station is used to define the various features of the water column which will be continuously referred to during the following discussion. The "mixed layer" is about 15 m thick, except in the nearshore transect stations where it is not well defined. The "pycnocline" refers to the seasonal pycnocline that occurs simultaneously with steep gradients in temperature, salinity, and light transmission. A permanent pycnocline exists below the seasonal feature. The "clearest layers" denote the part of the water column in which light transmission is at a relative maximum. In the deeper stations, this background level of light transmission is fairly constant at about 60%, while in the shallower stations it drops to about 50%. Occasionally, a mid-depth turbid layer is present. (Although the terms "turbid" and "nepheloid" are synonymous, they will be retained here to distinguish between mid-depth and near-bottom features respectively.) Finally, at the bottom of the profile is the nepheloid layer, which includes that part of the light transmission profile where there is a decrease in percent transmission with increasing depth, after descending below a mid-depth "clear" region.

The nephelometer profiles did not extend to the seafloor and generally approached no closer than 10 to 15 m. In some of the records, there is evidence of clearer water immediately below the nepheloid layer and in others there appears to be a dramatic increase in turbidity as the seafloor is approached. This is the region of the benthic boundary layer, and it will require additional instrumentation before we understand all the phenomena associated with it.

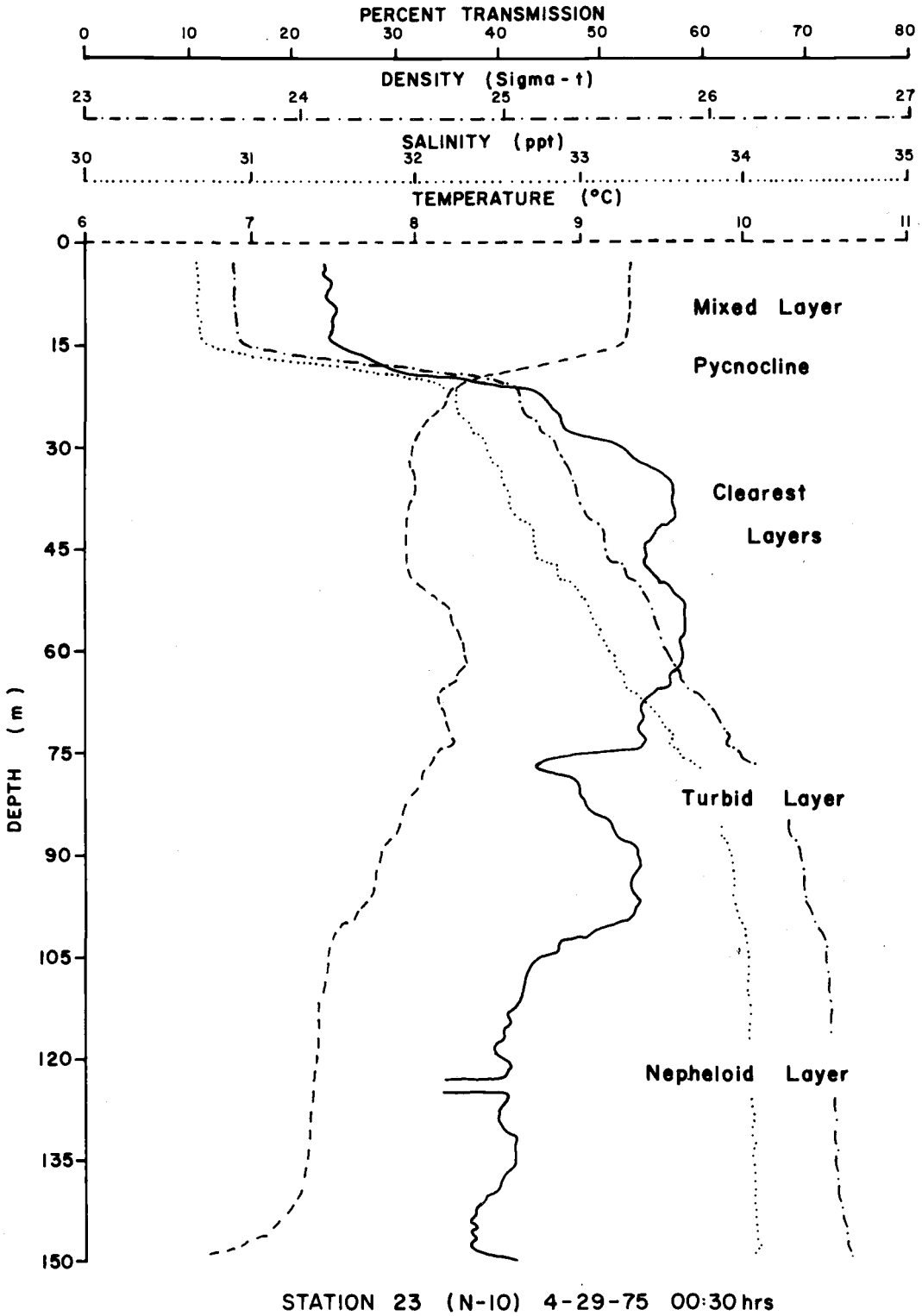

Figure 9. Example of data collected with the in situ nephelometer system. Terminology for the various optically-defined features is presented also.

Two other hydrographic features of the stations which should be noted are a warm water temperature anomally occurring about mid-depth in the deeper profiles (between about 50 and 80 m in Figure 9), and the permanent pycnocline (between about 20 and 80 m in Figure 9). Both of these features have implications involving upwelling. It has been demonstrated that the isopycnals along the base of the permanent pycnocline become inclined towards the coast during upwelling conditions, and that the warm water anomaly may represent relatively salty and warm surface water which is descending seaward along the inclined frontal layer (Mooers et al. 1976). At nearly all stations more than 4 nautical miles offshore (depths greater than 70 m) some decrease in light transmission corresponds to the base of this warm anomaly. In the study by Pak (1970) of the Columbia River plume, a correlation between warm water anomalies and increased light scattering is observed also (see Pak's Figures 2 and 6).

A comparison of near-bottom temperatures as a function of time suggests that relatively cold and salty water began to appear at Station A8 during the sampling period (see Figure 21). The observation fits the "two-celled" model of upwelling described by Mooers et al. (1976) very well and may be water advected from continental slope depths in a shoreward direction. However, the possibility of water being advected in an alongshore direction cannot be excluded at present. A change in the intensity of the nepheloid layer accompanies this change in bottom water character also, as is shown in Figure 21.

Gravimetric Analyses

Total suspended mass ranged from 126 to 2028 μgm/ℓ , with both the highest single value and greatest mean value occurring in the mixed layer samples. The order of decreasing mean TSM values is then nepheloid group, pycnocline group, and clearest layers. The TSM expected for a mid-depth turbid layer is estimated from light transmission records to be about the same as those values found in the nepheloid layer. The portion of TSM which was oxidizable was also highest in the mixed layer samples, averaging about 32%. The mean percent organic matter decreased in an almost linear fashion with an increase in depth, however, reaching a value of 14% for the nepheloid samples. There is the distinct possibility that the organic matter determined for the surface group of samples may be too low, since some of the rather fluid protoplasm of living cells may pass through Nuclepore filters. Laboratory experiments have revealed that these filters retain phytoplankton with varying efficiencies (P. Donaghay, personal communication).

Figure 10 summarizes the data for all stations. It is a composite of both transect and anchor stations and represents a geographical region about 9 nautical miles (E-W) by 4 nautical miles (N-S), ranging in depth from 37 to 163 m, during upwelling conditions for about three days in April, 1975. The characteristic light transmission value for each feature is included also and the high degree of correlation between percent transmission and TSM is immediately obvious.

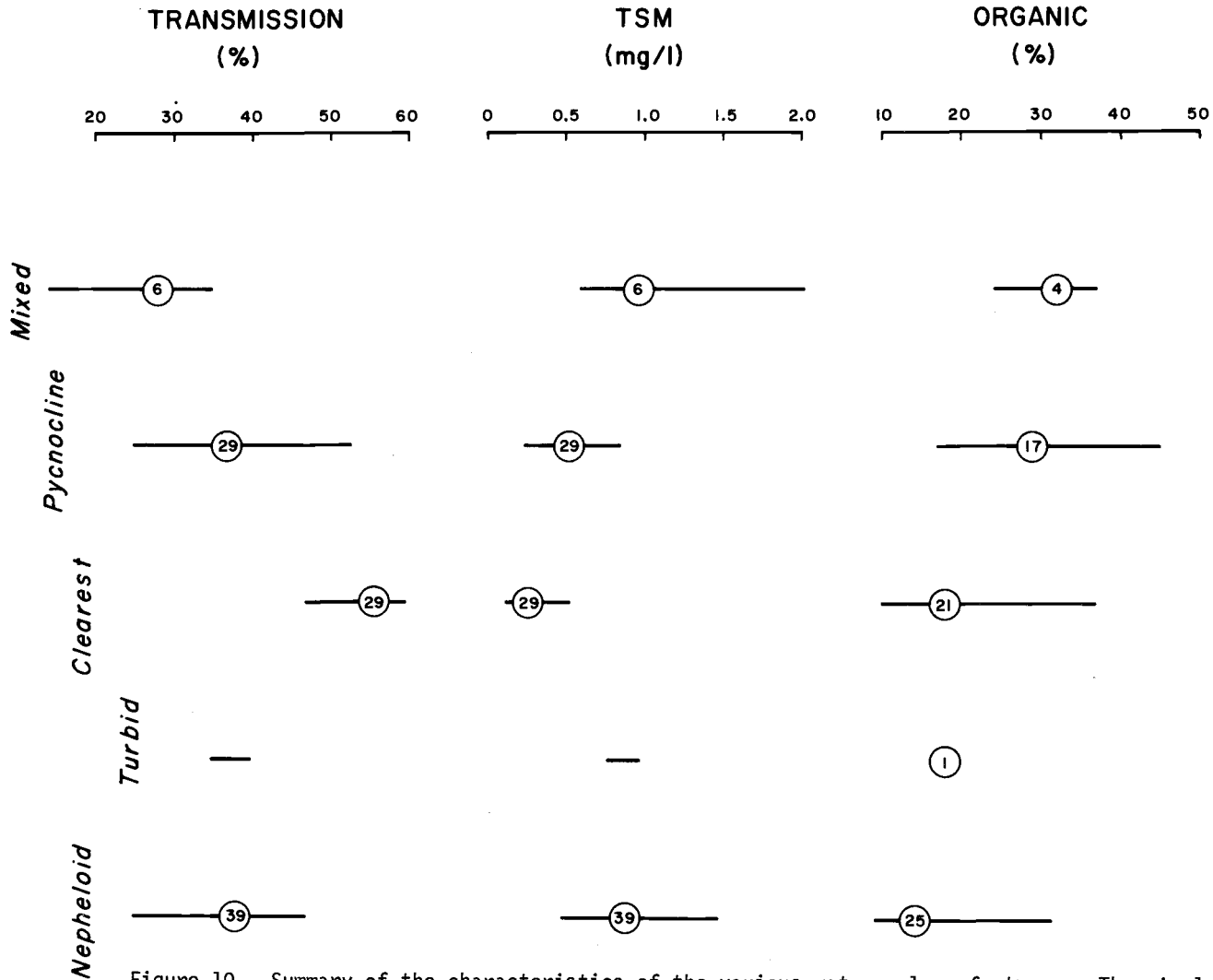

Figure 10. Summary of the characteristics of the various water column features. The circle centers indicate the mean value of the parameter and the enclosed number is the number of data points. The horizontal line indicates the range of observed values.

Particle Volume Concentrations

These measurements are tabulated in Appendix II. An "apparent" particle density (or wet bulk density) may be calculated by dividing TSM by volume concentration and a scatter plot of this relationship is shown in Figure 11. The range of densities for materials to be expected in the marine environment is from near 1 gm/cm^3 for plankton to about 3 gm/cm^3 for some clay minerals. Most non-living particles fall in the range 2 to 2.7 gm/cm^3. If the particulate matter is in an aggregate form, the apparent density may be around 1.5 (McCave, 1975).

As can be seen in the scatter plot, considerable variability exists for this data, with some obviously unrealistic values. These anomalous densities are probably the result of measurement discrepancies such as protoplasm being missed by filtration but recorded by the Coulter Counter. In addition, the Coulter Counter records the total volume of particles in their natural, suspended state, while gravimetric analysis records only dry weight. Both of these effects would lead to low apparent densities. An explanation for the anomalous high values is that the Coulter Counter does not record a certain size class of the material recovered by filtration, since the lower detection limit of the instrument was about 2-3 μm for this data. The filters should have retained all material larger than 0.4 μm. This would result in anomalously high density values. The relationship between suspended mass and beam attenuation (natural log of transmission) will reveal more evidence for this sampling discrepancy.

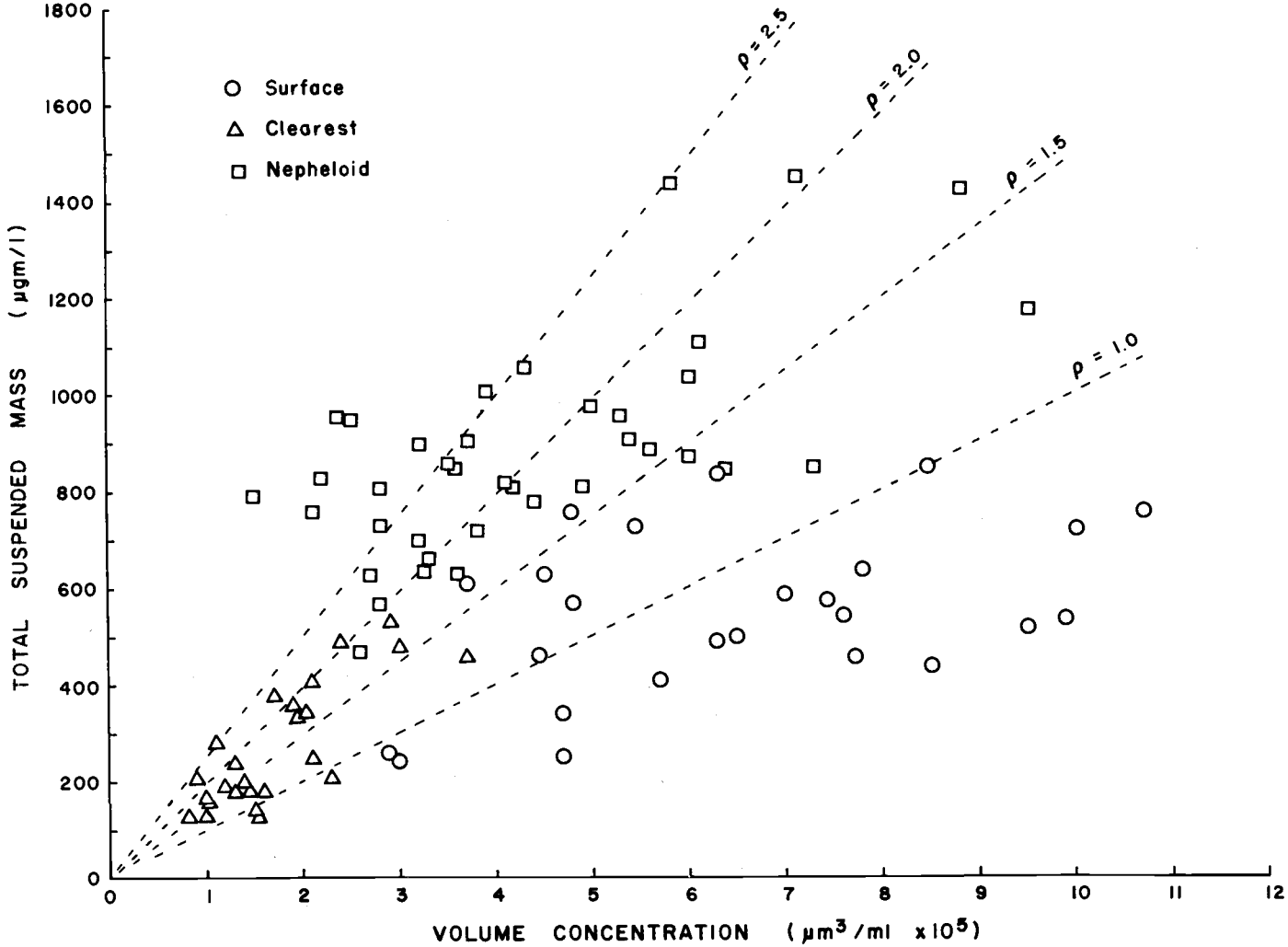

Figure 11. Relation between TSM and volume concentration showing apparent particle density (wet bulk density). Dashed lines represent densities of materials common in the marine environment.

Carbon and Nitrogen Values

Particulate carbon and nitrogen values are listed in Appendix II and are included for comparison with the percent organic matter determined by hydrogen peroxide leaching of filtered samples, which at present is an untested laboratory technique. The ratio C/N increased with depth, as has been observed in many studies (c.f. Gordon, 1971; Riley, 1970, for summary of recent literature). Values in the mixed and pycnocline layers averaged about 8, in the clearest layers about 11, and in the nepheloid layer about 12, although a considerably larger range of values was observed in this group compared to the others, with extreme values of 7 to 22 encountered.

While many investigations have sought to relate particulate carbon (PC) with organic matter by a simple factor, the consistency of results leaves much to be desired. The data from this study are plotted in Figure 12 and the lack of consistency is again encountered. If all PC is assumed to be in the form of oxidizable organic matter, a ratio of just over 1:1 is suggested for many of the data points. This is lower than the 2.8 value given for organic matter in surface sediment by Redfield (1963).

The aforementioned assumption is probably the main source of error in this type of analysis. Linear regression of the data by depth groups reveals that none of the groups yields a significant regression between PC and organic matter. They all produce regressions with positive PC intercepts when organic matter equals zero, however, which indicates a source of PC other than oxidizable organic matter. Hydrogen peroxide leaching of suspended particulate matter

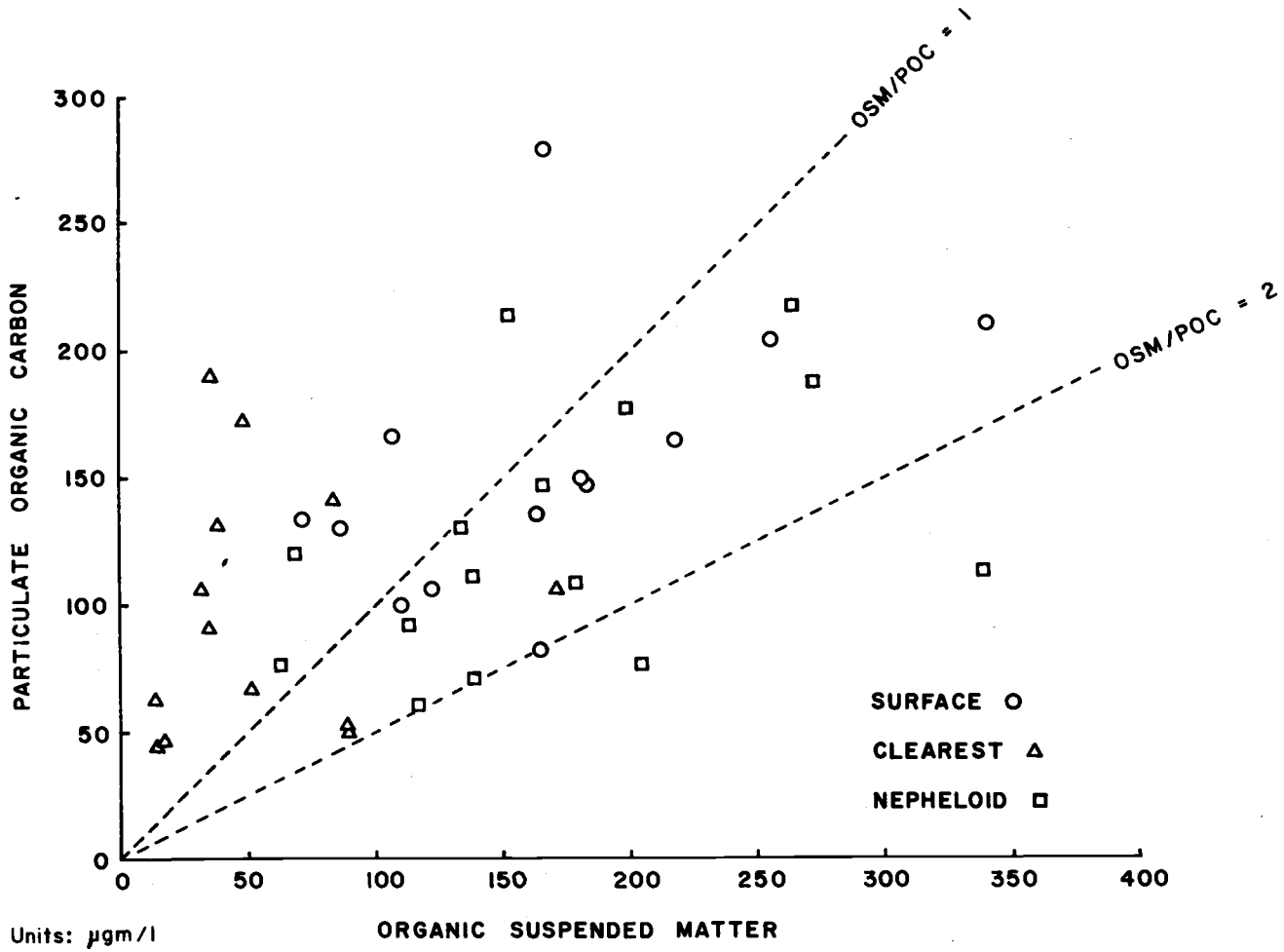

Figure 12. Relation between particulate organic carbon and oxidizable organic matter. The ratio OSM/POC is often reported to be about 2 for marine plankton but it is obviously quite variable in the continental shelf environment. Note the consistent grouping of the clearest layer data points.

may not affect carbon which is present as woody fibers, chiton, or industrial pollutants, yet these forms of carbon would tend to be measured by the high temperature combustion process of the CHN analyzer.

It might be significant that of the data points that are most anomalous in Figure 12 the majority come from the clearest layers in the water column. This suggests something other than random measurement error.

Similar attempts to relate particulate nitrogen to organic matter were unproductive and will not be pursued here. Any attempt to relate organic matter to other elements of biological importance will have to use more sophisticated techniques, since it is imperative to resolve the different classes of organic compounds -- even if only into "natural" and "manmade" categories -- before an understanding of the roles natural organic particles play in the sedimentological cycle will be attained.

X-Ray Mineralogy

The diffractograms of the six sample mounts are presented in Figure 13. They reveal an essentially homogeneous mineralogy for all samples, consisting of quartz, feldspars, illite, and chlorite. No expandable component is obvious. The lack of detection of carbonates and smectites is not unequivocal evidence for their absence in the water column, however. Carbonates may have been removed during peroxide leaching of organic material, although they are thought to be a negligible portion of the suspended material. The surface concentration of material on the X-ray planchet was about 3 to 5 mg/cm^2,

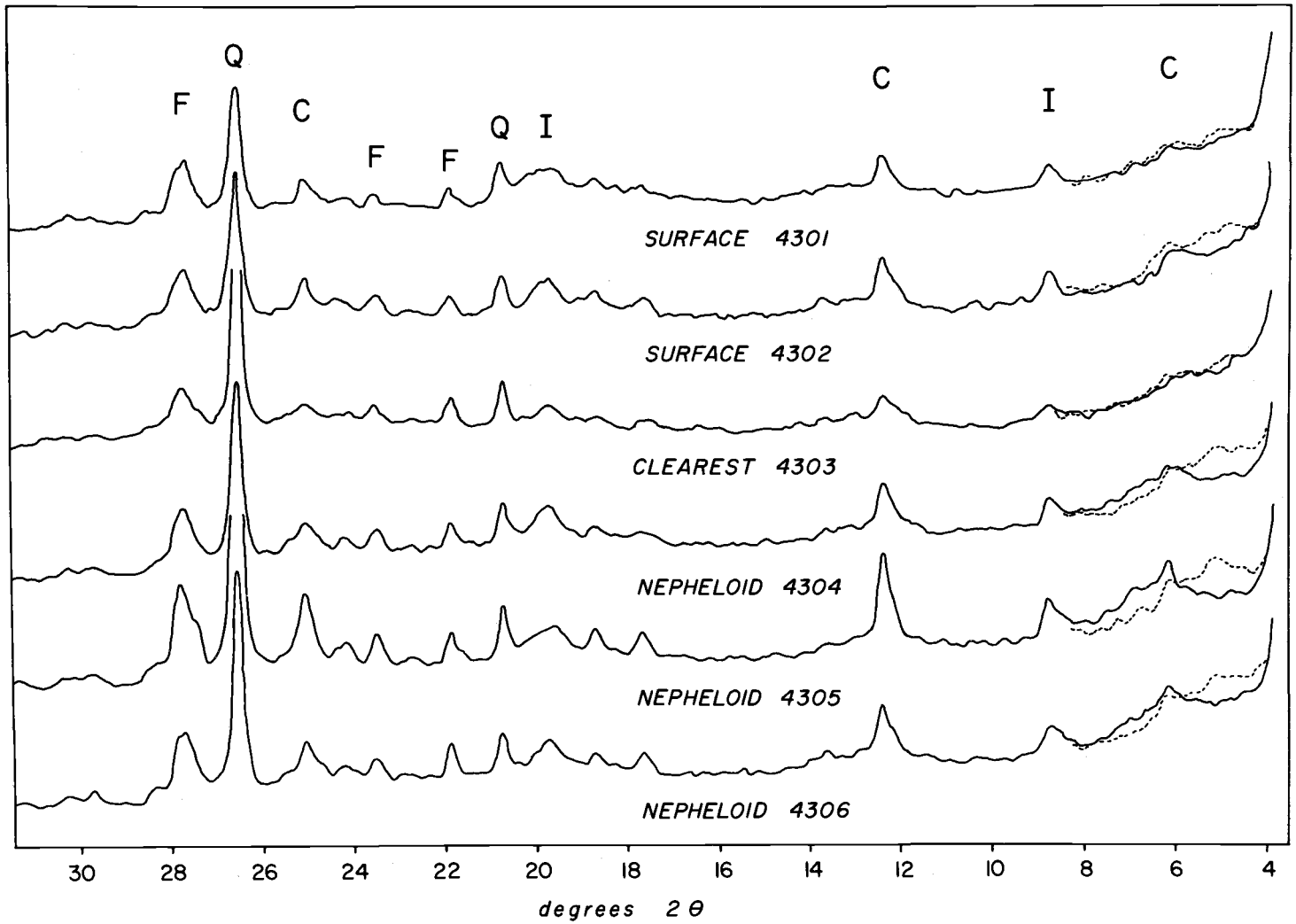

Figure 13. X-ray diffractograms of suspended particulate matter. Minerals are identified as follows: feldspar (F), quartz (Q), chlorite (C), and illite (I). The dotted line indicates the change in diffractogram after ethylene glycol solvation.

well above the 1.6 mg/cm^2 limit described by Tucholke (1974) below which an artificial depletion of smectites might be observed. It should be noted, however, that Tucholke's work dealt with samples of clay minerals only, and that the material in this study includes admixtures of other materials. Another consideration is that smectites, due to their fine-grained nature, may have been selectively missed during filtration at 0.4 μm, although it is unlikely that this loss would be significant either in terms of mass or effect on X-ray diffraction.

The diffractograms reveal no substantive differences in mineralogy among the water column features. This implies that either the suspended particle population becomes well mixed very quickly in shelf waters or that the mineralogies of the various sources for the suspended material are the same. Unfortunately, the minerals identified in the diffractograms are nearly ubiquitous in mid-latitude marine environments and provide no reliable tracers for particle sources. The single fine-grained mineral which may be used as a source indicator in this region is montmorillonite and it reflects a Columbia River source. Baker (1973a; 1976) has used montmorillonite in suspended material to trace the northwestward transport of particles from the Columbia down canyons on Nitinat Fan. R. Karlin and L. D. Kulm (1977, unpublished research at O.S.U.) have summarized the distribution of clay minerals in surface sediments on the slope and abyssal plains off the Pacific Northwest coast. They demonstrate the dispersal of Columbia River sediment by the montmorillonite pattern also, although it is not certain that the trends they depict

reflect only modern dispersal dynamics. Surface sediment clay mineralogy on the continental shelf has not yet been compiled and the work is in progress at O.S.U.

Although the relatively warm, fresh water of the Columbia River plume flows southward at the surface to the region of sampling in this study, its major axis (as defined by light scattering) is somewhat seaward of the shelf and is located over the continental slope (Pak, 1970). Whether or not this plume is a major source for the suspended matter observed in shelf waters today is uncertain from the mineralogical data. On the basis of discharge alone, the Columbia delivers much more material than any other Oregon coastal river to the continental shelf (Curtis et al., 1973).

R. Karlin and L. D. Kulm in their work postulate a southern source for some of the clay minerals observed on the Pacific Northwest borderland. They note that the discharges of Northern California rivers are considerably larger than the Oregon rivers and that the clay mineralogy of their suspended loads is the same as that observed in surface sediments off Oregon although the proportions of various minerals may vary significantly.

Northward transport of particles from more southerly latitudes is quite possible by means of the Davidson Current -- a northward flow along the continental slope which, during the summer months, includes deep, northward motion along the shelf also (Huyer et al., 1975). Presumably, this water could be dragged onshore during upwelling conditions to act as a source of particulate matter. This material may not be depositionally important, however, and may be

just passing through with the advected water.

Considering the high energy environment of the Oregon shelf, it seems very likely that resuspended seafloor sediment is the source of a significant portion of the material observed in suspension. All depths along the shelf are affected by storm waves at some time or another, and the strong vertical mixing associated with upwelling events would surely help to distribute resuspended material at certain times of the year. While it is unlikely that suspended particle mineralogy will be the clue to learning the source of the material, studies involving the processes at work at the benthic boundary layer and the distribution of suspended mass in relation to the current field will accomplish this goal.

Discussion

Introduction to Beam Attenuation and Suspended Particulates

More and more frequently reports of correlation between optical properties and suspended particulate matter are appearing in the literature (c.f. Baker, 1976; Biscaye and Eittreim, 1974; Owen, 1974; Eittreim and Ewing, 1972; Plank et al., 1972; Carder et al., 1971; Maksimov and Shlafman, 1970). In most cases, the approach is strictly empirical, with little effort devoted to explaining the physical significance between the measured optical property and the suspended particles. For obvious logistical reasons, it would be very desirable for sedimentologists to be able to determine the amount of suspended particulate matter by an *in situ* profiling instrument as opposed to the laborious and time-consuming methods of water sampling

and filtration or Coulter counting.

The next two sections will demonstrate just how precise prediction of total suspended mass can be and will attempt to provide some insight as to the physical significance of the optical measurement. For the reader's convenience, a brief summary of beam attenuation in seawater is presented first and is condensed from a chapter in Jerlov (1968 or 1976).

The total beam attenuation coefficient (c) is defined as the sum of light intensity loss over a given distance in seawater due to the combined effects of scattering and absorption of the light beam -- both by water itself and by suspended particulate matter. Scattering and absorption by particle-free water may be considered constant for wavelengths in the visible spectrum, being unaffected by changes in salinity and temperature. For red light with a wavelength of 660 nm (the wavelength of the light source of the O.S.U. instrument), absorption due to dissolved organic substances (yellow matter) is negligible. These essentially constant components of the beam attenuation coefficient sum to a value estimated to be between 0.33 m^{-1} and 0.43 m^{-1} (see Tyler et al., 1974, for summary of beam attenuation coefficients for particle-free water).

Therefore, the primary influence affecting the beam attenuation coefficient in seawater containing at least moderate numbers of particles is the variability introduced by scattering and absorption by suspended particulate matter. A combination of particulate parameters -- number, size, and composition -- is the source of this variability. The coefficients observed throughout this investigation

varied from about 0.5 to 2.0 m^{-1}; hence, if particle-free seawater accounts for 0.4 m^{-1}, the contribution by particles ranges from 0.1 to 1.6 m^{-1}.

If the slope of the particle size distribution is constant, the relationship between beam attenuation and number of particles will be linear, provided that the scattering efficiency of the particles is the same in all size classes (Zaneveld, 1973). This holds for lithogenous particles larger than about 2 μm and organic particles larger than about 7 μm. Particles smaller than these diameters exhibit reduced scattering efficiencies, which may cause a departure from linearity (see Beardsley et al., 1970, for discussion of scattering efficiency). The number of particles may be expressed in terms of number, mass, or volume concentrations. A laboratory experiment by Gossé (1974) demonstrates linearity for quartz particles of various size classes. The main influences on scattering efficiency are the size, index of refraction, and absorption of each particle. Particle density becomes a consideration as well if attenuation is being related to some other variable involving mass measurements.

It is apparent that the attenuation coefficient in seawater cannot be precisely explained by a single particle parameter, such as mass or volume concentration, unless the other parameters of the particle population are constant throughout the region of sampling. This is seldom the case in the ocean where wide variations in particle characteristics exist in both vertical and horizontal directions. Therefore, any relationship between observations of attenuation and suspended particulate matter is at best an average, and the variability

observed about that relationship is a measure of the heterogeneous nature of the particle population, i.e., the variability in the number of particles, their size distribution, and their composition.

Beam Attenuation and Total Suspended Mass

The Oregon suspended matter data have been divided into three groups for regression analysis. The few samples from the mixed layer have been included with those from the pycnocline to form a surface group, and the "turbid layer" samples have been combined with the nepheloid layer samples to form a nepheloid group.

The results of linear regression on each group are presented in Figure 14. The most striking difference observed is the increased variability about regression for the surface group compared with the others. Numerous possibilities exist to explain this, such as sampling error in the collection of simultaneous data in regions of steep gradients, the effect on c due to refraction of light from the transmitted beam in regions of steep density gradients, and a greater variability in c because of increased "patchiness" of particles of varying composition, size distribution, etc. None of these possibilities seems to be the prime cause, however, since they should produce the same variability in regressions of c on volume concentration and this variability is not apparent (see Figure 16).

The best explanation may be the lack of detection of some suspended mass in a few of the samples, due to reduced filtering efficiency in surface water. Evidence for this is the unrealistically low "apparent" density for several samples from the surface group

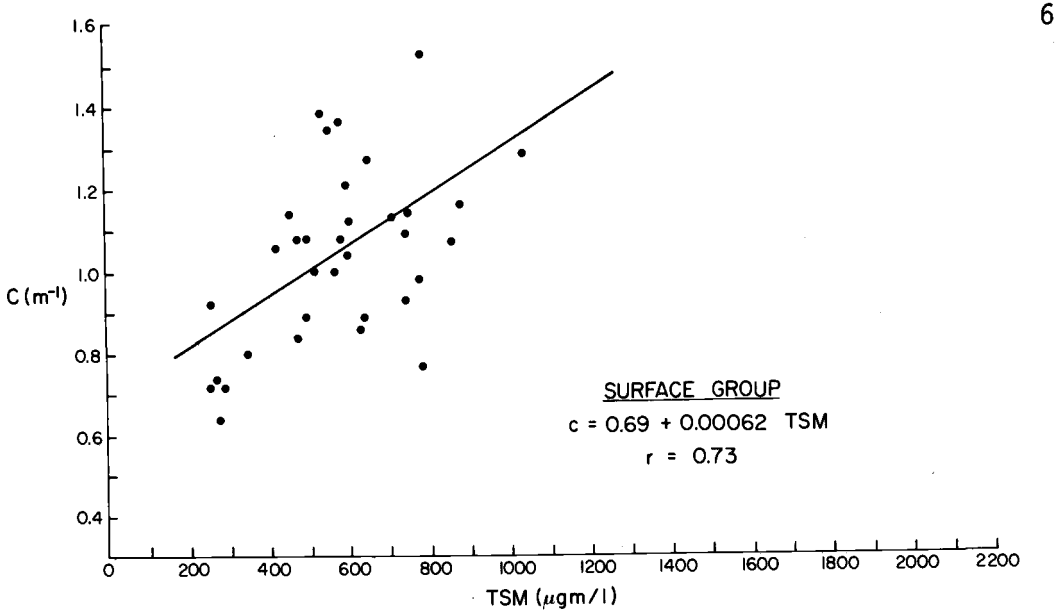

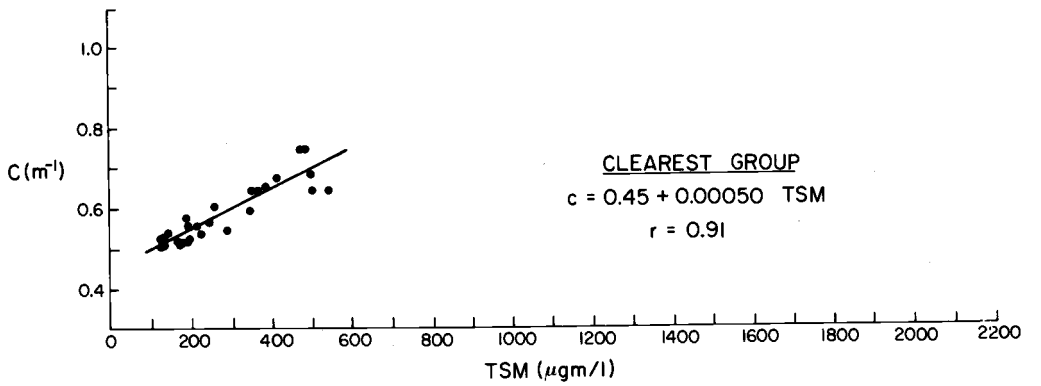

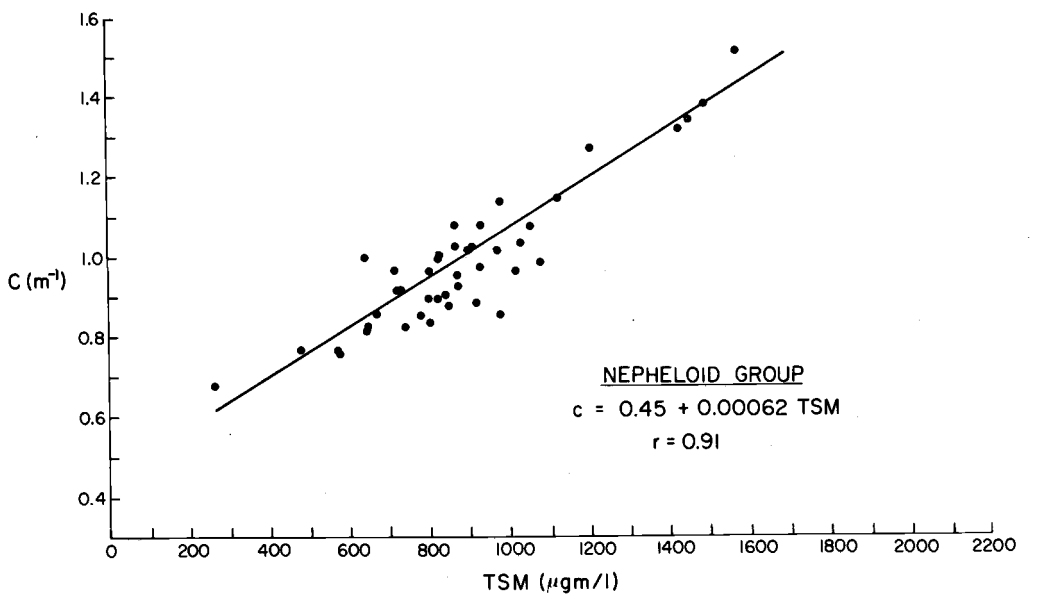

Figure 14. Scatter plots and regression lines for beam attenuation (c) as a function of TSM.

(refer to Figure 11). Some particulate matter has probably not been collected and weighed during filtering that has been recorded as volume by the Coulter Counter, resulting in the low density values. The alternative -- recording too great a volume -- is less likely, since we should then observe increased variability in the regression of c on volume concentration. We can visualize this by assuming that much of the material in suspension in the surface layers is protoplasm and that this fairly fluid material may be sucked through the filter during vacuum filtration. Roth et al. (1975) show photomicrographs of collapsed coccolithospheres on membrane filters and point out the uncertainty of whether or not some protoplasm may have been removed during filtration. The amount not collected would vary from sample to sample and would result in an increased variance in the regression of c on TSM. Unpublished research by the O.S.U. Phytoplankton group (P. Donaghay, personal communication) demonstrates that Nuclepore filters are the least efficient collectors of plankton compared to other types of membrane filters. Whereas glass fiber membranes retained about 97% of the organic material in test samples, Nuclepore filters retained only 70 to 90% with considerable variability.

The hypothesis of material being missed by filtration can be tested to a limited degree by removing those surface samples with "apparent" densities of less than 1.0 gm/cm^3 from the data for regression. When this is done, the regression becomes more comparable to the deeper groups with respect to the zero TSM intercept and also develops a slightly steeper slope -- a reflection of the true decrease

in average particle density in surface waters (Figure 15a). The variability about regression is also significantly reduced. Removing these data points from the regression of c on volume concentration does not change that regression appreciably (Figure 15b).

The regressions for the clearest and nepheloid groups seem very similar. The slope of the line for the clearest group is somewhat less than that for the nepheloid group but the regression is based on a limited range of TSM values, which would tend to decrease the reliability of the calculated slope. In fact, 95% confidence intervals on the true slope for each group overlap (Snedecor and Cochran, 1967, page 158).

Note that the zero TSM intercepts for the clearest and nepheloid groups are the same and have a value of c equal to 0.45 m^{-1}. The intercept of the surface group approaches that value also as the anomalous low density data points are removed. In addition, the regressions of c on volume concentration indicate this value for the zero particle intercept (refer to Figure 16). Recalling that the accepted value for particle-free seawater is between 0.33 and 0.43 m^{-1} for this nephelometer, we may speculate on the source of this small discrepancy. One possible explanation is a dissolved component which increases attenuation. Dissolved organic matter may affect attenuation at some wavelengths but the influence should not exceed 0.01 m^{-1} for this instrument, even in organic-rich coastal waters (Jerlov, 1968). A second possibility is that a constant amount of the suspended load was not measured by filtration. If this were true, between 60 and 200 $\mu gm/\ell$ of material (presumably smaller than 0.4 μm) would have to

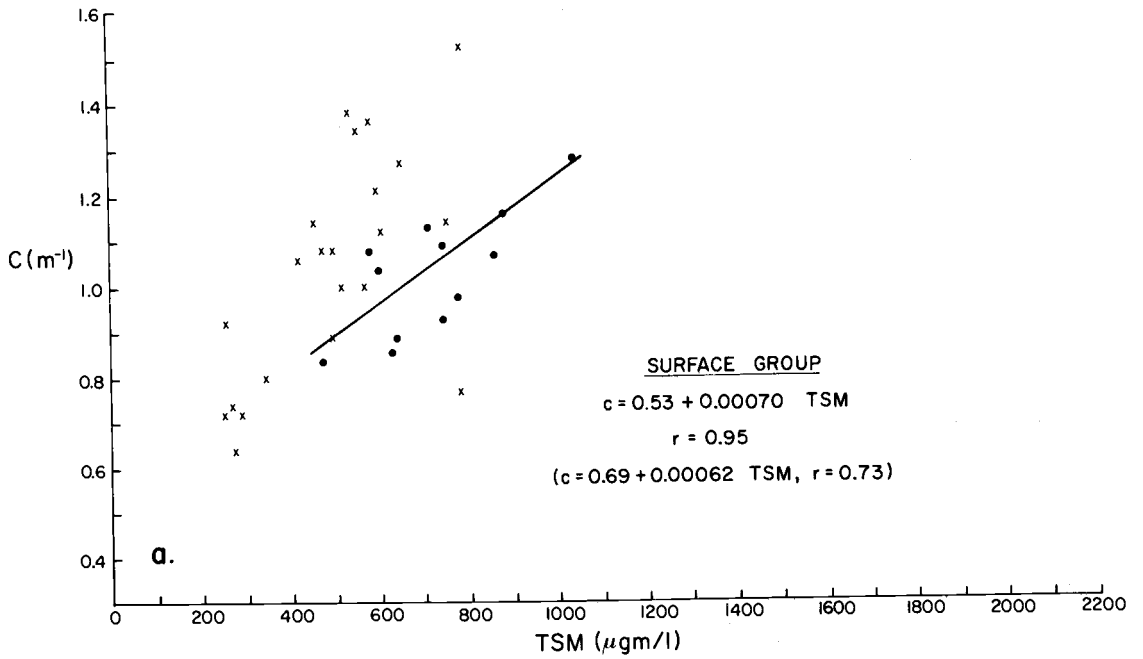

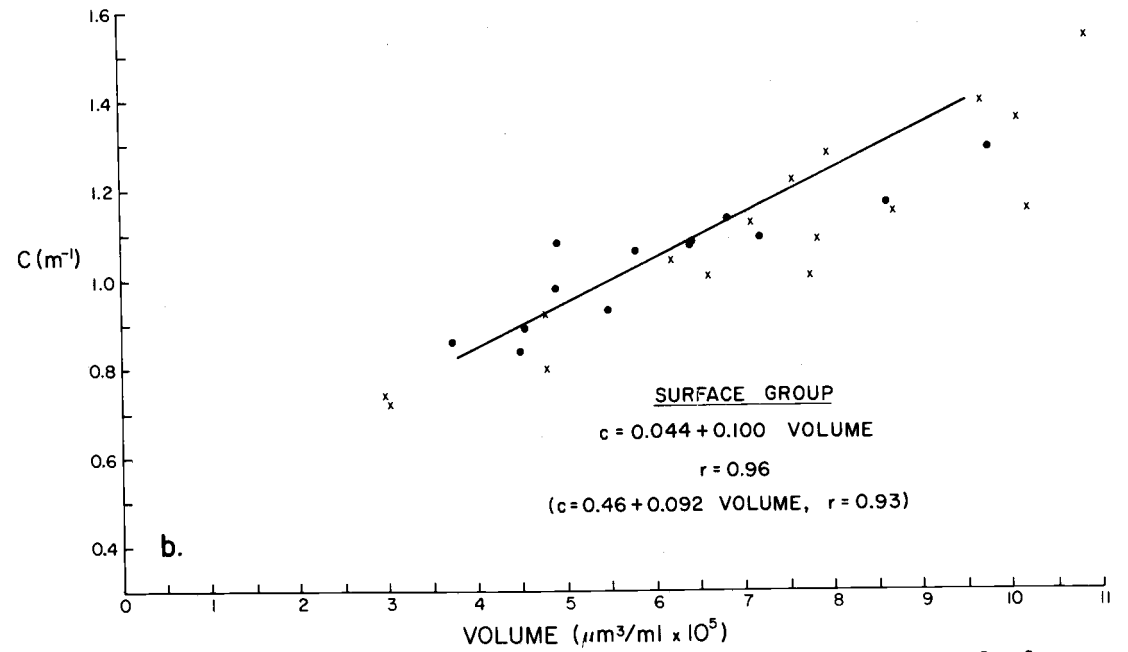

Figure 15. Effect on surface group regressions due to removal of data points with low apparent densities ($\rho < 1.0$ gm/cm^3). "x" indicates a deleted data point. The equations in parentheses represent the original complete set of data.

pass through the filter for each sample and a constant volume would also have to be missed -- a coincidence which seems unlikely. Even if a great number of these very small particles was present, their contribution to attenuation might be relatively small since sub-micrometer lithogenous particles become inefficient scatterers compared to those larger than about 2 μm (c.f. Beardsley et al., 1970). Finally, the offset could be due to instrument design or error in the published values for particle-free water.

It seems reasonable to conclude that the regression of c on TSM for surface water is not nearly as reliable as the regressions for samples taken from below the pycnocline. This is the result of varying filtering efficiencies, perhaps due to increased protoplasm in the water.

Beam Attenuation and Volume Concentration

The same data groups were used for regressions of c on volume concentrations and the results are shown in Figure 16. While the variability about the regressions lines seems comparable in each group, the intercept and slope of the nepheloid group appear different from the two shallower groups. Once again, we look to the technique used to measure the particles for an explanation, since the variability is not observed in the corresponding regressions of c on TSM (refer to Figure 14). The Coulter Counter has a lower detection limit of 2 to 3 μm. Assuming that an appreciable number of the suspended particles in the nepheloid layer is in the size range 0.4 to 3 μm, the measured volume concentrations would be too low. This would

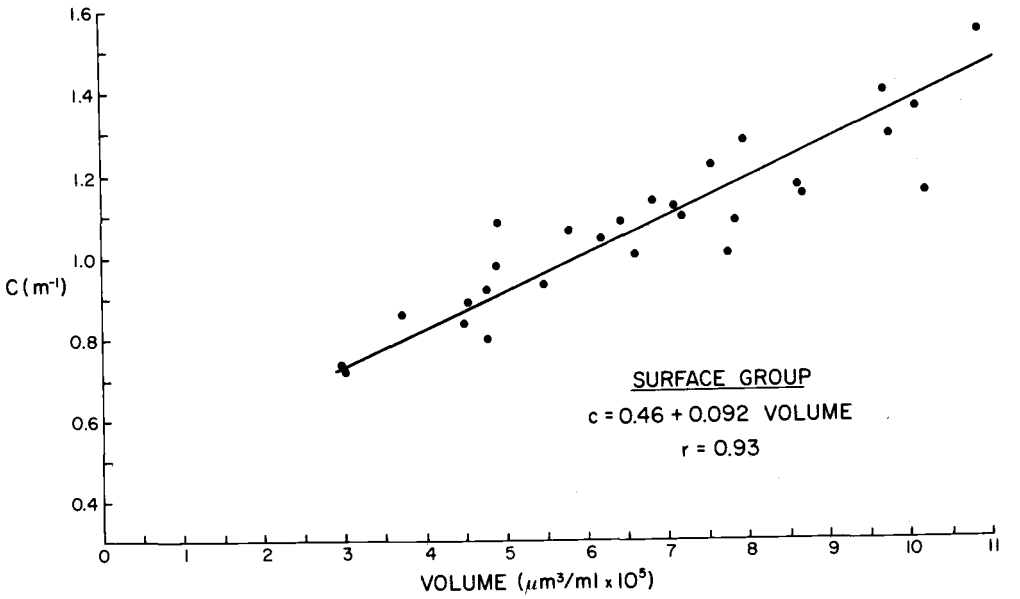

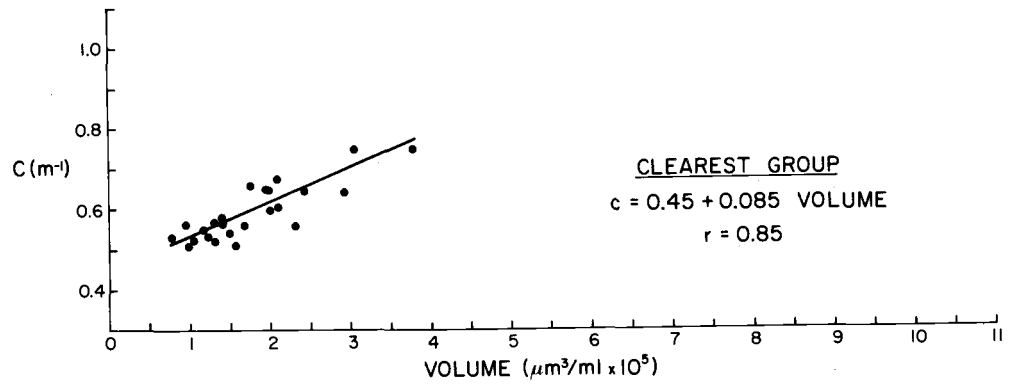

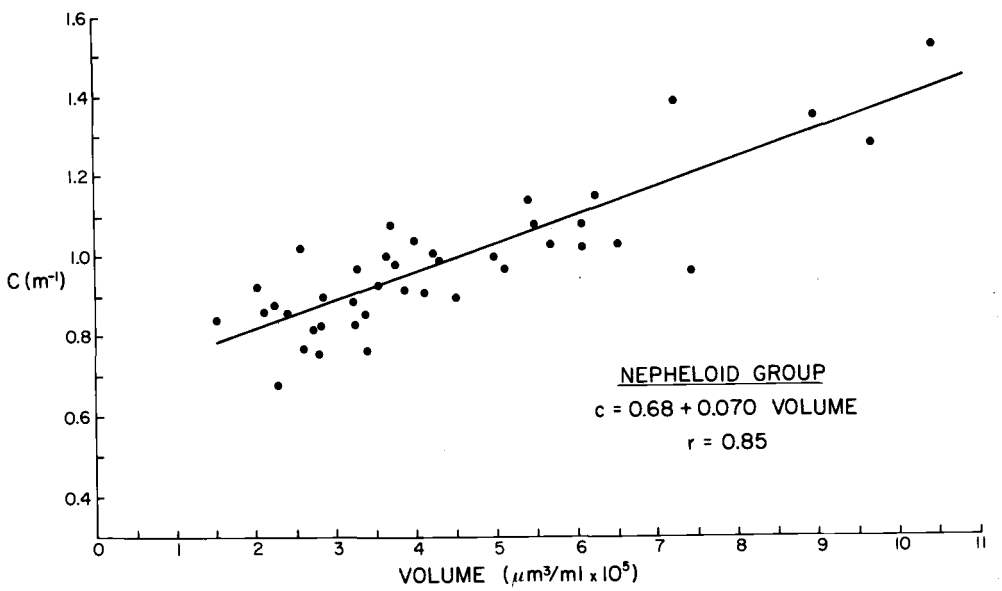

Figure 16. Scatter plots and regression lines for beam attenuation (c) as a function of volume concentration.

result in unusually high "apparent" densities for the particles, since filtering at 0.4 μm would collect these particles. Inspection of Figure 11 again reveals several nepheloid samples which do have unrealistically high densities. Based on the mineralogy observed in the X-ray diffractograms, only chlorite and illite may have densities approaching 3 gm/cm^3, with the other mineral components being about 2.6. Certainly the 14% organic matter in the nepheloid samples should tend to produce a lower average density also.

If we remove those samples with densities of 3 gm/cm^3 or greater from the data set, the regression of c on volume produces a lower intercept and steeper slope. Such removal makes the regression more comparable to the surface and clearest groups (Figure 17a). Removal of these samples from the corresponding regression of c on TSM produces essentially no change in that line (Figure 17b). Hence, it seems reasonable to conclude that the regression presented here for the nepheloid group does not provide the most accurate information due to the omission of a group of particles smaller than about 3 μm (but larger than 0.4 μm) from the volume concentration values.

Predicting TSM from Measurements of Attenuation

Variability of the total attenuation coefficient is primarily a function of the number of suspended particulates present. If the composition remains constant in all size classes, the relation of c to number of particles is linear. It can be seen from the scatter plots in Figure 14 that the relation is reasonably linear in the clearest and nepheloid groups and about the same for those two groups.

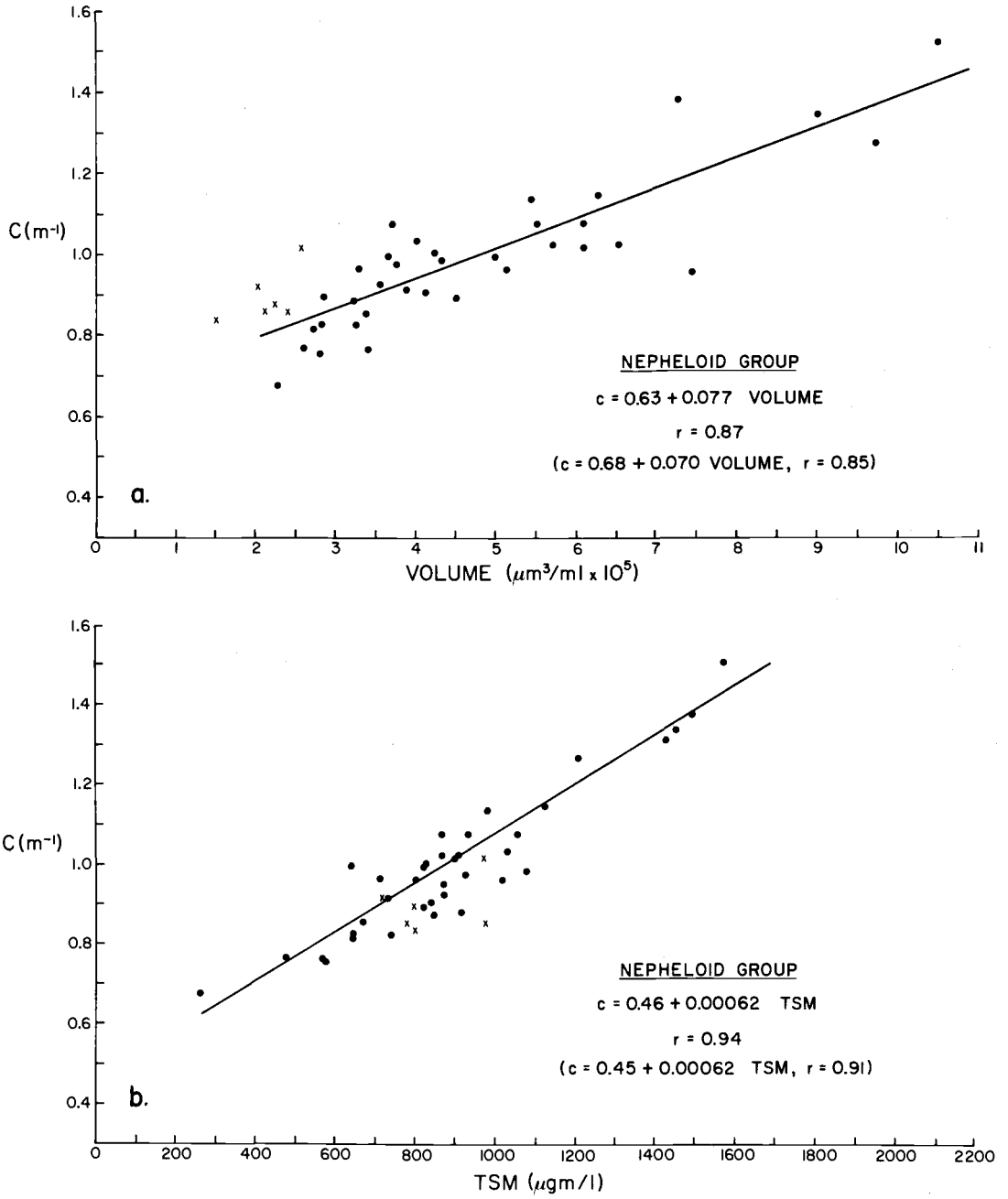

Figure 17. Effect on nepheloid group regressions due to removal of data points with high apparent densities ($\rho \geq 3.0$ gm/cm^3). "x" indicates a deleted data point. The equations in parentheses represent the original complete set of data.

The suggestion is that the composition and size distribution slope are nearly constant for these groups. This is not strictly true, of course, but the differences do not seem to have a great enough influence on c to cause serious difficulties with using a linear approximation to predict TSM from attenuation.

Figure 18 shows the 95% confidence intervals for a predicted mean value of TSM for any given observation of c. The regressions for the clearest and nepheloid groups are the same as those presented in Figure 14. The regression for the surface group is somewhat speculative, being based on the assumption that the particle-free intercept is 0.45 m^{-1}. Data points with "apparent" densities less than 1.0 gm/cm^3 have also been eliminated. The resulting equation will have to suffice until a better method to measure the mass of suspended material in surface waters is devised. A graph of the uncertainty of a predicted mean value for TSM (95% confidence interval) is presented in Figure 19. It was constructed from the regressions in Figure 18.

Conversion of Attenuation Profiles to Suspended Mass

Having established relations between beam attenuation and total suspended mass which have relatively low levels of uncertainty in the prediction of TSM from c (Figure 19), it is possible to convert all the optical profiles from the cruise to suspended mass profiles. It has been shown that particle populations of different compositions will produce correspondingly different regression equations, and *a priori*, a separate regression has been calculated for the various

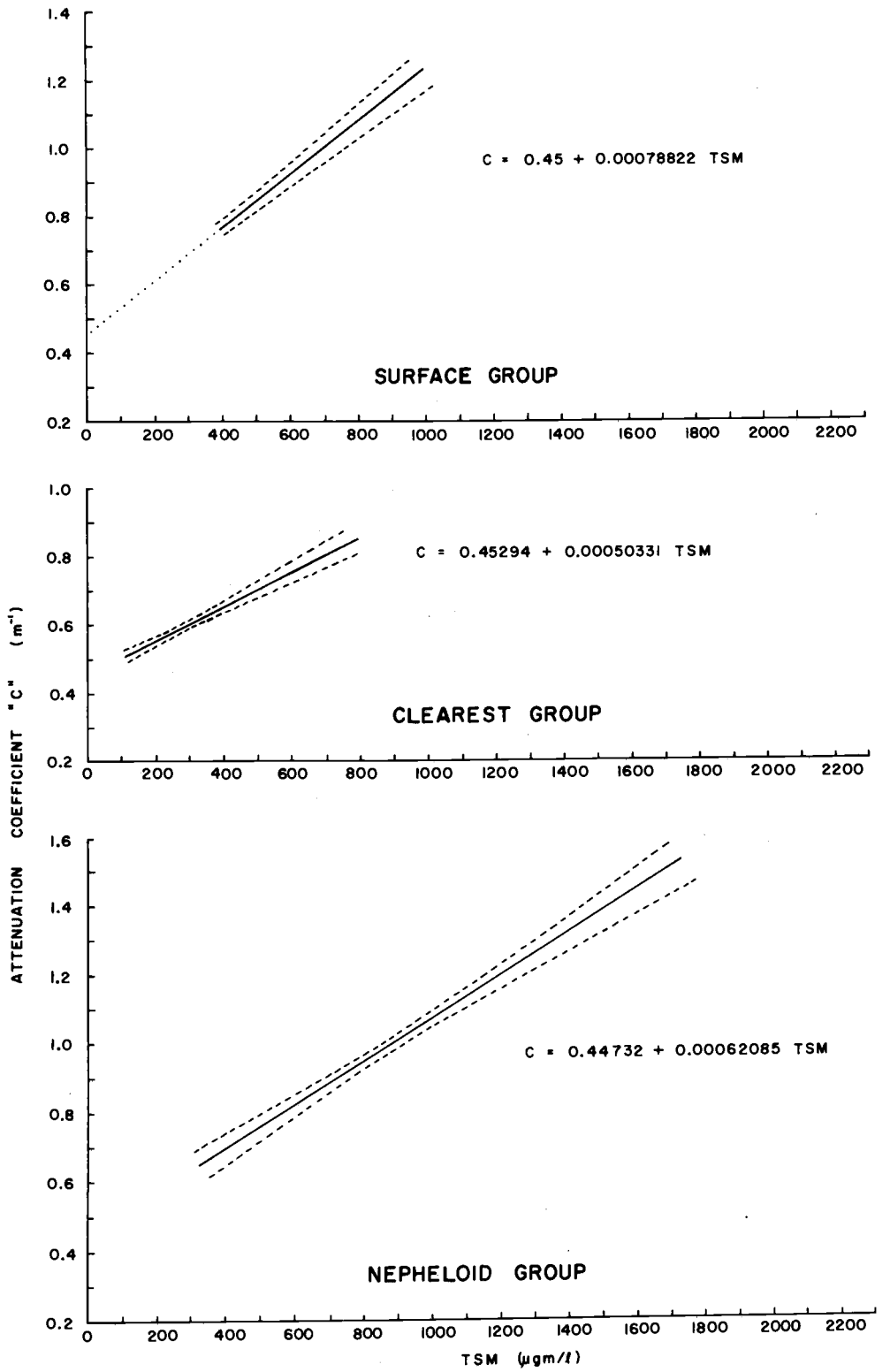

Figure 18. Regression lines with 95% confidence intervals for three depth features. The equation for the surface group has been "forced" through c equals 0.45 when TSM equals zero. Number of significant figures in equations is not indicative of precision.

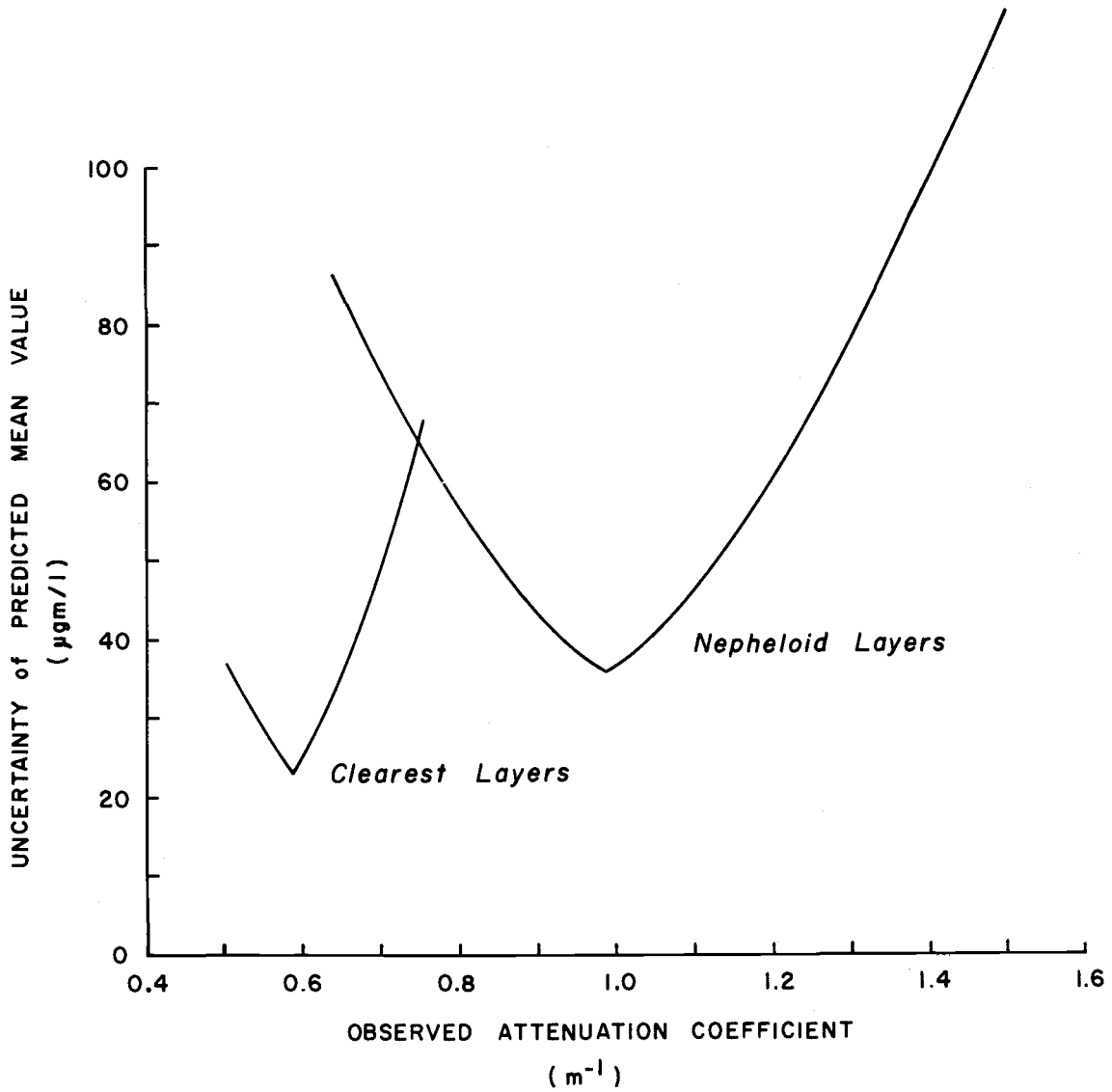

Figure 19. Uncertainty of predicted mean values of TSM for observations of attenuation coefficient. Plus or minus the uncertainty gives a 95% confidence interval. The curves were derived from the equations in Figure 18.

features of the water column. In order to use the predictive powers of regression, however, a balance must be established between theory and practicality; i.e., the character of the particles in the clearest layer may be quite different from those in the nepheloid layer yet both have a similar effect on c. The filtered samples used to calibrate the c vs TSM relationship from the clearest layers do not extend over the entire range of c observed in those portions of the nephelometer profiles classified as "clearest layers." Hence, during the conversion process, predictions of TSM would be made for values of c beyond the valid range of the calibration data.

For these reasons, the combined data from below the pycnocline were used as the data base for predicting TSM from observed attenuation (see Table VII for the actual equations). It should be noted that the regression for the combined group produces lower levels of uncertainty for the predicted mean TSM value than those suggested by Figure 18 or 19. This is due primarily to the increased number of data points in the regression.

Two methods of accomplishing the actual conversion were tried and a comparison of the results for Station A8-2 are presented in Table VII. In the first method, a profile of c versus depth was plotted. The features of the water column were defined by depth boundaries and the area in each segment under the profile was measured by polar planimeter. A mean value for attenuation for the feature was determined and converted to suspended mass using either the surface group equation (for mixed layer and pycnocline features) or the deep group equation (for features below the pycnocline). It

TABLE VII. COMPARISON OF TWO METHODS FOR INTEGRATING MASS PROFILES

Feature (Station A8-2)	Planimeter Method (mg/cm^2)	Mathematical Method (mg/cm^2)
Mixed Layer (4-16 m)	1.13	1.23
Pycnocline (16-31 m)	0.59	0.55
Clearest Layer (31-68 m)	0.75	0.74
Nepheloid Layer (68-112 m)	3.00	3.14
(112-120 m)	?	?
TOTAL	5.47	5.68

EQUATIONS: Surface Group TSM = (c-0.45)/0.00078822

Deep Group TSM = (c-0.42254)/0.00064352

is important to note that this method is valid only if a linear relationship exists between c and mass; measuring areas under the profile of percent transmission as a function of depth would be invalid, since it is the natural logarithm of transmission which is a linear function of suspended mass.

The second conversion method involved several steps in the reduction of the nephelometer system's data. The first step was minor smoothing of the c values into one meter depth increments. An overlay of the original profile with the smoothed profile revealed no significant differences in the character of the profile. Attenuation was then converted to mass concentration using either of two equations, depending on which portion of the profile was being converted. Finally, the resulting mass values were interpolated in 100 $\mu gm/\ell$ increments and the corresponding depths were determined. The 95% confidence intervals for predicted mean TSM are generally better than $\pm$ 70 $\mu gm/\ell$ so that the 100 $\mu gm/\ell$ resolution chosen for interpolation is reasonable. A running summation of the mass concentration by depth increment was also calculated, providing an integrated mass profile for the water column.

The two different methods of conversion produce very similar results (Table VII). Five other profiles were also used to compare the methods and it was found that neither produced consistently higher nor lower results. The total mass per area of seafloor by each method was within a range of 0.5 mg/cm^2.

To the author's knowledge, there are no previous studies from the continental shelf of the Pacific Northwest with which to compare

these results directly. Baker (1973b) has used similar techniques to estimate suspended mass per area of seafloor over Nitinat Fan on the continental slope off Washington. He calculated values in the range of 4.7 to 9.4 mg/cm^2 for the inorganic fraction but includes only the water column between 200 m and 20 m off the seafloor. The differing optical measurements and methods used in each study would make conclusions formed from a comparison of results questionable. The conversion calculations of Baker are incorrect in that they are based on a regression of inorganic mass concentration as a function of scattering. Physically, of course, this is not the case. By regressing scattering as a function of inorganic mass (using the same data points), the resulting equation becomes more reasonable, since it acquires a small scattering intercept when mass is set at zero (see Figure 20). Predictions of inorganic mass from scattering using the correct regression will result in lower mass concentrations for scattering values less than 5 and higher concentrations when scattering exceeds 5. A problem with the strictly empirical relationship still exists, however, in that the nephelometer design (see Sternberg et al., 1974) is such that the response to particle mass may not be linear in any case (J.R.V. Zaneveld, personal communication). If the scattering-particle mass relationship is not linear the planimeter methods Baker used to convert scattering profiles to integrated mass are also invalid.

Variability in TSM During Cruise Y7504C

Having now documented the conversion of an optical measurement

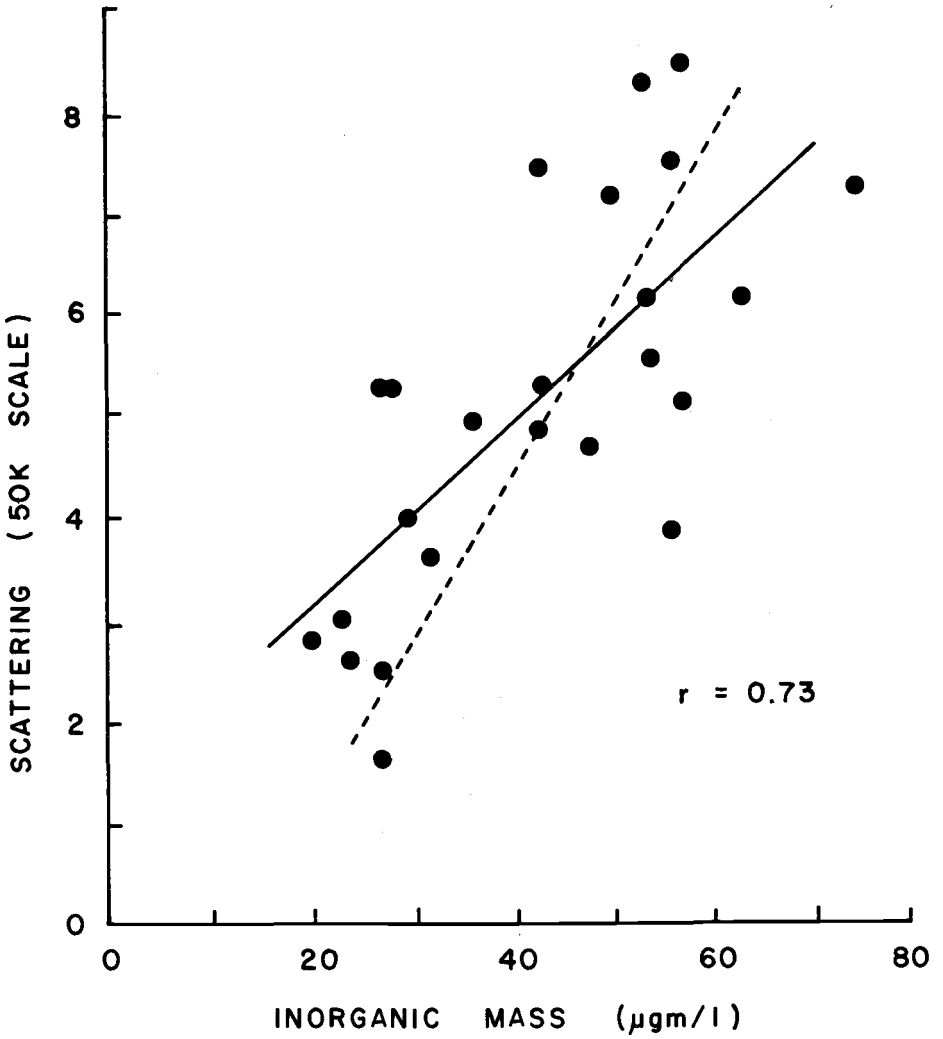

Figure 20. Calibration curve for scattering nephelometer described by Baker (1973). Solid line is regression of scattering as a function of suspended mass; dashed line is the regression used by Baker in which mass is a function of scattering.

into an estimate of suspended mass, it is possible to investigate the distribution of suspended particulate matter on a much finer scale than heretofore possible. The profiles of attenuation from Y7504C were converted to mass profiles using the mathematical methods just described. Mass values in increments of 100 μgm/ℓ were plotted against depth for each of the stations and the data points were contoured. The resulting sections are presented in Figures 22 through 25.

In order to interpret the distribution of suspended mass revealed in these figures, some description of the water mass movements is required since the two features are closely related. The cruise occurred during the upwelling season off Oregon and the winds during the entire sampling period were from the northwest or north at from 10 to 20 knots. Mooers et al.(1976) provide a complete description of the dynamics of coastal upwelling off Oregon. They propose a two-celled circulation model for onshore-offshore water motions. Their model also includes a southward surface flow, a northward deep flow, and an "inclined frontal layer" which separates the water column into an upper and lower regime. This layer is coincident with the base of the permanent pycnocline and occurs between the 26.0 and 25.5 isopycnals (sigma-t) for the data they present. Another prominent feature they describe is an anomalously warm water mass at mid-depths, which they interpret to be warm, dense surface water which has sunk and moved offshore along the "inclined frontal layer." The range of current speeds to be expected in the upwelling regime have been observed to be on the order of 10 to 30

cm/sec at a distance of 10 km offshore (op. cit. Table 2).

During the sampling period, upwelling became more well-developed than prior to the cruise. This was revealed by changes in various hydrographic parameters at the anchor stations. Figure 21 illustrates these changes. In the figure, the temperature and transmission profiles of Transect Station N8 have been chosen as "standards" with which to compare profiles from subsequent nephelometer casts at Anchor Station 8. Note that N8 and A8-1 have nearly identical profiles in spite of being separated by about 4 nautical miles and 5 hours time. The most obvious change is the intrusion of cold water at Anchor Station 8 during the 36 hour period. This is accompanied by a significant change in the optical properties of the nepheloid layer as well, in that the intruding cold water is substantially less turbid. The total mass in the water column is listed in Table VIII for all the stations, and consistent changes in mass distribution are also indicated for Anchor Station 8.

A second development which follows these changes is the appearance of warm, turbid water in the surface layers and an increase in the intensity of the mid-depth warm water anomaly. The whole surface regime becomes more turbid during the duration of sampling. By referring to the appropriate time frame in the mass cross section (Figure 22), the magnitude of the changes in the surface waters can be seen. The changes occur rapidly, as is evident in the development of the turbid "lens" at about 2000 hours on April 29. With appropriate current field information it would be possible to evaluate the size of these various "patches" of particle-laden waters.

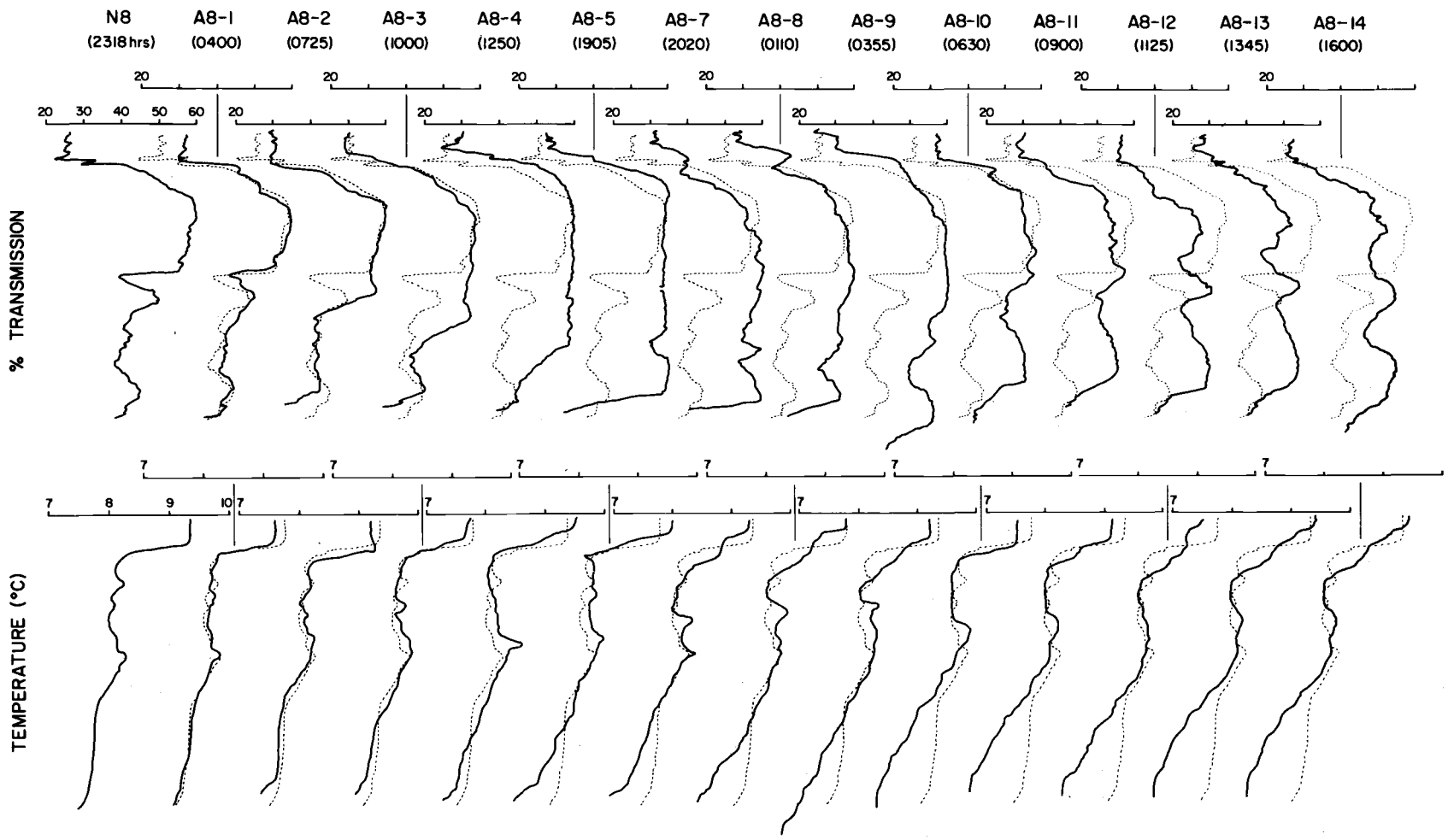

Figure 21. Light transmission and temperature profiles of Anchor Station Eight compared to profiles of Transect Station N8 (dashed lines) showing relative changes in the characteristics of the water column as time progresses.

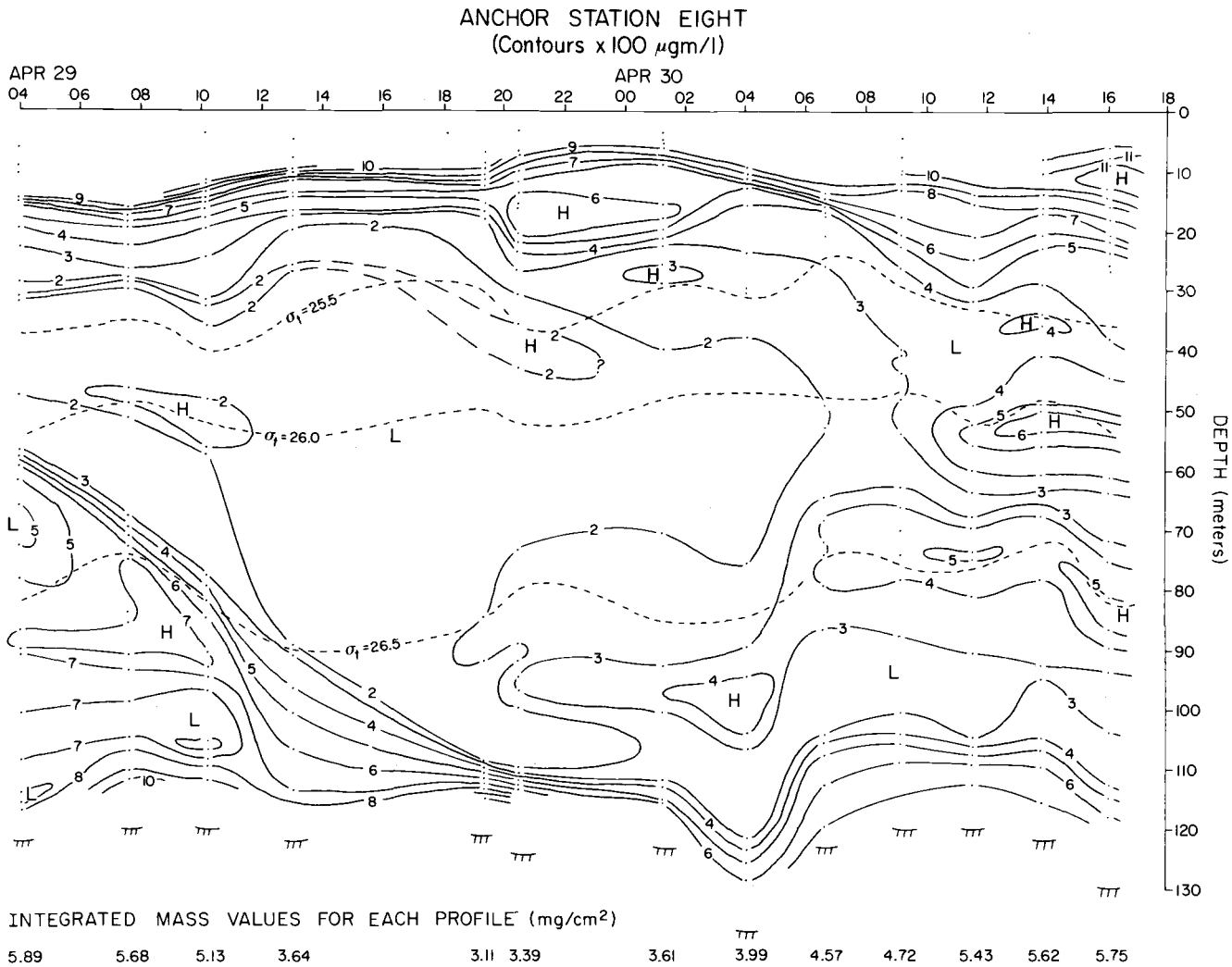

Figure 22. TSM distribution as a function of time at Anchor Station Eight. Dashed contours are water density. "Integrated mass" refers to the total amount of suspended material in a column of water with a cross-sectional area of one cm^2.

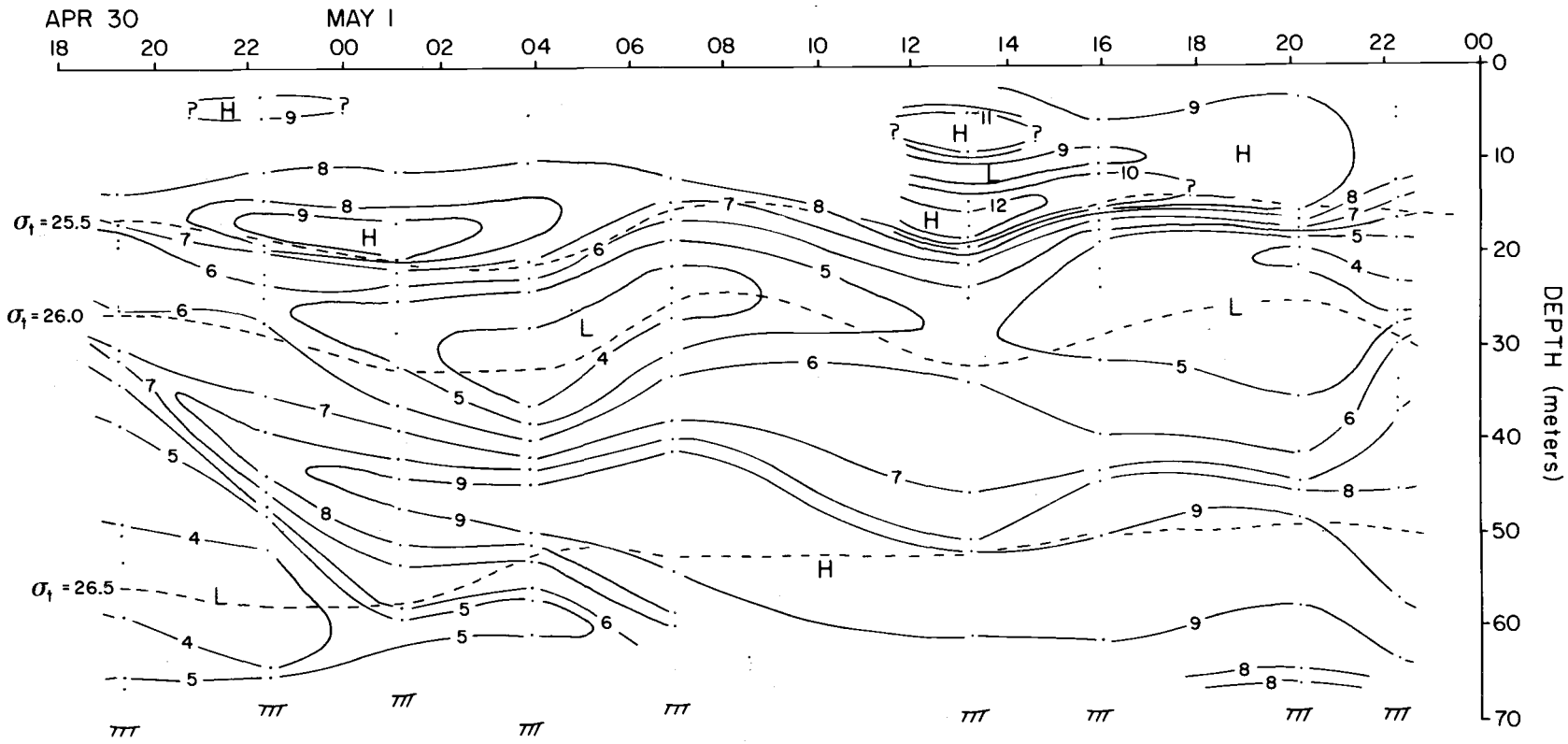

INTEGRATED MASS VALUES FOR EACH PROFILE (mg/cm^2)

3.43	4.04	4.05	3.68	4.37		4.99	4.78	4.65	4.43

Figure 23. TSM distribution as a function of time at Anchor Station Four.

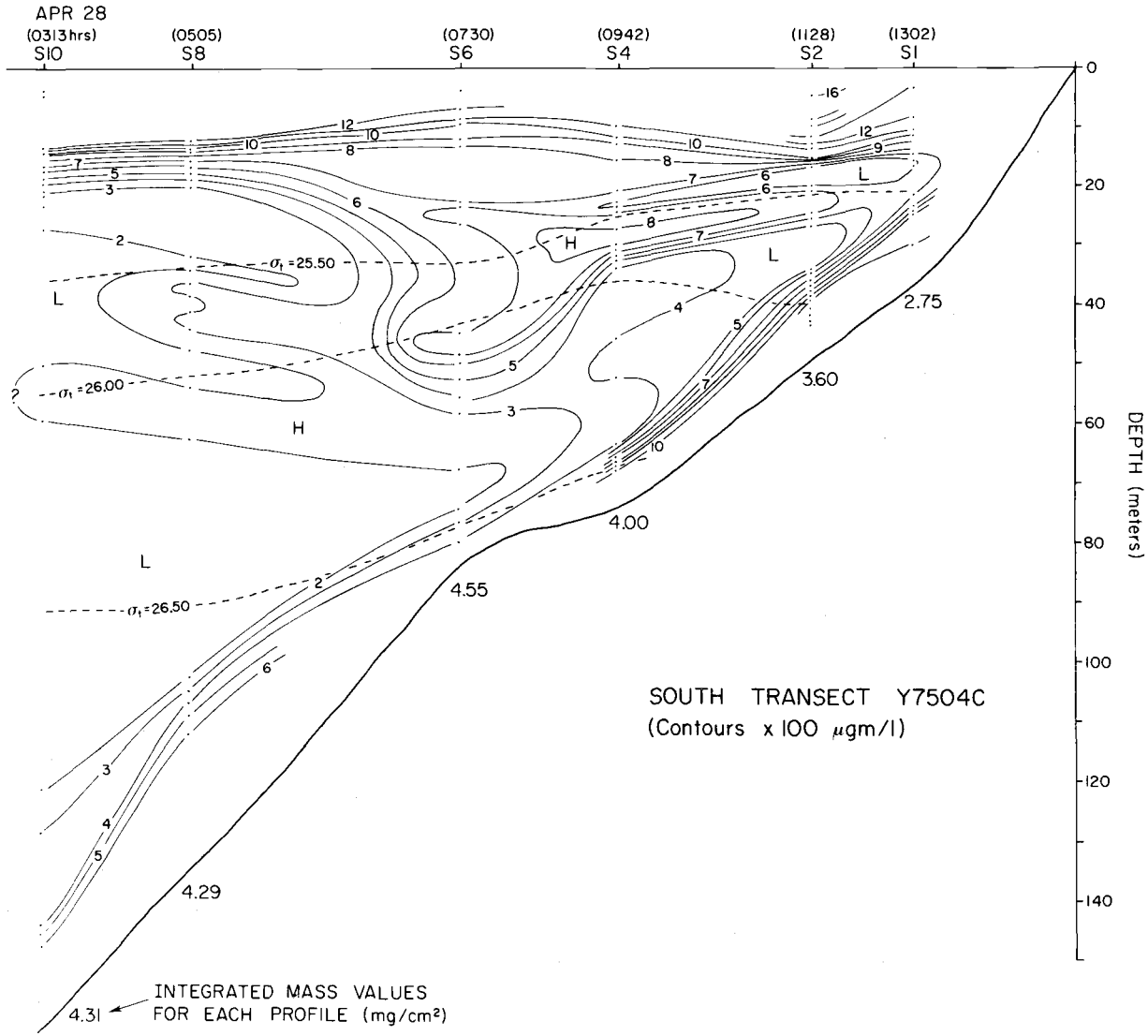

Figure 24. TSM distribution as a function of distance offshore for South Transect.

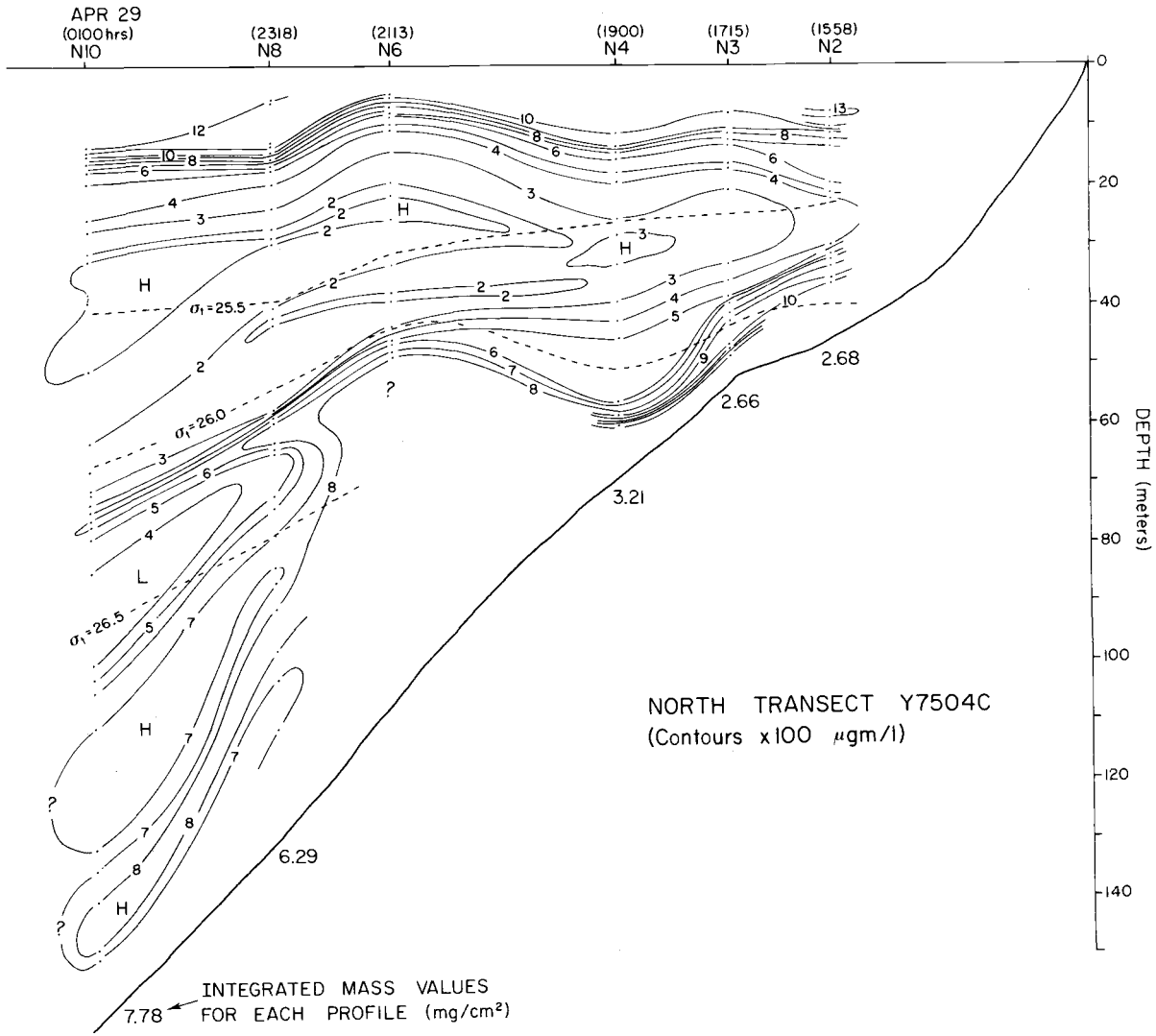

Figure 25. TSM distribution as a function of distance offshore for North Transect.

All of these anchor station observations are consistent with the following sequence of events. At the onset of the coastal upwelling season the base of the permanent pycnocline becomes inclined towards the coast. Occasionally, increased winds from the north boost the intensity of upwelling causing relatively cold, salty and clear water to move shoreward beneath the inclined frontal layer. This water ultimately reaches the surface where it is warmed, and its particulate load increased by the enhanced surface productivity. Once at the surface it is transported in a seaward direction until it reaches a region of relatively lower ambient density. Here it begins to sink, carrying along a newly-acquired load of particles. That this motion may occur in pulses rather than as a smooth, continuous flow is suggested by the changes in integrated mass per seafloor area. Referring to Table VIII, it can be seen that integrated mass decreases from a high at the beginning of Anchor Station 8 to a low about halfway through, and back high again near the end. The implication is that water begins to descend from the surface only after a sufficient volume (or perhaps duration of motion) of cold water has been moved shoreward. Both transect sections (Figure 24 and 25) indicate subsurface zones of relatively high TSM which are inclined towards the shore. In a general fashion, these zones correspond to the inclined frontal layer which is roughly defined by the dotted 26.0 and 25.5 isopycnals in the figures.

It is difficult to interpret the TSM structures depicted in Figures 24 and 25 very specifically, since they combine both geographical and temporal variations -- the latter being significant

TABLE VIII. MASS PER UNIT AREA OF SEAFLOOR

Transect Stations	(Time)	Total mass (mg/cm^2)
	Apr 28	
11S-10	(0255)	4.31
12S-8	(0450)	4.29
13S-6	(0710)	4.55
14S-4	(0930)	4.00
15S-2	(1140)	3.60
16S-1	(1255)	2.75
18N-2	(1545)	2.68
19N-3	(1705)	2.66
20N-4	(1850)	3.21
21N-6	(2100)	4.50
22N-8	(2305)	6.29
	Apr 29	
23N-10	(0030)	7.78

Anchor Station	(Time)	Total mass (mg/cm^2)
24A8-1	(0345)	5.89
25A8-2	(0745)	5.68
26A8-3	(1000)	5.13
27A8-4	(1250)	3.64
29A8-6	(1905)	3.11
30A8-7	(2020)	3.39
	Apr 30	
31A8-8	(0110)	3.61
32A8-9	(0355)	3.99
33A8-10	(0630)	4.57
34A8-11	(0900)	4.72
35A8-12	(1125)	5.43
36A8-13	(1345)	5.62
37A8-14	(1600)	5.75

Anchor Station	(Time)	Total mass (mg/cm^2)
38A4-1	(1855)	3.43
39A4-2	(2200)	4.04
	May 1	
40A4-3	(0055)	4.05
41A4-4	(0453)	3.68
42A4-5	(0650)	4.37
44A4-7	(1300)	4.99
45A4-8	(1550)	4.78
46A4-9	(1900)	5.65
47A4-10	(2210)	4.43

as seen in the Anchor Station figures. But they do fit the general upwelling model. Starting at S10 in Figure 24 and proceeding shoreward, the intrusion of clear water in the lower half of the water column is obvious. At S6, TSM in excess of 800 μgm/ℓ exists in a layer which is coincident with the inclined frontal layer. At S1, the influence of upwelled, clear water is still visible as "lenses" of relatively low TSM. Continuing on to N2 in Figure 25, the general level of TSM seems slightly lower and at N4 and N6, the prominent high which was observed at about 30 m in the Southern Transect is no longer present. The enclosed highs at this depth now are of low intensity -- between 300 and 400 μgm/ℓ . Why did the South Transect high disappear? Dilution by mixing is one possibility and an assessment of this could be made by using input from this data in a mixing model. A second possibility is suggested by the structures observed at N10. Note the presence of several "lenses" of relatively more turbid water which were not observed at S10 22 hours earlier. These could reflect the 800 μgm/ℓ turbid layer observed earlier at S4 and S6 after it has descended and moved further offshore. If these turbid features are the same material, an offshore component of motion of about 10 cm/sec is indicated.

Another phenomenon is revealed by the isopycnals in Figures 22 through 25. There is a clear correlation between density and TSM gradients at the surface, particularly at Anchor Station 4 (Figure 23) and occasionally at other depths. This probably reflects internal waves moving across the continental shelf (full treatment of the subject can be found in Mooers, 1970). Where periodicity is well-

defined, as in Figure 23, a 12 hour wavelength is indicated.

REFERENCES CITED

Anderson, J.U., 1961. An improved pretreatment for mineralogical analysis of samples containing organic matter. Proc. 10th National Conf. on Clays and Clay Minerals, 1961: pp 380-388.

Baker, E.T., 1973a. Distribution and composition of suspended sediment in the bottom waters of the Washington continental shelf and slope. Jour. Sed. Petrol. 43:812-822.

Baker, E.T., 1973b. Nephelometry and mineralogy of suspended particulate matter in the waters over the Washington continental slope and Nitinat deep-sea fan. Ph.D. thesis, University of Washington, Seattle. 142 pp.

Baker, E.T., 1976. Distribution, composition and transport of suspended particulate matter in the vicinity of Willapa submarine canyon, Washington. Geol. Soc. Amer. Bull. 87(4):625-632.

Beardsley, G.F., Jr., H. Pak, K. Carder and B. Lundgren, 1970. Light scattering and suspended particles in the eastern equatorial Pacific Ocean. Jour. Geophys. Res. 75(15):2837-2845.

Beer, R.M., J. P. Dauphin and T.S. Sholes, 1974. A deep-sea in situ suspended sediment sampling system. Mar. Geol. 17:M35-M44.

Bertine, K.K. and P.D. LaFleur, 1972. Aids to analysis. In: Marine Pollution Monitoring: Strategies for a National Program. E.D. Goldberg, convener. (Deliberations of a workshop at Santa Catalina Marine Biological Laboratory, University of Southern California, Oct., 1972.)

Biscaye, P.E. and S.L. Eittreim, 1974. Variations in benthic boundary layer phenomena: nepheloid layer in the North American Basin. In: Suspended Solids in Water. R.J. Gibbs (editor). Plenum Press, New York, pp 227-260.

Bishop, J.K.B. and J. M. Edmond, 1976. A new large volume filtration system for the sampling of oceanic particulate matter. Jour. Mar. Res. 34(2):187-198.

Bridges, R.M., 1970. Design considerations for oceanic systems. Bendix Technical Journal 3(1):16-25.

Carder, K.L., G.F. Beardsley, Jr. and H. Pak, 1971. Particle size distribution in the eastern equatorial Pacific. Jour. Geophys. Res. 76(21):5070-5077.

Carder, K.L., P.R. Betzer and D.W. Eggimann, 1974. Physical, chemical, and optical measurements of suspended-particle concentrations:

their intercomparison and application to the West African Shelf. In: Suspended Solids in Water, R.J. Gibbs (editor). Plenum Press, New York, pp 173-.

Carroll, D., 1970. Clay minerals in Arctic Ocean sea-floor sediments. Jour. Sed. Petrol. 40(3):814-821.

Clark, D.L., 1969. Paleoecology and sedimentation in part of the Arctic Basin. Arctic(22):233-245.

Coachman, L.K. and K. Aagaard., 1974. Physical oceanography of the Arctic and Subarctic Seas. In: Marine Geology and Oceanography of the Arctic Seas, Y. Herman (editor). Springer-Verlag, New York, pp 1-72.

Coachman, L.K., 1969. Physical oceanography in the Arctic Ocean: 1968. Arctic 22(3):14-224.

Coachman, L.K. and C.A. Barnes, 1963. The movement of Atlantic water in the Arctic Ocean. Arctic 16(1):8-16.

Cranston, R.E. and D.E. Buckley, 1972. The application and performance of microfilters in analysis of suspended particulate matter. Unpublished manuscript. (Report Series BI-R-72-7, Bedford Institute of Oceanography, Dartmouth, Nova Scotia.)

Curtis, W.E., J.K. Culbertson and E.D. Chase, 1973. Fluvial-sediment discharge to the oceans from the conterminous U.S. U.S. Geol. Surv. Cir. 670, 17 pp.

Darby, D.A., L.H. Burckle and D.L. Clark, 1974. Airborne dust on the Arctic pack ice, its composition and fallout rate. Earth and Planet. Sci. Letters 24:166-172.

Eittreim, S. and M. Ewing, 1972. Suspended particulate matter in the deep waters of the North American Basin. Studies in Physical Oceanography. Vol. 2, Gordon (editor), Gordon and Breach Science Pub., New York, 1972:123-167.

Feely, R.A., 1976. Evidence for aggregate formation in a nepheloid layer and its possible role in the sedimentation of particulate matter. Mar. Geol. 20:M7-M13.

Gordon, D.C., 1970. Some studies on the distribution and composition of particulate organic carbon in the North Atlantic Ocean. Deep-Sea Res. 17:233-243.

Gordon, D.C., Jr., 1970. A microscopic study of organic particles in the North Atlantic Ocean. Deep-Sea Res. 17(1):175-185.

Gordon, D.C., Jr., 1971. Distribution of particulate organic carbon and nitrogen at an oceanic station in the central Pacific. Deep-Sea Res. 18:1127-1134.

Gossé, J.G., 1974. Tyndall measurements on quartz particles at 90°. Rijkswaterstaat. Directie Waterhuishouding en Waterbeweging Fysische Afdeling, Nota FA 7403. (Hague, Netherlands).

Green, K.E., 1960. Ecology of some Arctic foraminifera. In: Scientific Studies at Fletchers Ice Island T-3 (1952-1955), Vol. I., pp 59-82.

Hamilton, E.L., 1976. Variations of density and porosity with depth in deep-sea sediments. Jour. Sed. Petrol. 46(2):280-300.

Hamilton, E.L., 1974. Prediction of deep-sea sediment properties: state-of-the-art. In: Deep-Sea Sediments: Physical and Mechanical Properties, A.L. Inderbitzen (editor). Plenum Press, New York, 497 pp.

Harlett, J.C., 1972. Sediment transport on the northern Oregon continental shelf. Ph.D. thesis, Oregon State University, Corvallis. 120 pp.

Harlett, J.C. and L.D. Kulm, 1973. Suspended sediment transport on the northern Oregon continental shelf. Geol. Soc. Amer. Bull. 84:3815-3826.

Hopkins, T.L., 1969. Zooplankton standing crop in the Arctic Basin. Limnol. Oceanog. 14:80-85.

Hunkins, K., E.M. Thorndike and G. Mathieu, 1969. Nepheloid layers and bottom currents in the Arctic Ocean. Jour. Geophys. Res. 74(28):6995-7008.

Huyer, A., R.D. Pillsbury and R.L. Smith, 1975. Seasonal variation of the alongshore velocity field over the continental shelf off Oregon. Limnol. and Oceanog. 20:90-95.

Jackson, M.L., 1958. Soil Chemical Analysis. Prentice-Hall, Inc., New Jersey, 498 pp. Chapter 9: Organic matter determinations for soils, pp 205-225.

Jacobs, M.G. and M. Ewing, 1969. Suspended particulate matter: concentration in the major oceans. Science 163(3865):380-383.

Jerlov, N.G., 1968. Optical Oceanography. Elsevier, Amsterdam. 110 pp.

Jerlov, N.G., 1976. Marine Optics. Elsevier, Amsterdam. 212 pp.

Keller, G.H., 1971. Engineering properties of Greenland and Norwegian basin sediments. Proc. of First Int'l. Conf. on Port and Ocean Engineering under Arctic Conditions, Vol. II, pp 1285-1311.

Kinney, P.J., M.E. Arhelger and D.C. Burrell, 1970. Chemical characteristics of water masses in the Amerasian Basin of the Arctic Ocean. Jour. Geophys. Res. 75(21):4097-4104.

Kinney, P.J., T.C. Loder and Joanne Groves, 1971. Particulate and dissolved organic matter in the Amerasian Basin of the Arctic Ocean. Limnol. and Oceanog. 16(1):132-137.

Komar, P.D., L.D. Kulm and J.C. Harlett, 1974. Observations and analysis of bottom turbid layers on the Oregon continental shelf. Jour. Geol. 82(1):104-111.

Kranck, Kate, 1975. Sediment deposition from flocculated suspensions. Sedimentology (22):111-123.

Lee, Homa, J., 1973. Measurements and estimates of engineering and other physical properties, Leg 19. In: Initial Reports of the Deep Sea Drilling Project, Vol. 19, J.S. Creager, D.W. Seholl, et al., 1973. Washington (U.S. GPO), pp 701-720.

Maksimov, A.N. and M.M. Shlafman, 1970. Possibility of determining the concentration of suspended matter by an optical method. Oceanology 10(4):565-568.

McCave, I.N., 1975. Vertical flux of particles in the ocean. Deep-Sea Res. 22:491-502.

McCrone, W.C. and J.G. Delly, 1973. The Particle Atlas: an encyclopedia of techniques for small particle identification. 2nd Ed., Ann Arbor Science Publishers, 4 vol.

Molnia, B.F., 1974. A rapid and accurate method for the analysis of calcium carbonate in small samples. Jour. Sed. Petrol. 44(2): 589-590.

Momsen, D.F. and J.C. Clerici, 1971. First silver zinc batteries used in deep submergence. Mar. Tech. Soc. Jour. 5(2):31-36.

Mooers, C.N.K., 1970. The interaction of an internal tide with the frontal zone of a coastal upwelling region. Ph.D. dissertation, Oregon State University, Corvallis. 480 pp.

Mooers, C.N.K., C.A. Collins and R.L. Smith, 1976. The dynamic structure of the frontal zone in the coastal upwelling region off Oregon. Jour. Phys. Oceanog. 6(1):3-21.

Neshyba, S., G.F. Beardsley, Jr., V.T. Neal and K. Carder, 1968. Light scattering in the central Arctic Ocean: some winter profiles. Science 162:1267-1268.

Owen, R.W., Jr., 1974. Optically effective area of particle ensembles in the sea. Limnol. and Oceanog. 19(4):584-590.

Pak, H., 1970. The Columbia River as a source of marine light scattering particles. Ph.D. thesis, Oregon State University, Corvallis. 110 pp.

Peterson, R.E., 1976. A deep-sea in situ suspended sediment sampling system: comment. Mar. Geol. 21:59-62.

Plank, W.S., H. Pak and J.R.V. Zaneveld, 1972. Light scattering and suspended matter in nepheloid layers. Jour. Geophys. Res. 77(9):1689-1694.

Redfield, A.C., B.H. Ketchum and F.A. Richards, 1963. The influence of organisms on the composition of seawater. In: The Sea, M.A. Hill (editor), pp 26-77.

Riley, G.A., 1970. Particulate organic matter in seawater. Adv. Mar. Biol. 8:1-118.

Roth, P.H., M.M. Mullin and W.H. Berger, 1975. Coccolith sedimentation by fecal pellets: laboratory experiments and field observations. Geol. Soc. Amer. Bull. 86:1079-1084.

Smith, R.C., 1973. Optical properties of the Arctic upper water. Arctic 26(4):303-313.

Snedecor, G.W. and W.C. Cochran, 1967. Statistical Methods, 6th Ed., Iowa State University Press, Iowa. 593 pp.

Spencer, D.W. and P.L. Sachs, 1970. Some aspects of the distribution, chemistry and mineralogy of suspended matter in the Gulf of Maine. Mar. Geol. 9:117-136.

Sternberg, R.W., E.T. Baker, D.A. McManus, S. Smith and D.R. Morrison, 1974. An integrating nephelometer for measuring particle concentrations in the deep sea. Deep-Sea Res. 21:887-892.

Tucholke, Brian E., 1974. Determination of montmorillonite in small samples and implications for suspended matter studies. Jour. Sed. Petrol. 44(1):254-258.

Tyler, J.E., R.W. Austin and T.J. Petzold, 1974. Beam transmissiometers for oceanographic measurements. In: Suspended Solids in Water, R.J. Gibbs (editor). Plenum Press, New York.

Zaneveld, J.R.V., 1973. Variation of optical sea parameters with depth. In: Optics of the Sea, lecture series No. 61, AGARD, NATO, France.

APPENDICES

APPENDIX I. ARCTIC OCEAN DATA

Column 1. Filter number

2. Day, November, 1973/time, Barrow, Alaska

3. Sample depth, meters

4. Total Suspended Mass, μgm/ℓ

5. Maximum and minimum values of TSM due to analytical errors; "D" indicates values deleted from average mass calculations for the depths sampled (see text)

6. Organic Suspended Mass, μgm/ℓ

Appendix I cont.

1	2	3	4	5		6
T-3-1	16/1440	1220	29.9	28.5-31.3	D	
T-3-2	16/2030	1220	31.4	28.8-34.0	D	
T-3-3	16/2030	1220	24.6	22.0-27.3	D	
T-3-6	17/0915	1220	13.6	11.7-15.5	D	3.5
T-3-7	17/2025	1220	17.7	16.4-19.0	D	
T-3-8	18/1430	1214	6.8	5.4--8.2		
T-3-10	18/1430	1220	14.6	13.5-15.6	D	
T-3-11	18/1945	1214	8.1	6.8--9.5		
T-3-12	18/1945	1220	9.6	8.7-10.6	D	
T-3-13	19/1000	1214				
T-3-13	19/1330	1214				
T-3-13	19/1630	1214	4.5	4.1--5.0		
T-3-14	19/1000	1220	12.4	11.4-13.4	D	
T-3-16	19/1630	1220	10.9	9.9-11.8	D	2.5
T-3-17	20/1030	1220				
T-3-17	20/1545	1220	11.2	10.5-11.9	D	
T-3-18	20/1030	1214				
T-3-18	20/1545	1214	5.9	5.2--6.6		
T-3-19	21/1015	594	6.6	5.3--8.0		
T-3-20	21/1015	600	12.1	11.1-13.0	D	
T-3-21	21/1500	594				
T-3-21	23/1000	594				
T-3-21	23/1445	594	5.2	4.7--5.6		
T-3-22	21/1500	600	12.0	11.0-13.0	D	
T-3-23	23/1000	600	13.0	12.0-14.0	D	
T-3-24	23/1445	600	11.8	10.8-12.8	D	
T-3-28	23/2100	594	7.0	5.6--8.3		1.4
T-3-29	23/2100	600	11.1	10.0-12.2	D	4.7
T-3-30	24/1715	594				
T-3-30	25/1100	594	5.7	5.1--6.4		

Appendix I cont.

1	2	3	4	5	6
T-3-32	24/1715	600	8.7	7.7--9.7	
T-3-33	25/1100	600	7.3	6.1--8.5	
T-3-34	25/1630	1220			
T-3-34	25/2130	1220	6.4	5.9--6.9	
T-3-36	25/1630	1214			
T-3-36	25/2130	1214	3.3	2.7--4.0	
T-3-41	26/1245	44	10.4	9.1-11.8	
T-3-42	26/1245	50	7.9	6.7--9.1	
T-3-44	26/1545	44	4.0	2.6--5.4	
T-3-45	26/1545	50	6.4	5.4--7.5	
T-3-52	27/1000	50	7.3	6.2--8.3	
T-3-53	27/1000	44	10.4	9.1-11.7	
T-3-54	27/1430	44	7.3	6.0--8.6	
T-3-56	27/1430	50	6.2	5.0--7.3	
T-3-57	27/2000	144	7.7	6.3--9.0	
T-3-58	27/2000	150	9.4	8.4-10.5	
T-3-59	28/1100	144	8.5	7.1--9.8	4.9
T-3-61	28/1100	150	10.3	9.3-11.4	6.1
T-3-64	28/1530	50	8.3	7.3--9.4	3.6
T-3-66	28/2000	144	9.7	8.4-11.1	
T-3-67	28/2000	150	8.8	7.6-10.0	
T-3-68	29/0915	144	9.4	8.1-10.7	
T-3-69	29/0915	150	8.4	7.5--9.4	

APPENDIX II. OREGON CONTINENTAL SHELF DATA, Y7504C

Column	1.	Station number
	2.	Seafloor depth -- sample depth, meters
	3.	Local time, starting April 28, 1975
	4.	Filter number; "N" = nepheloid, "T" = turbid, "C" = clearest, "P" = pycnocline, and "M" = mixed
	5.	Total Suspended Mass, μgm/ℓ
	6.	Organic Suspended Mass, μgm/ℓ
	7.	Percent organic matter
	8.	Particulate Organic Carbon, μgm/ℓ
	9.	Particulate Organic Nitrogen, μgm/ℓ
	10.	Carbon/Nitrogen ratio
	11.	Organic matter/Carbon ratio
	12.	Percent light transmission
	13.	Volume concentration, X 10^5 μm^3/ml
	14.	Particle density, gm/cm^3

Appendix II cont.

1	2	3	4	5	6	7	8	9	10	11	12	13	14
11S10	163-149	313	7N	633	198	31	178	10	17.1	1.1	44	2.67	2.4
11S10	163-090	313	8C	172	31	18	-0	-0	-0	-0	60	1.04	1.7
11S10	163-019	313	21P	282	110	39	100	12	8.4	1.1	49	-0	-0
12S8	136-126	505	9N	658	68	10	121	5	22.8	.6	42	3.32	2.0
12S8	136-086	505	10C	181	17	11	47	4	13.1	.4	60	1.03	1.6
12S8	136-020	505	11P	461	107	23	167	15	11.5	.6	43	4.42	1.0
13S6	83-082	730	12N	467	63	14	77	8	9.7	.8	46	2.55	1.8
13S6	83-070	730	13C	281	32	11	107	8	14.1	.3	58	1.13	2.5
13S6	83-041	730	14P	614	140	23	-0	-0	-0	-0	42	3.67	1.7
14S4	75-069	942	16N	1105	179	16	109	7	14.9	1.6	32	6.13	1.8
14S4	75-060	942	17C	341	89	26	54	5	11.3	1.7	52	1.96	1.7
14S4	75-030	942	18P	761	165	22	82	10	7.9	2.0	38	4.82	1.6
15S2	50-045	1128	19N	1400	153	11	215	26	8.2	.7	27	-0	-0
15S2	50-032	1128	20C	498	49	10	173	22	7.8	.3	50	-0	-0
16S1	37-033	1302	23N	1184	338	29	114	16	7.1	3.0	28	9.52	1.2
16S1	37-020	1302	22C	463	171	37	106	13	7.9	1.6	47	3.71	1.2
16S1	37-010	1302	24M	1011	340	34	213	27	7.8	1.6	28	9.58	1.1
17N1	37-028	1434	25N	1425	263	18	219	27	8.1	1.2	26	8.81	1.6
17N1	37-018	1434	26T	1539	272	18	188	28	6.8	1.4	22	10.27	1.5
17N1	37-009	1434	27M	2028	490	24	171	23	7.6	2.9	14	13.93	1.5
18N2	47-041	1558	28N	914	133	15	131	17	7.8	1.0	34	5.39	1.7
18N2	47-029	1558	29C	531	84	16	142	12	12.1	.6	52	2.89	1.8
18N2	47-014	1558	30P	727	181	25	150	19	7.9	1.2	39	5.39	1.3
19N3	53-049	1715	31N	1461	167	11	148	14	10.4	1.1	25	7.11	2.1
19N3	53-030	1715	32C	179	36	20	190	20	9.3	.2	56	1.38	1.3
19N3	53-012	1715	33P	626	122	20	107	15	7.4	1.1	41	4.47	1.4
20N4	70-056	1900	34N	1036	204	20	77	9	8.2	2.6	34	5.96	1.7
20N4	70-036	1900	35C	357	90	25	51	5	9.6	1.8	52	1.88	1.9
20N4	70-011	1900	36P	487	218	45	165	22	7.4	1.3	34	6.32	.8
21N6	105-105	2113	37N	1443	138	10	112	10	11.5	1.2	-0	5.78	2.5

Appendix II cont.

1	2	3	4	5	6	7	8	9	10	11	12	13	14
21N6	105-037	2113	38C	184	35	19	-0	-0	-0	-0	57	1.63	1.1
21N6	105-011	2113	39P	409	163	40	136	16	8.6	1.2	35	5.70	.7
22N8	130-117	2318	41N	1057	113	11	93	7	14.1	1.2	37	4.25	2.5
22N8	130-029	2318	42C	207	39	19	132	11	12.3	.3	57	2.28	.9
22N8	130-018	2318	43P	765	184	24	148	16	9.4	1.2	46	-0	-0
23N10	160-149	100	44N	907	139	15	71	7	10.4	2.0	38	3.68	2.5
23N10	160-051	100	45C	219	52	24	68	6	11.7	.8	59	-0	-0
23N10	160-011	100	46M	765	256	33	205	27	7.7	1.2	22	10.65	.7
24A8-1	122-115	403	47N	998	-0	-0	-0	-0	-0	-0	38	-0	-0
24A8-1	122-041	403	48C	186	-0	-0	-0	-0	-0	-0	59	-0	-0
24A8-1	122-023	403	49P	266	-0	-0	-0	-0	-0	-0	53	-0	-0
25A8-2	120-111	737	50N	850	-0	-0	-0	-0	-0	-0	34	3.63	2.3
25A8-2	120-039	737	51C	126	-0	-0	-0	-0	-0	-0	59	-0	-0
25A8-2	120-021	737	52P	261	-0	-0	-0	-0	-0	-0	48	2.91	.9
26A8-3	120-113	1011	53N	963	107	11	-0	-0	-0	-0	32	5.32	1.8
26A8-3	120-058	1011	54C	202	35	17	91	7	12.8	.4	57	1.39	1.5
26A8-3	120-010	1011	55P	521	166	32	280	36	7.7	.6	25	9.52	.5
27A8-4	122-115	1302	56N	1011	-0	-0	-0	-0	-0	-0	35	3.92	2.6
27A8-4	122-060	1302	57C	138	-0	-0	-0	-0	-0	-0	59	1.47	.9
27A8-4	122-009	1302	58P	539	-0	-0	-0	-0	-0	-0	26	9.90	.5
28A8-5	123-117	1717	59N	953	117	12	61	4	13.9	1.9	36	2.52	3.8
28A8-5	123-059	1717	60C	128	14	11	64	5	12.5	.2	59	.76	1.7
28A8-5	123-012	1717	61P	242	72	30	134	18	7.5	.5	49	2.96	.8
29A8-6	121-113	1921	62N	855	-0	-0	-0	-0	-0	-0	40	3.48	2.5
29A8-6	121-059	1921	63C	190	-0	-0	-0	-0	-0	-0	59	1.20	1.6
29A8-6	121-007	1921	64P	443	-0	-0	-0	-0	-0	-0	32	8.53	.5
30A8-7	124-115	2030	66N	831	104	12	-0	-0	-0	-0	42	2.19	3.8
30A8-7	124-057	2030	67C	128	15	11	46	7	7.0	.3	60	.96	1.3
30A8-7	124-012	2030	68P	248	87	35	131	38	3.4	.7	40	4.69	.5
31A8-8	123-116	119	69N	805	-0	-0	-0	-0	-0	-0	41	2.79	2.9

Appendix II cont.

1	2	3	4	5	6	7	8	9	10	11	12	13	14
31A8-8	123-059	119	70C	135	-0	-0	-0	-0	-0	-0	60	1.54	.9
31A8-8	123-012	119	71P	336	-0	-0	-0	-0	-0	-0	45	4.71	.7
32A8-9	137-130	407	72N	727	77	11	-0	-0	-0	-0	44	2.78	2.6
32A8-9	137-053	407	73C	176	46	26	-0	-0	-0	-0	59	1.31	1.3
32A8-9	137-010	407	74P	590	167	28	-0	-0	-0	-0	33	6.97	.8
33A8-10	123-119	640	75N	959	-0	-0	-0	-0	-0	-0	42	2.35	4.1
33A8-10	123-059	640	76C	237	-0	-0	-0	-0	-0	-0	57	1.29	1.8
33A8-10	123-008	640	77M	693	-0	-0	-0	-0	-0	-0	32	6.71	1.0
34A8-11	120-113	912	78N	898	117	13	-0	-0	-0	-0	41	3.16	2.8
34A8-11	120-059	912	79C	207	37	18	-0	-0	-0	-0	57	.93	2.2
34A8-11	120-012	912	80P	566	187	33	-0	-0	-0	-0	34	4.83	1.2
35A8-12	120-115	1133	81N	824	-0	-0	-0	-0	-0	-0	40	4.05	2.0
35A8-12	120-060	1133	82T	254	-0	-0	-0	-0	-0	-0	50	2.22	1.1
35A8-12	120-012	1133	84P	860	-0	-0	-0	-0	-0	-0	31	8.47	1.0
36A8-13	122-116	1355	85N	783	73	9	-0	-0	-0	-0	41	4.42	1.8
36A8-13	122-061	1355	86C	339	74	22	-0	-0	-0	-0	55	1.96	1.7
36A8-13	122-012	1355	87P	636	213	33	-0	-0	-0	-0	28	7.82	.8
37A8-14	130-123	1608	88N	715	-0	-0	-0	-0	-0	-0	40	3.80	1.9
37A8-14	130-061	1608	89C	253	-0	-0	-0	-0	-0	-0	54	2.06	1.2
37A8-14	130-012	1608	91P	461	-0	-0	-0	-0	-0	-0	34	7.71	.6
38A4-1	70-066	1910	92N	763	-0	-0	-0	-0	-0	-0	42	2.07	3.7
38A4-1	70-056	1910	93C	377	-0	-0	-0	-0	-0	-0	52	1.73	2.2
38A4-1	70-011	1910	94P	554	-0	-0	-0	-0	-0	-0	37	7.62	.7
39A4-2	68-064	2217	95C	492	66	13	-0	-0	-0	-0	52	2.38	2.1
39A4-2	68-055	2217	96C	406	67	17	-0	-0	-0	-0	51	2.05	2.0
39A4-2	68-011	2217	97P	840	-0	-0	-0	-0	-0	-0	34	6.29	1.3
40A4-3	67-062	103	98N	566	-0	-0	-0	-0	-0	-0	47	2.75	2.1
40A4-3	67-056	103	99T	561	-0	-0	-0	-0	-0	-0	46	3.35	1.7
40A4-3	67-012	103	101M	727	-0	-0	-0	-0	-0	-0	34	7.07	1.0
41A4-4	67-063	357	102N	634	102	16	-0	-0	-0	-0	44	3.19	2.0
41A4-4	67-055	357	103C	475	63	13	-0	-0	-0	-0	47	3.01	1.6

Appendix II cont.

1	2	3	4	5	6	7	8	9	10	11	12	13	14
41A4-4	67-011	357	104M	585	219	37	-0	-0	-0	-0	35	6.09	1.0
42A4-5	70-065	657	105N	785	-0	-0	-0	-0	-0	-0	43	1.47	5.3
42A4-5	70-056	657	106T	705	-0	-0	-0	-0	-0	-0	40	1.98	3.6
42A4-5	70-012	657	107P	482	-0	-0	-0	-0	-0	-0	41	-0	-0
43A4-6	68-047	1003	109N	627	87	14	-0	-0	-0	-0	37	3.58	1.8
44A4-7	67-062	1310	111N	781	-0	-0	-0	-0	-0	-0	38	5.03	1.6
44A4-7	67-056	1310	112N	880	-0	-0	-0	-0	-0	-0	36	5.97	1.5
44A4-7	67-011	1310	113P	733	-0	-0	-0	-0	-0	-0	32	10.01	.7
45A4-8	69-066	1600	114N	805	101	13	-0	-0	-0	-0	37	4.89	1.6
45A4-8	69-056	1600	116N	850	95	11	-0	-0	-0	-0	36	6.41	1.3
45A4-8	69-012	1600	117P	567	112	20	-0	-0	-0	-0	26	-0	-0
46A4-9	69-065	2014	118N	853	-0	-0	-0	-0	-0	-0	38	7.31	1.2
46A4-9	69-050	2014	119N	891	-0	-0	-0	-0	-0	-0	36	5.58	1.6
46A4-9	69-011	2014	120P	582	-0	-0	-0	-0	-0	-0	30	7.43	.8
47A4-10	69-067	2220	121N	700	108	15	-0	-0	-0	-0	38	3.22	2.2
47A4-10	69-054	2220	122N	812	102	13	-0	-0	-0	-0	36	4.15	2.0
47A4-10	69-009	2220	123P	503	84	17	-0	-0	-0	-0	37	6.51	.8

APPENDIX III. REGRESSION EQUATIONS FOR Y7504C

All regression calculations were performed using the O.S.U. "SIPS" computer program. The values in parentheses under "intercept" and "slope" are 95% confidence intervals calculated according to Snedecor and Cochran, 1967, pp 153-154. A double asterisk (**) indicates a significance greater than alpha = 0.01, a single asterisk (*) indicates significance between 0.05 and 0.01, and "N.S." means the significance is less than 0.05.

The mean square of residuals (variance about regression) is provided to allow comparison of various regressions. The larger mean square is divided by the smaller, and the result compared to an F distribution table, with the null hypothesis H_0: variance 1 = variance 2 (Snedecor and Cochran, 1967, p 117).

Units:

Attenuation coefficient (m^{-1})

Total suspended mass ($\mu gm/\ell$)

Suspended volume (X 10^5 $\mu m^3/ml$)

Notes:

(1) Data with calculated densities less than 1 gm/cm^3 have been removed.

(2) Same as (1) above, and "forced" through c = 0.45 m^{-1} when TSM equals zero.

(3) Data with calculated densities greater than 3 gm/cm^3 have been removed.

ATTENUATION COEFFICIENT = (intercept) + (slope) TOTAL SUSPENDED MASS

Feature	Intercept	Slope	No. Samples	Correlation coefficient	Variance
Mixed Layer	0.76	0.00060	6	0.90	0.02912
	(33-119)	(20-99)		*	(d.f.=4)
Pycnocline Layer	0.74	0.00050	29	0.44	0.03418
	(52-97)	(9-91)		*	(d.f.=27)
Combined Surface Group	0.69	0.00062	35	0.73	0.03245
	(55-83)	(41-82)		**	(d.f.=33)
Adjusted Surface Group(1)	0.53	0.00070	13	0.96	0.00812
	(40-66)	(56-85)		**	(d.f.=11)
"Zeroed" Surface Group(2)	0.45	0.00079	13	0.99	0.00879
	(n.a.)	(72-85)		**	(d.f.=12)

Clearest Layer	0.45	0.00050	29	0.91	0.00094
	(43-48)	(41-60)		**	(d.f.=27)

ATTENUATION COEFFICIENT = (intercept) + (slope) TOTAL SUSPENDED MASS, continued

Feature	Intercept	Slope	No. Samples	Correlation coefficient	Variance
Turbid Layer	0.45	0.00067	4	0.99	0.00365
	(21-70)	(40-95)		*	(d.f.=2)
Nepheloid Layer	0.45	0.00061	39	0.88	0.00504
	(36-55)	(50-71)		**	(d.f.=37)
Combined Nepheloid Group	0.45	0.00062	43	0.91	0.00504
	(37-53)	(53-71)		**	(d.f.=41)
Adjusted Nepheloid Group(3)	0.46	0.00062	37	0.94	0.00422
	(38-53)	(54-70)		**	(d.f.=35)

Combined Below Pycnocline Group	0.42	0.00064	72	0.97	0.00350
	(39-45)	(61-68)		**	(d.f.=70)

ATTENUATION COEFFICIENT = (intercept) + (slope) SUSPENDED VOLUME

Feature	Intercept	Slope	No. Samples	Correlation coefficient	Variance
Mixed Layer	0.29	0.012	6	0.98	0.00622
	(-2 to 60)	(-21 to 44)		**	(d.f.=4)
Pycnocline Layer	0.57	0.074	24	0.88	0.00703
	(45-68)	(57-91)		**	(d.f.=22)
Combined Surface Group	0.46	0.092	30	0.93	0.00909
	(36-57)	(77-106)		**	(d.f.=28)
Adjusted Surface Group(1)	0.44	0.100	13	0.96	0.00783
	(30-59)	(98-102)		**	(d.f.=11)

Clearest Layer	0.45	0.085	25	0.85	0.00143
	(40-49)	(62-107)		**	(d.f.=23)

ATTENUATION COEFFICIENT = (intercept) + (slope) SUSPENDED VOLUME, continued

Feature	Intercept	Slope	No. samples	Correlation coefficient	Variance
Turbid Layer	0.57	0.090	4	0.94	0.02406
	(2-112)	(-9 to 188)		N.S.	(d.f.=2)
Nepheloid Layer	0.71	0.062	37	0.82	0.00705
	(64-78)	(47-77)		**	(d.f.=35)
Combined Nepheloid Group	0.68	0.070	41	0.85	0.00824
	(61-75)	(56-83)		**	(d.f.=39)
Adjusted Nepheloid Group(3)	0.63	0.077	35	0.87	0.00795
	(55-71)	(62-93)		**	(d.f.=33)

APPENDIX IV. EQUIPMENT AND TECHNIQUES

In Situ Filtering Equipment

Introduction

As the need for larger samples of suspended material arises, one must consider in situ collection. Spencer and Sachs (1970) provide a good description of an in situ pump/filtering system which processes sea water at a rate of up to 180 ℓ/hr with 0.45 μm filters, can be used to depths of at least 5700 m, and is described as "convenient and reliable." They include a simple and inexpensive scheme for utilizing automobile batteries as a power source, one of the more nagging problems encountered in designing this type of equipment. One deficiency in their design is the method by which the volume of water processed is measured -- they must extrapolate flow rates below 1.5 ℓ/min. A similar configuration for in situ filtering was used by Baker (1973), differing only in the power source design and type of flowmeter used. By using a larger diameter filter, he claimed success at processing up to 400 ℓ/hr of continental slope water off Washington.

A third description can be found in Beer et al. (1974). The significant differences in their design are the use of an A.C. pump/motor and incorporation of a commercially available turbine flowmeter which seems to be a definite improvement over other flow recording schemes. It is questionable whether or not the use of an A.C. motor in their design is of any advantage. The conversion of power from D.C., which is available from storage batteries if a conducting cable is not used, results in some loss of efficiency. Their claims of collecting up to 100 mg of sediment per filter (two are used) and continuous operation for as long as 24 hours on batteries would represent a highly desirable achievement. However, the equipment did not have a chance to prove itself by actually doing so before being lost at sea. Additional comments on their article can be found in Peterson (1976). Recently, an in situ filtration system capable of filtering several thousand liters has been described (Bishop and Edmond, 1976).

The system the author has constructed during his research has been designed around what seem to be the best parts of the previously described systems. Figure 26a is a diagram of the system and a description of each of the components follows.

Submersible Pump/Motor

This unit was obtained from Pelagic Electronics (174 Lakeshore Drive, East Falmouth, Massachusetts 02536) and consists of a pressure

compensated 6 volt D.C. motor which drives an attached impeller pump. The current requirement in the system was 16 amperes (no load) and 18 amperes (full load). The maximum flow rate of the pump, according to the manufacturer, is 20 ℓ/min at minimum flow restriction. With our filtering system, it moved about 4 ℓ/min of particle-free water in the laboratory and a maximum of 1.5 ℓ/min at depth in the ocean. The primary flow restrictions are the two 142 mm 0.4 μm Nuclepore filters, with additional restrictions due to the system's plumbing and turbine flowmeter. The reduced rate during ocean use is presumably due to entrapment of particulate matter, and also to environmental conditions -- especially increased seawater viscosity and reduced battery power at low temperatures.

It is difficult to estimate the maximum filter area beyond which there would be no flow rate increase for the pump, due to the variety of flow restrictions involved. The results of Baker (1973) suggest that using a single 293 mm filter (about twice the filter area of this system) increases the flow rate significantly. One might also consider a larger pore size filter.

Filter Holders

Two Millipore polyvinyl chloride holders, each containing a 142 mm 0.4 μm Nuclepore filter, were used. These holders are rugged, relatively inexpensive, and they minimize contamination problems. They provide a total effective filtering area of about 225 cm^2, which is well below the capacity of the pump. The screen and screen support are uncoated stainless steel, and a Dacron mesh was used between the screen and the filter to enhance flow through the filter. Some investigators have suggested Teflon coatings for these steel parts, and also for the "O" rings used to seal the holder, since the usual rubber parts can contribute to contamination during elemental analysis.

Flowmeter

A Cox Model LF-3-6 turbine flowmeter (Cox Instrument, 15300 Fullerton, Detroit, Michigan 48227) was installed between the filter holders and the pump inlet to measure flow rate, as suggested by Beer et al. (1974). This instrument will sense flow rates between about 0.5 and 5.0 ℓ/min and its signal is easily converted to a recorder display. The only alteration to the unit as supplied by the manufacturer was the potting of the electrical connections to withstand high pressures. The flowmeter was flushed with ethanol after each use at the suggestion of a Cox company engineer.

In addition to the calibration curve provided by the manufacturer, the flowmeter was calibrated using the filter system's circuitry. This was done by regulating the flow of water to the

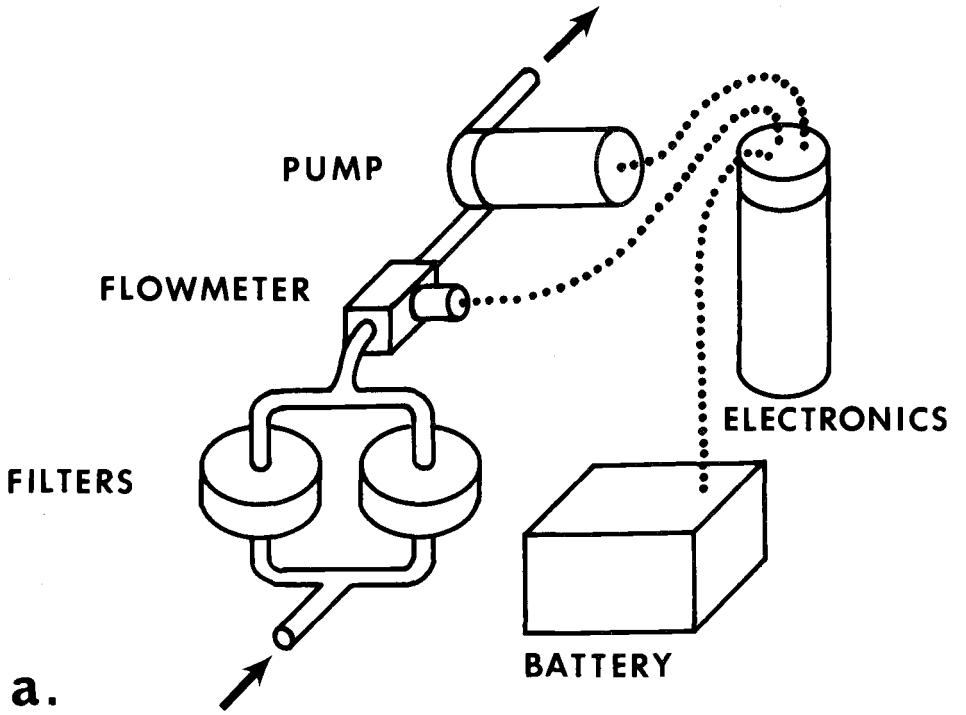

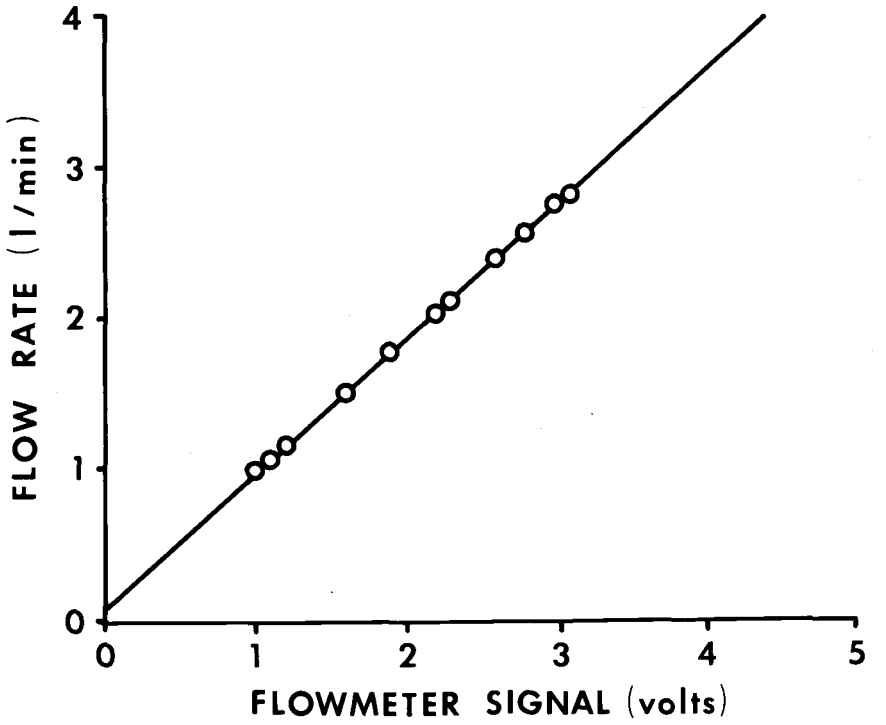

Figure 26. Component diagram of in situ filtering system (a) and calibration curve for flowmeter (b).

flowmeter by means of a valve, recording the time required to fill a 4 liter flask, and noting the voltage signal sent to the Rustrak recorder. The resulting calibration curve is presented in Figure 26b and was used for all subsequent flow rate determinations.

Electronics

All the electrical components were contained in a single pressure case. These included a Rustrak recorder for the processed signal from the flowmeter and relays to switch the pump motor on and off. The system could be operated by means of a signal sent down a conducting cable or by programming the Rustrak to act as a timer. Mr. R. Bartz, of the Optical Oceanography group at O.S.U., devised a simple and reliable switching scheme. A pair of contacts was installed in the Rustrak which rode along the chart paper. Strips of aluminum foil were positioned at selected points along the chart paper which, when the contacts rode over them, closed a circuit causing the pump to start or stop, depending on the position of a latching relay which alternated the function. Thus, a pair of foil strips separated by an hour's worth of chart paper would allow the pump to run for an hour. The Rustrak was equipped with an optional inverter motor to provide accurately timed chart paper motion. The switching system never malfunctioned during its testing periods and actual submerged operation.

Schematics for the flowmeter circuit and the switching relay circuit are presented in Figure 29 and were designed by R. Bartz.

Power Supply

The power demands of the pump motor require an efficient (i.e. high power-to-weight ratio) power source, and lead-acid batteries are currently the most practical source, although silver-zinc batteries may be a reasonable choice also (see Momsen and Clerici, 1971). The technology for using lead-acid batteries in a submerged, high pressure environment has resulted from their selection as the primary power source for small submersibles. The basic requirements for enclosing a lead-acid battery in a pressure compensated case are described in Bridges (1970). The difference between designs for submersibles, and a design appropriate for a submerged filtering system, is that the latter must be frequently recharged aboard ship, a complicating factor since it usually involves draining the insulating oil from the battery case. This step can be omitted only if a very slow "trickle" charge is made, which may be impractical at sea due to time constraints.

Following is a list of considerations to be made in the design of any liquid electrolyte battery system for submerged use:

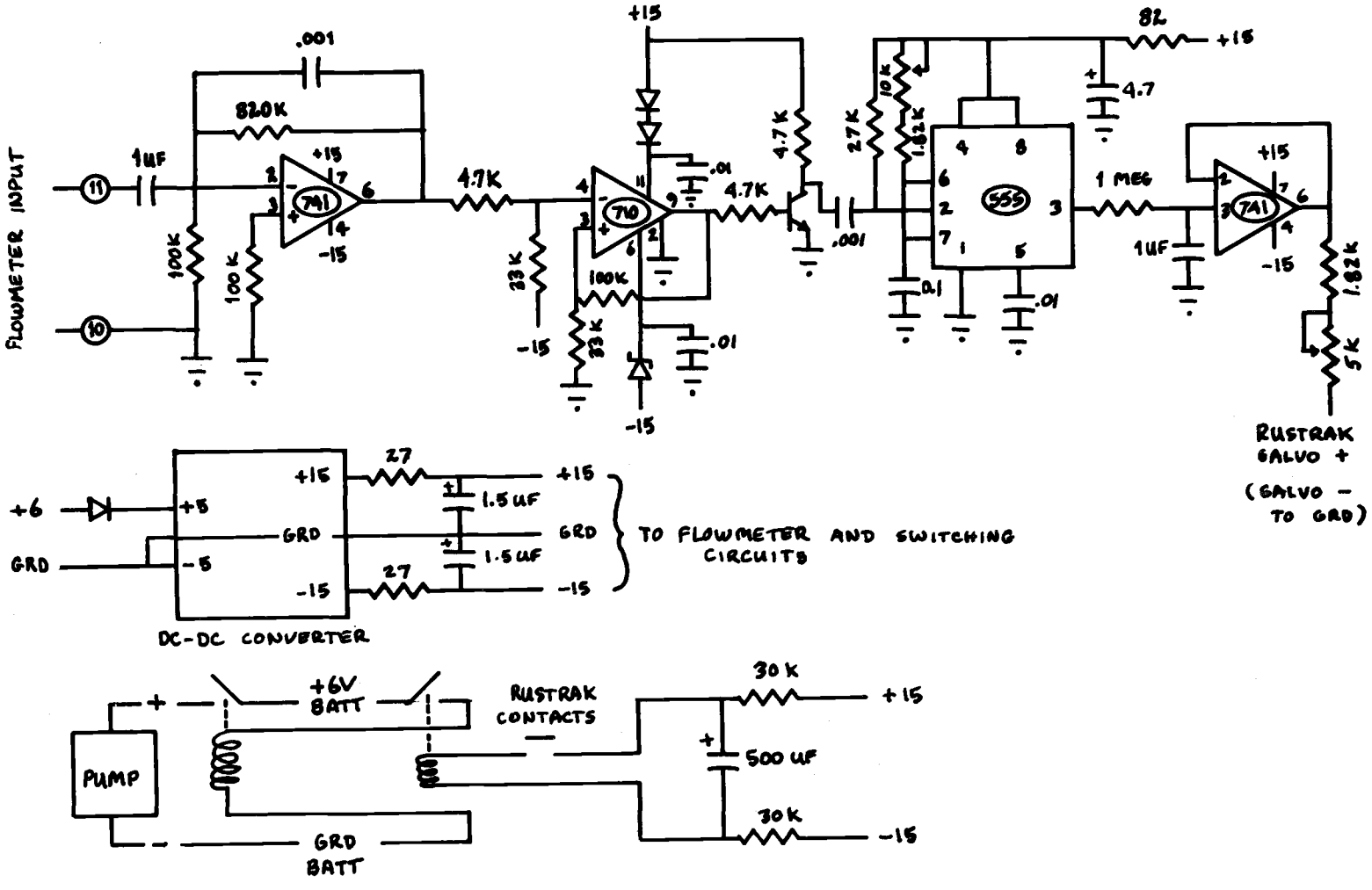

Figure 27. Schematics for flowmeter and switching circuits of in situ filtering system.

1. Insulation of the battery plates, electrolyte, and all electrical connectors from contact with sea water.

2. Degassing the battery due to a) exsolution of gases after use at depth, and b) generation of gases during rapid recharging aboard ship.

3. Replenishment of electrolyte volume lost due to gas generation.

4. Loss of battery capacity due to low temperatures in the marine environment.

Two methods of submerging lead-acid batteries were tried during the course of this investigation. Though neither method was completely satisfactory, both worked in a limited fashion. The first design consisted of two 150 ampere truck batteries mounted in a polyvinyl chloride case. A piston was installed on the lid of the case to allow for differential thermal expansion of the insulating oil and to provide some volume compensation due to gas generation. The piston was fitted with a gas venting screw also. The top of each cell, and the case itself, were filled with white mineral oil having a specific gravity between that of battery electrolyte and sea water. The system worked well until several recharging cycles had been accomplished, at which time it failed due to a short between the terminals. The design deficiency was the lack of a direct path for gas bubbles to leave the battery cells which resulted in the expulsion of oil and electrolyte as the gases expanded. The electrolyte, being denser than the insulating oil, collected on the top of the batteries until enough accumulated to cause a short circuit.

Sealing batteries in an oil-filled case is a usual method for submerged operation. Many applications (for instance, the STAR battery housing described in Bridges, 1970) do not require frequent recharging cycles and hence are less affected by gas generation. A discussion of the problem with Mr. R. Frye (Oceanographic Battery Company, 700 Americana Drive, Annapolis, Maryland 21403) resulted in his following suggestions:

1. Case construction following standard industry designs which are available from Oceanographic Battery Company.

2. Draining insulation oil from the case to a level below the cell vents, such that the recharging gases vent freely during rapid recharging.

3. Replenishing the electrolyte before closing the case for subsequent use.

The second design was inspired by that of Spencer and Sachs (1970) and requires no case or insulating oil. The terminals and connectors were insulated by potting compound, and the cell vent caps

replaced with a special cap made by gluing a plastic cylinder to the original vent cap. A balloon or rubber prophylactic was then attached to the cylinder. The entire battery and the special caps were filled with electrolyte prior to submersion. The scheme involves repeated handling of electrolyte on board ship and it is not recommended for general use. It could serve as a quick and inexpensive method in instances where only a few lowerings are needed, however.

Data Collected With In Situ System

The mass concentration data obtained during the Blanco Fracture Zone cruise are presented in Table IX. The weight change of each of the two 142 mm filters used per lowering was recorded and it was revealed that the filters did not collect samples equally even though the holders were plumbed in parallel. The weight change of each of the filters was summed and divided by the total volume of water processed. The volume was determined by visually estimating the mean flow voltage on the Rustrak record, converting this to a flow rate (see curve, Figure 26b), and multiplying by the time that the pump operated.

Data collected during the Hawaii-Oregon transit are presented in Table X. A new procedure for determining the mass of sediment was tried and involved immediately placing the wet 142 mm filters from the system in a glass jar filled with filtered distilled water. Upon return to the lab, the liquid and filter were subjected to ultrasonic agitation to resuspend the particles. This suspension was then re-filtered through a 47 mm filter and the weight change recorded. Unfortunately, complete removal of particles from the original filter did not always occur. Hence, the accuracy and precision may not be as reliable as with the method used for the Blanco samples.

Use of Nuclepore Filter Media

Description

Nuclepore filters are made by perforating a polycarbonate membrane with neutrons and etching the resulting cylindrical paths to an exact diameter (Nuclepore Corp., catalogue A, 1975). They were selected over the more generally used Millipore membrane by virtue of their desirable weighing characteristics -- low tare weight compared to Millipore, completely non-hygroscopic nature, and absence of a soluble wetting agent. They also offered potential for re-suspension of the particles collected on their surface by ultrasonic agitation. This is not feasible with other brands of filters, since they allow particles to become trapped within the filter as well as on its surface. Nuclepore filters have recently been used successfully

TABLE IX. BLANCO FRACTURE ZONE DATA (Y7407)

Station	Location (N/W)	Depth (m)	Filter	Mass Recovered (mg)	TSM (μgm/ℓ)
2	44-10.2/127-14.3	2863	B78	3.57	43
			B77	2.57	
3	43-56.2/127-33.0	2862	B76	14.31	139
			B75	10.17	
4	43-52.7/127-09.0	3120	B74	8.78	158
			B73	22.63	
5	43-38.1/127-13.2	2875	B72	8.97	302
			B71	33.30	
6	43-38.0/127-25.0	2941	B69	8.45	120
			B68	8.85	
7	43-29.9/127-22.9	3127	B66	26.34	230
			B65	15.05	
11	43-48.3/128-41.3	3340	B62	8.99	145
			B61	9.53	
12	43-28.3/128-48.2	3098	B59	8.88	548
			B58	21.05	
14	43-41.9/129-37.3	3132	B55	20.88	534
			B53	25.68	

Note: All samples were taken about 20 to 30 m off the bottom and from within the optically defined nepheloid layer.

TABLE X. HAWAII-OREGON TRANSIT DATA (YALOC 74 LEG 3)

Station	Location (N/W)	Seafloor (m)	Sample (m)	Filter	TSM (μgm/ℓ)
44	22-19.5/155-42.3	4500	4488	H-3	17
44	22-19.5/155-42.3	4500	4478	H-4	25*
45	22-19.5/155-44.4	4525	3500	H-5	3
45	22-19.5/155-44.4	4525	3490	H-6	43*
57	33-10.3/150-56.4	5597	5587	H-7	14
60	33-10.7/150-54.4	5590	3500	H-8	6
72	33-27.7/150-59.0	5514	5502	H-9	6
72	33-28.0/151-00.5	5520	3500	H-11	3

Note: Values marked with an asterisk were taken with a 30 liter Niskin bottle.

by other investigators of suspended particulates, particularly if gravimetric analysis is involved (c.f. Carder et al., 1974; Biscaye and Eittreim, 1974).

One of the disadvantages of Nuclepore filters is a somewhat lower flow rate compared to Millipore filters. They may also clog more quickly, resulting in a decreased amount of sea water being processed per filter. This is especially true if there is a significant amount of protoplasm in suspension, as in surface and coastal waters. They have been found to be less efficient at retaining living cells compared to other types of membrane filters (P. Donaghay, personal communication).

Salt Rinse

If sea water has been filtered, the salt water must be flushed before drying the filter for reweighing. This process is facilitated by the completely non-hygroscopic nature of Nuclepore filters since sea water remains as droplets on the filter surface, or within the collected particles, but not within the filter itself. The technique used in this study was to completely wet the filter surface with particle-free distilled water and vacuum filter all visible water droplets. This was repeated three times. Several filters were examined with a microscope after drying and no evidence of salt was visible. Unrinsed filters display areas of dendritic salt patterns after drying. The amount of salt retained on a filter is quite variable and cannot be reliably predicted.

Weighing Techniques

All weighing was done on a Sartorius semimicro balance. Repeated weighings of filters during the early course of the study showed a disturbing lack of consistency, in spite of adherence to previously described techniques. Further experimentation showed that static charge buildup was the problem and that the presence of polonium strips around the balance pan did not adequately eliminate the static charge influence. Passing both sides of the filter over a polonium strip several times before placing the filter on the balance pan did remove the charge, however, and results became much more consistent. When weighing filters with particles on them, the polonium strip was passed over the filter to reduce the possibility of material being lost due to unnecessary filter handling. The filter surface and strip always passed within 1 cm of each other. The weighing of the 142 mm filters used in the *in situ* filtering system was more difficult than the 47 mm filters, since it was harder to eliminate static charges from the larger filters.

During the Oregon continental shelf study, a single 47 mm filter was set aside as a balance control. It was weighed about five times

prior to each actual sample weighing session to "warm up" the balance and the operator. The fifth weight was recorded as the true value. It was then reweighed every tenth filter to monitor possible balance drift. The control filter was weighed a total of 59 times during 15 separate sessions, between 16 April and 4 September, 1975, with the resulting descriptive statistics:

Mean	1.8278×10^{-2} gm
Median	1.8280×10^{-2} gm
Variance	1.8545×10^{-10} gm
Std. Dev.	1.3617×10^{-5} gm

Normality of the weighing errors is suggested by a kurtosis close to 3 (2.89) for the distribution. The standard deviation of the weight differences (which were used to compute mass concentration values) was determined by doubling the variance for each weight measurement (1.85×10^{-10}) and taking the square root. The 95% confidence interval of the change in weight is $\pm 3.8 \times 10^{-5}$ gm for these measurements (Snedecor and Cochran, 1967). This was the weighing error used in the computation of the Arctic data and the Oregon continental shelf data.

Processing Effects on Filters

Tests were performed on Nuclepore filters to determine their weight stability during certain processing techniques. These included weight loss due to the passage of water, sodium hypochlorite (Chlorox), and hydrogen peroxide, and any weight loss associated with ultrasonic treatment. The unexpected discovery was that a rinse with 4 liters of particle-free distilled water caused a slight weight loss in the five test filters. Repeated rinses did not cause an additional loss. This rinse loss is at variance with the results of Cranston and Buckley (1972), who found no weight change after filtering particle-free water. However, their Nuclepore filters were all pre-treated by soaking in water prior to the experiments -- a procedure which would seem desirable in light of these results. The rinse weight loss detected in my experiments is small compared to the weighing error discussed above.

A significant weight loss was noted for Chlorox, which eliminated this fluid as a possible leaching agent for organic matter removal (Anderson, 1961) if a quantitative estimate was to be made by weight change. Treatment with 35% hydrogen peroxide warmed for 1/2 hour at about 70° C also caused a small but consistent weight loss which did not continue with repeated treatment, suggesting attack of a surface coating only. Ultrasonic agitation of six test filters submerged in water resulted in a loss of weight. When the water was

filtered through a second filter, however, an equivalent weight gain did not result, suggesting that the loss was not due to particles greater than 0.4 μm breaking off. An inquiry to Nuclepore engineers concerning the nature of this loss was unproductive.

Treatment with hydrogen peroxide and recording the change in weight of the filter plus particulate matter appeared to be promising as a quantitative or at least semi-quantitative estimate of organic material, since a constant correction factor for weight loss from the filter material could be applied. Molnia (1974) has used a similar weight change technique to estimate the amount of calcium carbonate in sediment samples by leaching them with dilute hydrochloric acid. Digestion of organics by hydrogen peroxide is described by Jackson (1958) as it pertains to soils analysis and has been used routinely in the removal of organic material from marine sediments.

The technique is to place the filter in a small evaporating dish, add about 10 ml of 35% hydrogen peroxide (buffered to pH = 7 if carbonates are present), cover, and heat in a water bath at 60 to 70° C for 1/2 hour. An additional 2 ml of peroxide is added after the first 15 minutes. The filter should be turned particle side down during the digestion process. It is then carefully placed onto a filter holder and the peroxide, plus any loose particles, is refiltered through it. Three or four complete flushings with filtered distilled water remove all traces of peroxide and the treatment is complete. The filter is finally air-dried and reweighed.

Repeated treatments were performed on six of the Oregon continental shelf samples which covered a range of organic matter proportions, and only a minor additional weight loss occurred. It is possible that this additional loss is due to the repeated filtering, causing particles to break down into sizes which may pass through the filter, and not necessarily due to continued organic leaching. A summary of the processing experiments is presented in Table XI. Additional information concerning the use of Nuclepore filters in the analysis of suspended particulate matter may be found in an unpublished manuscript by Cranston and Buckley (1972), which is available from Nuclepore.

Filters as Mounting Media

Slides for optical microscopy of the Arctic samples were prepared by cutting a 5 by 15 mm section from the filter, in a direction extending from the center to the outer edge. The section was then mounted on a microscope slide under a cover slip using a suitable medium. It should be noted that particles will be moved off the filter surface by the mounting medium during preparation of the slide. Therefore, an attempt should be made to contain the medium within the area under the cover slip; otherwise, both filter and excess medium must be examined for particles.

TABLE XI. EFFECTS OF VARIOUS TREATMENTS ON NUCLEPORE FILTERS

	Treatment	Effect	Remarks
1.	Filtration of 4 ℓ of particle-free water	Weight loss of 12 μgm from 47 mm filters	No additional loss with repeated treatments
2.	1/2 hour soak in warm 35% hydrogen peroxide	Weight loss of 62 μgm from 47 mm filters	No additional loss with repeated treatments
3.	Repeated 1/2 hour soaks in warm 35% hydrogen peroxide; actual sample filters	Very minor additional weight loss after initial leach of organic matter	This additional loss is probably due to effects of repeated filtration
4.	Ultrasonic agitation in particle-free water	Weight loss of 413 μgm from 142 mm filters	Small but variable additional loss with repeated treatments, averaging 70 μgm; weight loss is not in the form of particles greater than 0.4 μm; about 100 μgm of loss may be due to effects of treatment #1

Hyrax was chosen as the mounting medium because of its high refractive index (1.70). Although the filters (with indices of 1.62 and 1.58) may become nearly transparent in media with similar indices such as Permount (1.58) or Caedex (1.56), many natural materials also have indices in this range which makes them difficult to observe. The use of Hyrax is especially helpful in the study of diatoms (see McCrone, 1973, volume II, for additional information on mounting media for particles). Although Hyrax causes an increased contrast of the pores in the filters, it was not a major problem.

The mounting technique is to place a small drop of Hyrax on both a cover slip and a slide, with each warmed just enough to make the Hyrax melt. Place the filter section "face down" on the cover slip and position the cover slip and section on the slide. Apply additional heat until large, "boiling," bubbles form in the Hyrax. Then cool by placing on a counter top. The large bubbles should contract to nothing.

Mounts for scanning electron microscopy of the Arctic samples were prepared by fixing a square of filter 5 mm on a side to an aluminum pedestal using two-sided tape. Spray adhesive and aluminum paint were also used and found to work equally well as adhesives. The sample was gold-coated in a vacuum evaporator.

Mounts for X-ray diffraction of the Oregon samples were produced by combining the resuspended material from filters that had been leached of organic matter. Resuspension was accomplished by placing a 47 mm filter in a small glass vial filled with particle-free distilled water to which a peptizer has been added, allowing the filter to soak overnight, and then subjecting the vial to ultrasonic agitation. The suspension was allowed to settle for several days and the filter gently removed. The vial was decanted of the clear liquid and the concentrated suspensions from several filters were combined. The resulting suspension was vacuum-filtered onto pressed silver planchets for X-ray diffraction. For the Oregon continental shelf samples, the combined suspension resulted in about 10 mg of inorganic material being mounted on a planchet with a surface area of 3 cm^2.

Resuspension and recovery were essentially complete in most cases, as monitored by weighing the cleaned filter and comparing it to the original tare of the filter. Weight loss from the original tare value due to water rinse, peroxide leach, and ultrasonic agitation was considered for the recovery estimation. An average of 98% recovery was found, with slightly lower values occurring for surface samples (see Table IV in Chapter III).